UNIVERSITÀ DEGLI STUDI DELL'AQUILA
DIPARTIMENTO DI INGEGNERIA CIVILE, EDILE-ARCHITETTURA, AMBIENTALE

Ph.D.ICEAA

Dottorato di Ricerca in Ingegneria Civile, Edile-Architettura, Ambientale

Curriculum Ingegneria Civile

XXXII ciclo

HYDRO-SEDIMENTARY DYNAMICS OF INTERMITTENT RIVER SYSTEMS: THE CELONE STREAM, PUGLIA (S-E ITALY)

SSD ICAR/02 – Costruzioni Idrauliche, Marittime e Idrologia

Candidato

RAFFAELE DI PILLO

Coordinatore del corso

Prof. MARCELLO DI RISIO

Tutor

Prof.ssa MARIA TERESA TODISCO

Co-Tutor

Dott. Ing. ANNA MARIA DE GIROLAMO

A.A. 2018/2019

UNIVERSITA' DEGLI STUDI DELL'AQUILA

DIPARTIMENTO DICEAA

Dipartimento di Ingegneria Civile, Edile-Architettura e Ambientale

Dottorato di ricerca ICEAA
In Ingegneria Civile, Edile-Architettura e Ambientale

XXXII Ciclo

SSD – ICAR/02 Costruzioni idrauliche, marittime ed Idrologia

HYDRO-SEDIMENTARY DYNAMICS OF INTERMITTENT RIVER SYSTEMS:

The Celone stream, Puglia (S-E Italy)

Coordinatore del Dottorato

Prof. Marcello Di Risio

Tutor

Prof.ssa Maria Teresa Todisco

Co-tutor

Dr. Eng. Anna Maria De Girolamo

Dottoranda: Ing. Raffaele Di Pillo

Nature always tends to act in the simplest way

D. Bernoulli

ANALITICAL INDEX

00 – Extended Abstract

This PhD thesis is carried out as part of a co-tutoring project between the University of L'Aquila and the Institute for Water Research (IRSA) of the National Research Council (CNR) based in Bari, it examines the erosion-transport-sedimentation dynamics of a small mediterranean watershed togheter with its ephemeral, intermittent river system.

The study was made possible thanks to the disposability of experimental data, made available by the hosting Institute (IRSA, Bari). The result of these samplings, carried out in particular on the Celone river (FG, Puglia, Italy), have been useful in characterizing the hydro sedimentary dynamic of the Celone itself, located in the Daunia's Apennines of northern Puglia, but could be also useful for a wide range of other similar basins, in fact, the pedological, morphological, climatic, land use, geological and hydraulic characteristics of this territory make it particular in its kind, but also similar to a large part of pedo-mountain basins widespread in the mountainous areas of Italy (Apennines, Sub-Apennines). The data set consists of continuous discharge measurements (Q) and discrete concentration of suspended solids (SSC) samplings, collected at "Masseria Pirro" gauging station located 8 km upstream the Capaccio (Torrebianca) reservoir, and entirely managed by the institute.

Another aspect to point out is that this study is part of a larger project on a European scale so this research was supported by European Community's Seventh Framework Programme, FP7/2007-2011, MIRAGE project.

After briefly recalling, in the first chapter, some elements of hydrology useful to better identify the processes that have subsequently been deepened, we started by identifying the state of the art through a preparatory framing work, on a basin scale, of the territory and by the examination of historical collection of data available on a multi-year basis (not always easy to find).

In the Mediterranean regions, almost all watercourses are affected by erosion and soil degradation (Jones et al. 2012), which has led over the years to a substantial increase in the study of erosive (de Vente 2009) transport (Gentile et al. 2010, Gallart et al. 2013, De Girolamo et al. 2015) and sedimentation phenomena of suspended solids in waterways (Tzoraki et al. 2007).

The quantification of the sediment load transported, in particular, becomes of great theoretical and practical interest when we think that through it we can reach a more correct quantification of the soil loss, which exacerbates numerous Apulian basins, together with its related ecological and managerial aspects, such as the delivery of nutrients and pollutants, the silting of reservoirs or the morphological and plano-altimetric variation of river basins (D'Ambrosio et al. 2019, Di Pillo et al. 2019).

The proposed study therefore starts from a theoretical system concerning the suspended solid transport problems, already widely developed over the years (Walling & Webb 1985, 1988) through numerous formulations, all widely diversified from each other according to different factors: territorial (land use, vegetation cover etc ..), climatic (humidity, rain days and heights etc ..) and more strictly hydraulic (flow rate regime etc ..) and is aimed at characterizing the phenomenon of SS transport in its almost-totality, therefore trying to (i) quantify the total load of suspended sediment transported to the closing section of the basin, (ii) Identify the sediment source areas, (iii) identify the drivers of the suspended sediment transport phenomenon and (iv) give a qualitative and quantitative evaluation of the silting phenomenon of the Capaccio reservoir, underlying the Celone river basin.

The flow-regime, the seasonality and the occurrence of particular events, will be studied as well as the total annual loads of suspended sediment calculated with different methods widely used in the literature. Subsequently, a statistical uncertainty analysis will be applied to these "output" data, aimed at assessing the reliability ranges related to each analyzed estimation method.

From this last step one can already understands one of the fundamental purposes of the study, which is precisely to provide an instrument capable of making it clear that there is a certain "range", within which the applicability and repeatability of certain methods of evaluation rather than others, it may be more or less correct for some basins rather than others.

In addition, the study finds *raison d'etre* also in perspective, as a tool for understanding the quality of the water and the correct management of the basin itself, it is underlined that the methods here proposed, even if below will be used only to evaluate the total suspended sediment loads, they can also be used for the quantification of the total annual loads of nutrients and pollutants, which can therefore lead to various chemical-environmental and ecological analyzes.

Subsequently, starting from the results of the analysis carried out by addressing the *load estimation problem* and observing that, as in similar basins, also in Celone river most of the suspended sediment transported during the year is conveyed during flood events, we proceeded to analyze at the event scale the erosion-transport-sedimentation dynamic.

After having obtained historical high resolution rainfall depth data, 30 min (± 0.5mm), of two different gauging stations belonging to the basin for the same study period (2010-2011) and after identifying a set of 18 independent variables, all competing in various capacities in influencing the studied phenomena, a Principal Component Analysis (PCA) was conducted, aimed at decreasing the variable's space, reducing it to the only components, the main ones, which are most able to describe them.

The event-scale analysis also made it possible to carry out a further study, concerning the Q-SSC hysteresis, or the non-linear relationship that occurs during a single event between the variation in discharge and suspended sediment concentration, over time. This study, already carried out by De Girolamo et al. 2015, has been revived through the indexing of hysteresis cycles by the introduction of specific HI index.

This methodology, even if it entails the loss of precision given by the observation of the single cycle in the traditional plot (Zhang et al. 2014), had the purpose of being able to make comparisons, both within the basin and with other basins, of different responses to different rainfall events. The application also made it possible to provide interesting indications regarding the location, more or less distant from the sampling point, of the sediment production areas, then compared with the results obtained by applying the FLORENCE model referred to in the subsequent chapter.

Finally, a physically based modeling of the instrumented watershed was carried out, starting from it, through a subdivision into sub-areas unit with homogeneous characteristics and through further multi-scenario modelling applied to them, those areas of the basin most likely to release and convey sediment to the watercourse will be identified. The same model will make it possible to give a first approach quantification the of the reservoir siltation, for the Torrebianca reservoir itself (8km downstream of the measurement station on the Celone river). This quantification will then be validated through the aforementioned suspended load estimates. Lastly, coupling these informations with the dam's characteristics i.e. material, average volume, maximum capacity, etc.., this will allow us to arrive at interesting considerations regarding the problems of loss of water storage capacity and its remediation.

01 – Introduction

1.1 General concepts

Water catchment

The term water catchment area, or drainage basin, indicates the portion of the earth's surface, limited by the line of watershed separation, within which the waters deriving from rainfall precipitation, from the melting of the snow, and any punctual or widespread sources are collected and run off.

Italian legislation (Law 183/89 on soil protection art. 1, paragraph 3) defines the river basin as:

"il territorio dal quale le acque pluviali o di fusione delle nevi e dei ghiacciai, defluendo in superficie, si raccolgono in un determinato corso d'acqua direttamente o a mezzo di affluenti, nonché il territorio che può essere allagato dalle acque del medesimo corso d'acqua, ivi compresi i suoi rami terminali con le foci in mare ed il litorale marittimo prospiciente; qualora un territorio possa essere allagato dalle acque di più corsi d'acqua, esso si intende ricadente nel bacino idrografico il cui bacino imbrifero montano ha la superficie maggiore".

It is necessary to detect the presence of sub-areas, in which drainage networks are often not fully developed or completely absent, such surface portions are however characterized as "sub-basins".

It is also fair to point out that the subdivision proposed below generally applies to mountain and / or hilly waterways, which generally have basins size in the order of tens of square kilometers (such as the one proposed by this work , 85,9 Km^2), in which it is not necessary to recognize "important" tributaries and therefore to make a subsequent division into any other spatial subsets:

From a morphological point of view, a water catchment area has three areas, generally easily distinguishable:

- The collection basin as a sediment and runoff producer. It is identified with the part of the system located at the highest altitudes, otherwise called the "headland" (upland or headwater).
- The transfer channel where sediment flows.
- Alluvial fans, or delta areas where the runoff is delivered to the container (sea, lake or other waterway). There is mainly deposition of the transported materials.

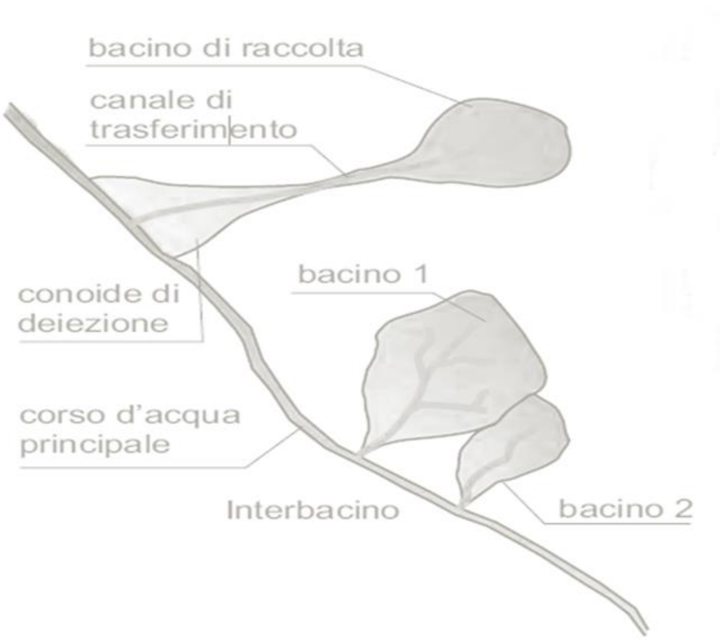

Fig.1. Water catchment

River Environment

River environment or ecosystem is defined as the set of abiotic factors, corresponding to the characteristics of the river habitat (composition of the seabed, temperature, lithology and geomorphology of the river basin, climatic factors, water, etc.), of the biotic factors corresponding to the characteristics of the communities that live in the habitat (man, fauna, flora) as well as the set of relationships that bind them and the dynamic processes to which they are subjects that contribute to the creation and development of a high amount of microhabitat and ecological systems that develop spatially and temporally at the same river basin or in different points with different characteristics within the basin.

The multidimensional approach to river systems, promoted by river ecology, refers to four specific dimensions: from bank to bank, from upstream to downstream, from upstream to downstream and the temporal dimension. To these dimensions correspond as many components, namely:

- the transversal component linked to the lateral dimension, consisting of the interrelationships with the territories and with the activities that take place in the adjacent environments;
- the longitudinal component represented by the succession of ecosystems starting from the source up to the mouth;
- the vertical component connected to the relationship between surface and groundwater;
- the temporal component fundamental to highlight the extreme variability of the river system over time,

resulting from climatic events, seasonal variations and sudden events such as floods.

This definition has gained importance especially in recent years, when communities began to look at river basins not only under the point of view of the exploiting of available resources i.e. hydroelectric and / or drinkable, but also as ecological-landscape resources, starting to become aware of the fact that these aspects are fundamental from the point of view of homeostatic capacities (ability to react and regenerate following an external disturbance), self-purifying and regeneration following erosion of a watercourse.

Therefore, the changes to be made in a certain basin, even if necessary to mitigate for example the hydraulic risk, which will be discussed later, or to determine a certain change, for example in the use of the soil of a certain area, must be weighed in reason of the fact that they will provoke changes whose effects could be devastating on such a fragile equilibrium, let us think, for example, of the creation of transversal obstacles that interrupt the longitudinal continuity of the watercourse (making its fundamental ecological corridor function disappear). It is however true that at the same time aspects related to safety and risk mitigation must not be overshadowed, both aspects should simply be carried forward hand in hand through the increasingly necessary collaboration of different professional figures.

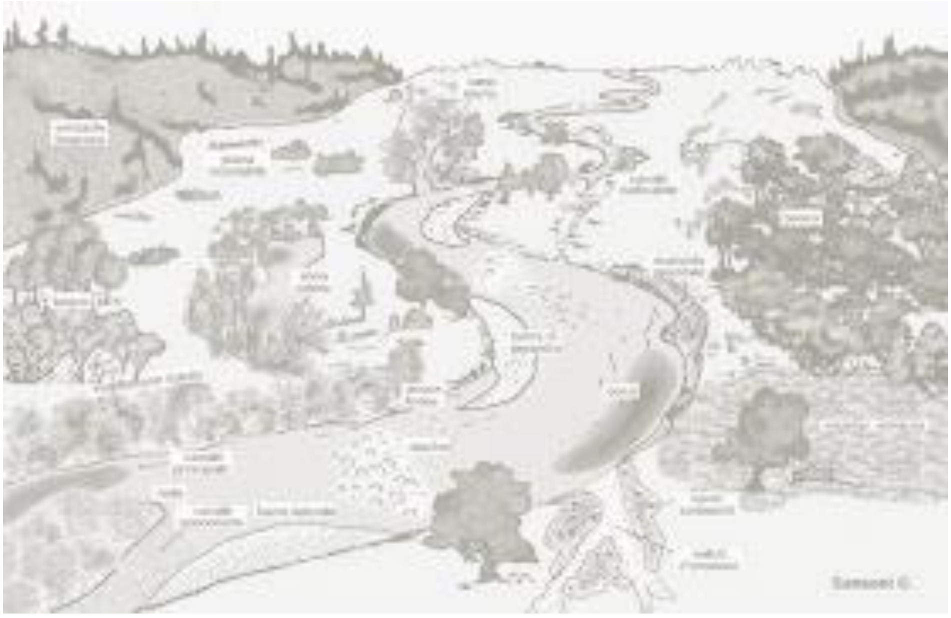

Fig.2. River Environment

Hydraulic Risk

To understand the concept of hydraulic risk, one must first understand some parameters related to it and through which it can be computed analytically:

- Risk (R): it is a subjective concept, linked to the interpretation of multiple concurrent factors, however for what has been said, it is necessary to give objective character in order to then proceed with a quantification. In general, it is the product of two factors, the danger and the expected damage. Specifically, we can distinguish two types of risk, the specific one and the total one.
- Hazard (H): or natural hazard and indicates the probability of a potentially harmful phenomenon occurring within an assigned time interval and within an assigned area. It is curious to note that the English term

hazard comes from Italian, in which it still maintains the meaning of a random fact, but mainly linked to human actions (gambling, to dare to do or say something). Naturally in the context of the hydraulic risk, the hazard will be understood as hydraulic and will be a factor dependent on variables related to the hydraulic and environmental physical characteristics of the watercourse or its hydrographic basin, such as for example the regime of rainfall or flow rates etc...

- Vulnerability (V): indicates the degree of losses caused to an asset or to a plurality of assets (exposed to risk) following the occurrence of a natural phenomenon of assigned entity. It is expressed referring to a range of values between 0 (no damage) and 1 (total loss).
- Specific Risk (Rs): indicates the extent of the damage expected as a result of a particular natural phenomenon. It is expressed with the product Rs = H x V.
- Element or asset subject to the risk (E): indicates the population, the properties, the economic activities, including public services, that are exposed to the danger of a natural event in a specific area.
- Total risk (Rt): indicates the expected number of deaths, injuries, property damaged or interruption of economic activities following a natural event and is therefore given by the product Rt = Rs x E = E x H x V.

This also following the approach dictated by the national legislation on the matter, Law 267/98. For the purpose of defining the risk, it also becomes necessary to establish the time frame within which it is decided to accept the occurrence of an event of equal or greater extent than the expected. This time frame can be equal to the expected life of the involved operas.

1.2 Hydrology

Some key hydrological concepts are briefly mentioned below such as: hydrological balance, rainfall inflow, infiltration, runoff, erosion and sediment transport.

Hydrological Balance

Previously, we mentioned the river watershed from a physical, geomorphological and water point of view but if we wanted to define it under a physical point of view, we can immediately say that it could be considered as an "open system", that is, a system capable of interacting with the surrounding environment by exchanging energy and matter. This interchange occurs precisely thanks to the passage of water in different forms and in different space-time conditions.

To correctly set up a hydrological balance problem, it will therefore be necessary to first define a spatial and temporal unit. The standard space unit on which these considerations are made is precisely the river basin, in this regard, in order to make a fair balance it will be necessary to acquire as basic cognitive elements: the identification of both surface and underground water bodies. As regards the time unit, the greatest difficulty will be due to the fact that the different interchange events between the system and the environment take place on widely different time scales (for example, one can refer to the different time scales on which rainfall instead of infiltration or evapotranspiration events occur), therefore it will be necessary to find a homogeneous temporal unit to which to report all the considered events. Generally, the average hydrological year is chosen, defined as the "virtual" year in which all the components of the hydrological cycle, calculated on the widest possible temporal basis and at the same time, present average values.

Once defined both temporal and spatial scale one can approach the water balance problem, evaluating inflow and outflow water volumes, therefore it will be:

$$P = Er + R + I \qquad (1)$$

Where:

P = rainfall volumes; Er = real evapotranspiration volumes; R = runoff volumes; I = infiltration volumes

It should be emphasized that this balance will be valid in the most general conditions, however, it may be influenced by the anthropic activities that through various practices of exploitation of the basins (for example, the water volumes taken for agricultural, industrial or drinking water supplies), will lead to the timely modification of the aforementioned balance sheet, it will however remain valid on average, thanks also to the practices of introducing water volumes (sewage purified water drains, grabbing and exchange water drains, etc...).

Another mandatory consideration concerns the quantification of budget terms, it will require the presence of frequent and widespread measures to better approximate the overall behaviour of the "basin" space unit. However, often the latter will be scarce or absent, limited to small portions of the basin, this aspect must be taken into account in the assessment of the balance, adopting appropriate tolerances, which, moreover, will almost always lead to an "estimate" of the hydrological balance.

A brief dissertation follows on the individual terms of the balance equation (Eq. 1).

Inflow

They represent the term to the left of the equation, generally defined with P (water inflow), specifically, it should be taken into account that these inflows can be of two types, direct (i.e. rainfall, snowmelt etc...) and indirect, or deriving from water domains adjacent as well as by numerous other factors, such as, for example, the presence of artificial inflow elements or the entry of volumes from other areas, not physically linked to the basin itself

Generally, these terms are difficult to quantify, the evaluation of the geological relationships between adjacent domains is, in fact, a function of a series of factors that are not immediately deducible, such as the difference in permeability between geological units, the size of the contact surfaces, the flow direction of the aquifers, elements that would lead to excessive complications in the evaluation of a term that in general will have less influence than the other.

Focusing therefore on what are the direct inflows, we will say that: they are mainly due to atmospheric events, both in the liquid state (rainfall), and in the solid and gaseous state (snowmelt, hailstorm and water vapor), generally for this case study (small foothill catchment) the latter could be considered comparable to the evapotranspiration lost volumes, therefore both excluded from the balance sheet.

Therefore, considering the positions made, the contributions due to rainfall events remain to be identified and understood. The study and characterization of the latter will be of fundamental importance in understanding the continuation of the work carried out, in fact considerations will be made regarding the rainfall regime in the instrumented basin, regarding the relationships between rainfall events and flood events (for example one can think to the delay between the peak of rainfall and the peak of discharge) and therefore how these can play an important role in the characterization of the phenomenon of the transport of both sediments and nutrients.

The quantification of a rain event will be expressed in millimetres of water, as if they fell on a horizontal plane and without undergoing evaporation or absorption processes. To obtain the volume of rainfall that has fallen on a given surface, simply multiply the projection of the latter on a horizontal plane by the aforementioned rainfall depth.

In particular, on the measurement of rainfall, it must be said that the measurements of the rainfall depth are made through rain gauges in stations spread throughout the national territory (one station approximately every 80 km^2)

depending on the measured quantities they will be divided into: Ordinary rain gauges (or snow-gauges in mountainous areas), used for the measurement of rainfall over the previous 24 hours; Recorders, in which the water is collected and conducted continuously to recorders, they fulfil the need to know the distribution and duration of the rains within 24 hours; Totalizers, used in those areas where due to particular environmental conditions it is not possible to take measurements over short periods, finally, for mountainous areas subject to considerable snowfall, we tend to trace the thickness of the snowpack, with direct measurements or through surveys or through the imagery-analysis.

These instruments are used, as far as being said, to measure the precipitation height, $h = V/A$, measured in mm, with V, precipitation volume and A area of the known surface, and the rain intensity $i = h/t$, generally expressed in mm/hour, with t, the time interval in which volume V is flowed.

The collection of these observations and their first processing, however, is carried out by the hydrographic offices and published in the "hydrological records".

This study made use of historical series (2010-2011) measuring rainfall height at 30 min (± 0.05mm) made available by the civil protection department, detached section of Modugno.

Outflow-Runoff

Always referring to Eq. 1. we can define the total runoff D as the sum of the quantities of surface runoff water and the quantities of infiltration water (D = R + I), this term will therefore identify the total water potential of the spatial domain considered, i.e. the maximum volume of theoretically usable water.

Generally, the determination of the outflow is a function of a series of basin's characteristic factors, such as, for example, basin's shape factors, average altitude, average slope, vegetation cover, the degree of imbibition of the soil characterized by its geo-lithological nature, which will determine the basin flow coefficient, this coefficient will represent the value of the ratio between the flowed net volume and the total volume (φ = D / P).

In the frequent case that the surface A of the basin is divided into several sub-surfaces Ai, each characterized by a coefficient φi, the weighted average coefficient φ for the entire area is: $\varphi = \frac{\sum \varphi i * Ai}{\sum Ai}$

The attribution of the flow coefficient remains subjective, however, the following corrective coefficients are added to this basic value, to better take into account the factors listed above:

φi = infiltration coefficient, takes into account the drainage capacity of the subsoil, for flood events that develop in time intervals of the order of hours, the outflow in the closing section is largely given by the surface flow, since the underground flow, fed from infiltration, it takes place in much longer times;

φp = difference in altitude, considers the average slope of the basin referred to the river, an element that obviously favors runoff;

φr = retention coefficient, assesses the tendency of the basin to retain water in natural depressions or to be drained by ditches or canals.

Since also the attribution of these values is subjective, it is therefore necessary to have a broader knowledge of the territory in order to best correlate these coefficients and condition of the soil.

Another fundamental parameter to take into consideration when talking about outflows is the concentration time tc, defined as the time that the fluid particle takes to flow into the closing section of the basin starting from the most distant point of the basin itself, it will be a function of the area and shape of the basin, in general we can consider it equal to the runoff time (used by the water particles to get to the compluvium line) plus the time that occurs to the particles to flow within the river rod, i.e. ratio between the sum of the path lengths and uniform motion velocity of the particle, these definitions are difficult to formulate, therefore numerous ad hoc formulations are widely used for the scope today, such as Giandotti 1934 or Aronica 1954 formulas, currently there are also many GIS applications that allow the calculation.

In conclusion, it is important to underline that a qualitative-quantitative modelling of these hydrological phenomena can be done through models developed by specific software (i.e. SWAT model), which through the introduction of input data concerning the physical and spatial characteristics of the basin are able to simulate the afore mentioned process of inflows-outflows.

Erosion

The modelling of the territory depends on several physical factors: the main one, in addition to the wind, is undoubtedly the water, which shapes the planet in the most effective way and with its incessant work. Flowing water dissipates part of its energy by friction; this loss of energy is transmitted to the riverbed in the form of a force which, in particular conditions, determines its displacement: the ability of the water to transport materials is directly proportional to this energy.

The quantities of soil eroded and transported to the sea, for all the emerged lands, were estimated at around 570 t km^{-2}; for the Po Valley basin, for example, the average is about 790 t km^{-2} (equal to about 0.5 mm $year^{-1}$). For the Arno river basin an average erosion of 3 mm $year^{-1}$ was assessed, for the studied basin, the Celone stream (Puglia, Italy) an erosion of more than 1mm $year^{-1}$ was calculated (De Girolamo et al. 2015).

The main consequence of river erosion is undoubtedly the transport of this material in the river grids, the solid transport precisely, will be directly related to the ability of the basin to produce transportable material (erodibility).

Horton (1945), defines a series of measurable parameters for the purpose of assessing the extent of erosion processes, among them we find the lithological characteristics of the soil, for which there is a relationship of direct proportionality with erodibility and inverse with permeability. There is again the vegetation cover of the land, i.e. there is a lower erodibility value where the vegetation is more dense, then there are anthropogenic activities (D'Ambrosio et al. 2019) that can have different effects depending on the type of land use (think for example of the cementation due to the industrial use of the land which will reduce the erodibility of the area, compared for example to land subjected to agricultural practices which will produce an increase of erodibility).

Also the drainage density (D), which correlates a linear property of a basin to an areal property, constitutes one of the most significant morphometric parameters for the quantitative evaluation of erosion in river basins; it is defined as the ratio between the total length of the river segments of a given basin $\sum (L)$ and the area A of the basin itself, $D = (\sum L)/A$. The drainage density is directly proportional to the intensity of the precipitations and the steepness of the slopes.

1.3 Sediment transport in Mediterranean watersheds

For what has been said so far, the key topic of the thesis work is the analysis and quantification of the sediment transport phenomenon in an intermittent river in the northern Apulia region, therefore we will provide the theoretical bases regarding "solid transport", coming from available literature sources.

Sediment Transport

The water, in its surface runoff process, dissipates energy by friction with the bed and the banks of the riverbed in which it flows, this energy under certain conditions, will be able to produce changes in the riverbed itself.

The movement phenomenon of sediments in the riverbed is generally linked to two aspects:

- Flow Characteristics: which, given the geometry of the river section and the discharge values, can be assessed through the well known laws of hydraulics.
- Sediment characteristics: in particular particle size distribution and cohesiveness.

Under the action of the hydrodynamic thrusts, the solid grains can be moved and transported downstream in different ways; We can recognize different transport mechanisms, the bed load transport, in which the grains move on the bottom of the riverbed, with rotational and / or sliding motions, more or less intermittent, from the phenomenon of suspended sediment transport, in which solid particles flow for long distances inside the current.

The different forms of transport are summarized below, proposing various formulations in the literature to highlight the relationship between flow characteristics and sediment characteristics, in the context of the transport problem.

Transpot mechanisms

The theoretical and experimental treatment of the phenomenon of sediment transport is relatively recent and mainly concerns the phenomena linked to non-cohesive materials (gravels and sands).

The hydraulic current of a watercourse, from the mobile bottom, may have the ability to detach the particles of the bottom and transport them for different distances, in particular, if the concentration of sediment in suspension is very low compared to the amount of water, solid transport can occur in two main ways:

- Suspended sediment transport: the solid particles move within the current, supported by its turbulent agitation and the transported material is generally the finest (clay, silt and sand);
- Bed load transport: the solid particles move by rolling or sliding on the bottom without ever abandoning it and the material transported is above all the coarsest (gravel, blocks). Another bed load transport mechanism is the so called by jumping or hopping, in which the particles proceed in successive sections falling on the bottom after abandoning it.

Incipient motion

The study of sediment transported by dragging on the bottom of the riverbed starts from the analysis of the conditions of incipient movements of solid particles.

To define the *limit of equilibrium* situation, also called *incipient motion*, we can start from those equations which generally include either the slope ic, or the discharge qc, which in this case assume the characteristic of "*critical*" conditions for the incipient movement

The incipient motion condition is therefore defined by an equation in which, in addition to the physical and geometric characteristics of the transported material (generally the diameter d), also the "critical" values of the motion variables appear.

A wide range of formulas and direct diagrams are proposed in the literature for the determination of the incipient movement conditions.

Here there are some formulas that are supposed to be the more expressive, either because they are recurrent in technical use, or because they are capable of interpreting experimental results in various conditions such as high slopes and coarse sediments:

Valentini's formula (1912), allows to calculate the critical slope (ic) for the incipient movement as a function of the degree of submergence (d / h) of the solid grains and their density Δ ($\Delta=\frac{\rho_s-\rho}{\rho}$, with $\rho_s = grain\ density,\ \rho = fluid\ density$):

$$i_c = 0{,}057\,\Delta\frac{d}{h} \qquad (2)$$

Bettes formula (1984), calculates the critical discharge (qc) as a function of the slope of the riverbed (i) and the characteristics of the solid grains (d):

$$\frac{q_c}{\sqrt{gd^2}} = \frac{0{,}134}{i} ln \frac{1{,}221}{i} \quad (3)$$

Bathurst *et al.* (1987) corrected this formula by changing the proportionality with i, also according to the different diameters of the solid grains (d):

$$\frac{q_c}{\sqrt{gd^2}} = 0{,}15 i^{-1{,}12} \quad (4)$$

$$\frac{q_c}{\sqrt{gd16^3}} = 0{,}21 i^{-1{,}12} \quad (5)$$

Finally, Graf and Suszka (1987), defined the condition of incipient movement through the index number φc (Index number of *Shields*, and can be interpreted as the relationship between the drag forces of the current and the stabilizing forces, immersed weight of the grains, $\varphi c = \frac{\tau * \rho}{g \Delta d}$, with τ = tangential stress on the bottom, directly attributable to the motion characteristics of the fluid current through τ = ρ * u ^ 2, with u = current velocity profile):

$$\varphi_c = 0{,}0042 * 10^{2{,}21} \quad (6)$$

Bed Load Transport

Once the threshold for the beginning of sediment movement has been determined, according to the characteristics of the overlying hydraulic current, the next step will be to determine the quantity of transported solid.

For bed load transport, we will overcame at different formulations, always given as a function of incipient motion and sediment characteristics respectively (this homogeneity of parameters will allow the coupling of formulations for the incipient motion with those for the quantification of the solid discharge), such formulations derive from the observation of the different types of movement of solid grains, which are sometimes considered complementary and not mutually exclusive:

Boundary layer of moving particles

Dragged by tangential forces, different thickness of solid particles are set in motion;

as depth increases, the solid layers are characterized by progressively decreasing speeds.

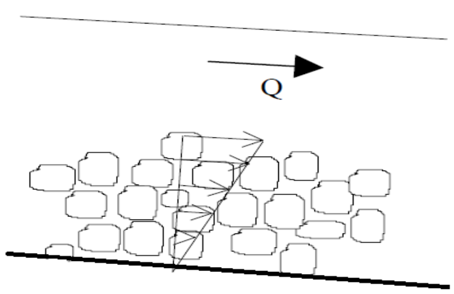

Fig.3. ***Boundary layer of moving particles***

Superficial motion

Only a surface layer of solid is considered to be in motion; the particles roll / crawl on the underlying ones that remain stationary.

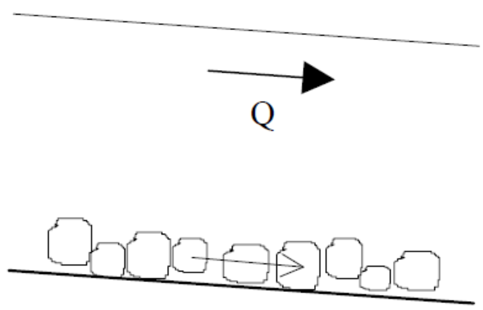

Fig.4. Superficial Motion

Bouncing

Particles motion is not schematized as a continuous phenomenon, but as a succession of finite "jumps" of the surface particles, followed by rest times.

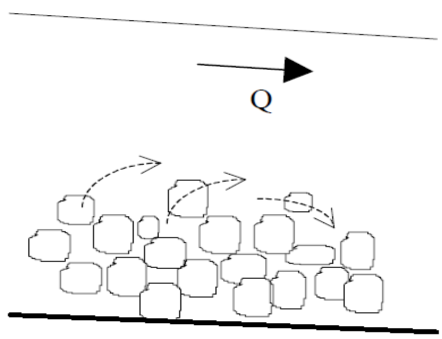

Fig.5. Bouncing

Starting from the different conceptual schemes, various formulas are determined that link the quantity of solid transported to the flow parameters, all of which lead to formulas of the type:

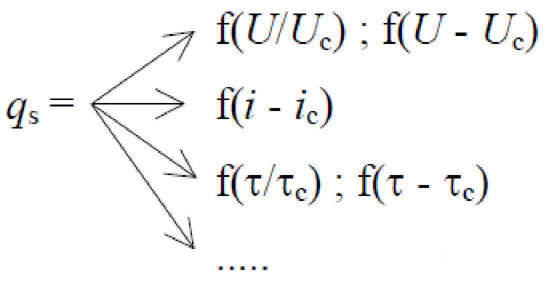

Fig.6. General structure of widely used bed load formulas

Solid discharge *qs* is often taken as dimensionless quantity, referring to the following index number:

$$\varphi = \frac{q}{\sqrt{d^3 g \Delta}} \qquad (7)$$

Following table summarizes some formulas widely used in literature to quantify bed load transport. These formulas must be used once exceeded the incipient motion threshold.

Schocklitsch (1962)	$q_s = \frac{2.5}{\rho_s / \rho} i^{1.5} (q - q_c)$
Bathurst *et al.* (1987) (Meyer-Peter e Müller modificato)	$\Phi = 8(\phi^* - \phi_c^\circ)^{1.5}$ $\phi^* = \frac{\rho u^{*2}}{\gamma \Delta d \cos\theta (\tan\beta - \tan\theta)}$
Suszka (1991)	$\Phi = 10.4\, \phi^{3/2} \left(1 - \frac{\phi_c^\circ}{\phi}\right)^{5/2}$
Meyer-Peter e Müller (1948)	$\Phi = 13.3 (\phi - \phi_c)^{1.5}$
Pezzoli (1979)	$q_s = d \sqrt{\frac{\tau}{\rho} \frac{2}{3}} \left(\frac{\tau}{\rho}\right)^{1/6} \left(\sqrt{\frac{\tau}{\tau_c}} - 1\right)^{5/3}$ $\tau = (\rho_s - \rho) g\, d\, \phi$

Tab 7. Bed load formulas widely used in literature

Having now available two different formulations, one that conceptually will tell us for which specific motion characteristics a certain range of solid grains will be handled and the latter which will allow us, once we are certain that we are above the afore mentioned critical thresholds to calculate the solid discharge, in the most appropriate way, When possible, the recommendation is to use homogeneous formulas with each other from both a conceptual point of view and from the source (or for the data on which they have been calibrated), in order to minimize the dispersion of the result.

Some possible combinations for the previously proposed formulas are listed below:

ABBINAMENTI	
Portata Solida	Incipiente Movimento
Schocklitsch	$\frac{q_c}{\sqrt{gd^3}} = 0.15 i^{-1.12}$
Bathurst et al.	$\phi_c^o = 0.047$
Suszka	$\phi_c^o = 0.0851\left(\frac{h}{d}\right)^{-0.266}$
Pezzoli	$\phi_c^o = 0.06\left(1 + 0.67\sqrt{\frac{d}{h}}\right)$ $\phi_c = \phi_c^o \cos\theta\left(1 - \frac{\tan\theta}{\tan\beta}\right)$

Fig.8. Possible combination of Incipient motion formulas and solid discharge formulas.

Although these formulas are useful in general cases and since there is no standard to refer for their use, some observations are still significant:

- The dispersion of results may be extremely high, beyond the obvious growing trend of qs with increasing q different formulas somewhat give scattered and variable values and gradients.
- When comparing the results, it is appropriate to consider the differences in the thresholds of incipient movement, when visible. Part of the dispersion of the curves is in fact attributable to a different assessment of the critical conditions.

Finally, we could conclude that, at least for relatively extreme situations, results will be susceptible to different approximations, related to different factors, this will make it difficult even to assess the order of magnitude of the phenomenon.

In reality, the possibility of estimating phenomena such as those under discussion must not be renounced, as long as you remember that the results must be evaluated on the basis of the approximations introduced, and with the awareness that, in the best of cases, it is possible to estimate the orders of magnitude connected to the phenomenon, and certainly not he precise values, moreover calculation models must necessarily be calibrated and validated with field values, they must be relative to precise watersheds or to comparable situations, Based on the historical data relating to the planimetric and altimetric evolution of the riverbed, the characteristics of the sediments, the solid volumes transported, it is necessary to choose the calculation model that proves to be most suitable for the specific situation and, if necessary, make reasoned corrections to the parameters relating to the current. and the sediments to be inserted in the model itself.

The main elements of choice and / or calibration are:

a) Grain size of the sediments, the characteristics of the cross sections, the resistance coefficient;

b) incipient movement threshold formula

c) solid discharge formulas.

Suspended sediment transport

For the calculation (the estimate) of the suspended sediment load, the starting point is made up of different theories for the evaluation of the concentration of solid particles suspended into the current. For this problem, two are the most used theories, respectively:

Dispersion-diffusion theory

It is based on the principle of " dispersed mass conservation ", considering the solid discharge as the sum of a diffuse flow and a convective flow; this derives from the fact that, assuming the solid particles as "suspended" in the liquid, then this system will behave as a two-phase mixture, therefore it will be possible to write a differential equation for the calculation of the concentration profile of solid particles:

$$w_s C + \varepsilon_s \frac{dC}{dy} = 0 \tag{8}$$

Eq. 8: first order differential equation with separable variables for the calculation of the concentration profile of the suspended solid particles

Terms have the following meanings:

w_s = falling speed of the solid particles in still water

ε_s = turbulent diffusion coefficient of the solid phase

C = concentration of solid particles transported in suspension

In it we can distinguish two terms, representative respectively: the flow of the particles that tend to settle (w_sC) and that of the particles that tend to be sustained due to the turbulent agitation ($\varepsilon_s dC$ / dy).

The integration of the equation for the determination of the concentration profile obviously requires knowledge of the distribution law of the turbulent diffusion coefficient of the solid phase, εs, along the vertical y.

Different solutions have been proposed for this equation, the most significant are reported:

Rouse (1987):

$$\frac{C}{C_a} = \left[\frac{D-y}{y}\frac{a}{D-a}\right]^{z_t} \quad (9)$$

Rouse (1987) solution for the evaluation of the concentration profile of the suspended particles.

Lane and Kalinske (1941):

$$C = C_a exp\left[-\frac{15w_s}{u*}\left(\frac{y-a}{D}\right)\right] \quad (10)$$

Lane and Kalinske (1941) solution for the evaluation of the concentration profile of the suspended particles.

In both we can highlight the presence of *D*, a term representative of the depth of the current and the coefficient *a* representative of the distance from the bottom, at which it is assumed that solid suspension transport begins, and *Ca* is the concentration at that altitude.

On *Ca* and *a*, it must be said that, in the presence of a moving bottom or coarse materials, the determination of the bottom itself is uncertain, therefore, the consequent determination of these parameters will take on a random character. Various theories have been proposed to solve the problem in the past, which depend substantially on the definition of *a* itself.

The ones that have found the greatest consensus are those of: Rouse (1937), Einstein (1950), Engenlund et al. (1976), and that of van Rijn (1984). For example, Rouse set the reference quota proportional to the water tie (a = 0.05D), while Einstein, considering the reference concentration as the concentration of the solid phase inside the bottom layer where the sediment transport occurs almost exclusively as transport at the bottom, assumed the height equal to twice the diameter of the largest particles and the concentration proportional to the solid discharge per unit of width of the bedload transport qb. Finally, Engenlund et al. and van Rijn expressed the concentration as a function of the mobility parameter of Shields and the average geometric diameter d50.

Gravitational Theory

The gravitational theory, introduced by Velikanov (1938), interprets the movement of solid particles within a two-dimensional, uniform and permanent current through an energetic approach. In fact, the basic hypothesis of the theory considers the loss of energy along a stream as the sum of an energy spent to overcome internal friction and an energy spent to continuously transport the particles upwards. The same author, later (Velikanov1954), assuming the solid phase separated from the liquid one and consequently the net vertical transport of both null, obtained the following expression:

$$C = C_a exp\left(-\int_a^y \frac{(y_s-y)w_s}{u\tau} dy\right) \quad (11)$$

Velikanov equation (1954) for the calculation of the concentration profile of the suspended solid particles from which the distribution of the concentrations along the vertical is obtained assuming a logarithmic law of speed and a linear law of tangential stresses.

Velikanov itslelf was criticized by the authors of the time and the biggest objection against his theory was the hypothesis of dealing separately with the solid phase and the liquid phase.

However, once known the vertical distribution of both the flow velocity "u" and the concentration "C", we will be able to calculate the suspended sediment discharge, per unit of width, simply by integrating on the water tie:

$$Qs = \int C * udy \quad (12)$$

02 – State of the Art

2.1 Hystorical data

Regard the Celone watershed, there are important historical data of turbid outflows, recorded in the years between 1965 and 1984, these data derive from a larger study carried out by PROGESA, of the University Aldo Moro of Bari.

In this regard, we need to highlight that, this study concerned the larger basin of the Candelaro river, of which the Celone is a confluent, furthermore, in this study, were taken turbidity records at San Vincenzo gauging station, downstream from Masseria Pirro gauging station.

However, the average sediment production evaluated in these studies, for the instrumented basin were around 200-220 t km^{-2}, these values will act as a reference in our studies, highlighting differences or similarities.

2.2 Monitoring Campaign

The monitoring campaign for the collection of data on which this work is based, was carried out by the IRSA staff of Bari, in the period of time between 1 July 2010 and 31 June 2011, 12 months in total.

The monitoring station was located at "Masseria Pirro", located about 8km upstream of the Torre Bianca reservoir, on the Celone river. Here, the riverbed has a regular, trapezoidal geometry.

This gauging station is the only one in the entire basin of the Candelaro river, of which the Celone is a sub basin, in which it is possible to carry out this type of measurement.

Fig.1. Gauging station for the continuous measurement of Q and discrete samplings of SSC

Measurement tools

The monitoring station consists of an ISCO Automatic sampler (model 6712FS; 24bottles; pumped volume 1l) inside it a data-logger is installed for data collection, the sampler is then connected to an ISCO-type flow meter 750 Area Velocity Flow Module.

The flow-meter allows us to measure the flow velocity (every 5 minutes) and the water tie, the measurement of the cross-sectional area is entered manually, the meter than proceeds to calculate the discharge in two steps, first calculates the wet section, area and subsequently, multiplying it by the velocity of the flow, calculates the discharge. These values are then averaged at 15 minutes intervals.

The sampler is made up of 24 bottles, for a total capacity of 1 liter per bottle, this sampler gives the possibility of sampling with different frequencies. In particular, there are two setting programs, with the first one IT takes samples at a regular time interval (monthly or fortnightly in the summer-autumn periods and one or two weekly samples for the winter and spring periods).The second setting allows us to create a sampling program according to the water tie, supplied by the aforementioned flow meter and connected to the sampler itself, the latter setting was therefore set to perform sampling with a frequency that varied from 15 min to 2 hours in correspondence with the flood events and therefore during the rising limb of the hydrograph, the frequency instead decreased during the falling limb, varying from 2 hours to 1 day.

This sampling strategy has been studied on the basis of the fact, that, as also known in the literature, for similar watersheds i.e. flashy and intermittent, most of the suspended sediment is conveyed during flood events (Alexandrov et al. 2007), hence the need is to detect these events.

The sampler was positioned so that it was submerged by the flow in accordance with the requirements of the US Geological service and in the centre of the riverbed section, having primarily verified that the lateral diffusion was sufficient to guarantee a homogeneous mix of suspended sediments in the sampling point, the total suspended solid concentration was than determined according to the standard analytical method APAt-IRSA (APAT-IRSA-CNR, 2002).

Sub daily data-set

Continuous measurements of discharge Q(t) and discrete measurements of Suspended Sediment Concentration SSC were ordered in a sub daily timeline to highlight minimum and maximum measured values of Q and SSC, also the seasonality variation in streamflow can be observed from the timeline (Fig xx).

23 different flood peaks can be distinguished, discharge values ranging from 0,36 m^3s^{-1} (14/07/2010), to 30,18 m^3s^{-1} (05/03/2011), the period of greatest frequency of flood events is between November and June, corresponding to the wet season. The dry season instead goes from June to October, when few flow events occurred.

The suspended sediment concentration samplings (CSS), for what has been said regarding the sampler setting, were more frequent during the floods, less frequent during driest periods, for them we observe a variation ranging from 0.005g l^{-1} to 37,6g l^{-1}.

Further observations of the sub-daily data set will be made during 4th chapter, were through a multivariate event-based analysis we will discuss about drivers of SS transport.

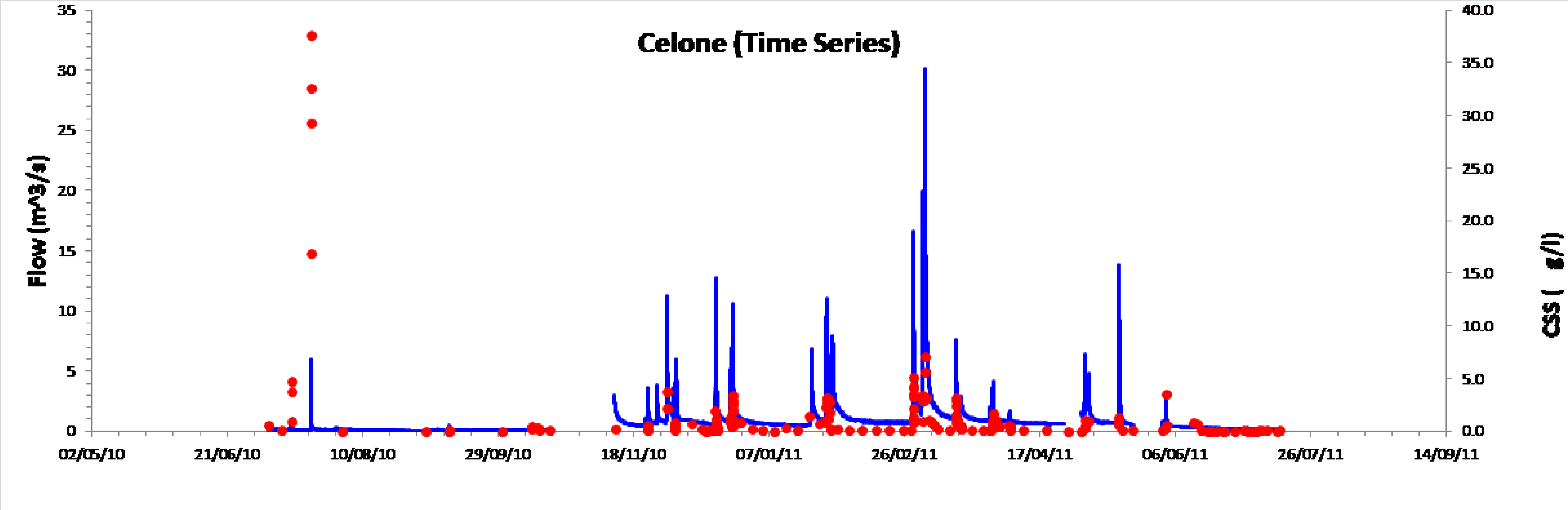

Fig.2. Sub daily time series of continuous measurements of Q [m3/s] and discrete sampling of SSC [g/l]

Daily data-set

In the 5th chapter the methodology through which the specific sediment production of the basin scale was estimated, required the use of data in daily format, both for the discharge Q and for the suspended sediment concentration CSS, therefore, we proceeded with the calculation of these values:

$$Q(daily) = \sum_{i=1}^{96} (q_i * 15 * 60)/86400 \qquad (1)$$

Where, qi is the instantaneous discharge measured every 15 minutes, 96 are the quarters of an hour that make up a day, 86400 are the seconds in a day. For the suspended sediment concentration, the daily equivalent was calculated, using the following formulation:

$$CSSeq = \frac{1}{VOL_{daly}} \sum_{i=1}^{n} \frac{(C_i + C_{i+1})}{2} * V_i \qquad (2)$$

Where: VOLdaily is the instantaneous volume of fluid transited in the time interval ts (start) -tf (end) of the measurement, Ci and Ci + 1 are two successive measured concentrations.

Vi is the fluid volume transited in the interval between Ci and Ci + 1.

In this way, we pass from a number n of observations made at sub-daily stage to a single equivalent daily concentration value, therefore to "sampled days".

These operations could lead the data set to no longer be representative of the specific behaviour of the streamflow, as this type of "intermittent" rivers are characterized by sudden floods, the so-called flash floods which therefore could hardly be compressed on a daily basis without losing characteristic information. This loss of characteristics will however be verified by the graphical comparison with the sub-daily dataset.

These transformations led to a compression of the data set at 365 daily discharge values and 88 equivalent daily concentration values, from figure 7, we can now highlight that the range of variation, for the average daily flows is between $0.004 < Q < 16.51 m^3 s^{-1}$, while the concentration range varied now between 0 < CSSdaily-eq < 6 mg l^{-1}.

Although the temporal distribution of the flood peaks and the values of the related CSS is comparable to the previous one, the effect of reducing the concentration peaks that had the transformation into a CSS equivalent daily can be observed, if in fact, looking at the first timeline, the peaks of CSS that reach about 37 mg l^{-1}, in the daily timeline remains contained around 0-10 mg l^{-1}, the same behaviour occurred with the discharge, while for the instantaneous ones peaks of 30,18 $m^3 s^{-1}$ were observed, now maximum values is around 16 $m^3 s^{-1}$.

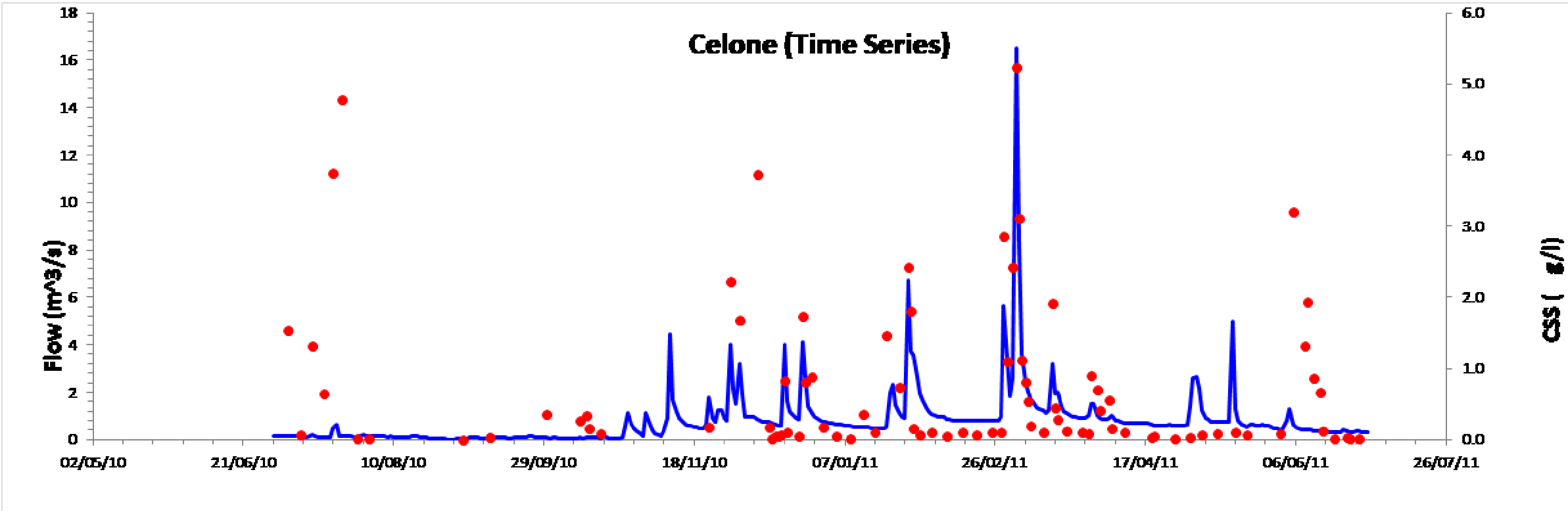

Fig.3. Daily time series of evaluated average daily Q [m3/s] and daily load SSC [g/l]

De Girolamo et al. 2018, Catena 165, 442-453

03 – The "Load estimation problem"

Abstract

Sampling strategies and methods used for estimating load can lead to large uncertainties in suspended sediment transport quantification, especially in rivers with a high variability in streamflow. The aim of this chapter is to evaluate suspended sediment load, using a number of direct estimation techniques, in order to find a suitable method for temporary river systems, and to assess the uncertainty associated with load estimation, due to the specific method applied. One year of continuous measurement of flow, and discrete sampling (n = 216) of suspended sediment concentrations, taken from 2010 to 2011 in the Celone River (SE, Italy), were used to estimate annual load. Averaging, ratio, and regression estimator methods were applied to the entire dataset, and to subsets of data, to calculate load. The results show a wide range of values, from 220 to 1123 t km^{-2} yr^{-1}, with respect to the applied suspended sediment load estimation techniques. Averaging methods resulted biased. Sediment rating curves underestimated load, while, if the back-transformation bias correction was used, load was overestimated. The ratio methods generally overestimate load. Increased precision and accuracy was achieved through applying data stratification, based on flow regime and seasonality. After applying three different flow regime stratifications, the annual load ranged from 240 to 606 t km^{-2} yr^{-1} and, using seasonal stratification, from 258 to 974 t km^{-2} yr^{-}

Key words: Temporary stream
Suspended sediment load
Load estimation techniques
Stratification of data
Uncertainty

[1]. It seems that ratio estimator methods, and the regression equations applied to the stratification on a flow regime basis, are more suitable for estimating load in temporary, flashy streams.

3.1 Introduction

Most of the river basins influenced by the Mediterranean climate are affected by erosion and soil degradation. During the last few decades, there has been a significant increase in studies of erosion (de Vente et al., 2009), sediment transport dynamics (Gentile et al., 2010; Bisantino et al., 2010; Gallart et al., 2013; Regüés and Nadal-Romero, 2013; García-Rama et al., 2016; López-Tarazón and Estrany, 2017; Kheirfam et al., 2017), and load estimation methodologies (Letcher et al., 2002; Tabatabaei et al., 2014). Several models have been developed for quantifying soil erosion by water and wind, which have been applied on regional (Kirkby et al., 2008; Panagos et al., 2015; Vigiak et al., 2017) and basinal scales (Abouabdillah et al., 2014; Bagarello et al., 2017; Ricci et al., 2018). Sediment load quantification is an important task in river basin management, as it provides the order of magnitude of soil loss. It is also fundamental in evaluating reservoir siltation, and the consequent loss of water reservoir capacity (Vericat and Batalla, 2006), and is necessary for calibrating models used to estimate erosion and sediment load. On the other hand, hydrological and sediment regimes are the basic drivers of water quality (Larned et al., 2010) and river ecosystems (Arthington, 2012; Wohl et al., 2015), and an accurate load estimation allows us to understand the impacts of anthropogenic activity on rivers. Sediment load, transported in a certain time interval through a section of river, is quantified by integration of instantaneous flux, which is the product of suspended sediment concentration (SSC) and discharge (Q). This simple equation, in several cases cannot be applied, due to limited data availability. In a number of basins, at the most, measurements of streamflow are available on a daily time-scale, whereas SSC measurements are generally taken on a weekly or monthly basis (De Girolamo and Lo Porto, 2012). Hence, to calculate sediment load, it is necessary to estimate the concentrations for those days when no measurements are available. This is the so-called "load estimation problem" (Lee et al., 2016). Several direct techniques have been developed for estimating suspended sediment load by using infrequent samples of SSC and continuous measurements of Q (Asselman, 2000). The characteristics of the dataset (i.e. number of samples), the dimensions of the river basin, and the flow regime, play an important role in choosing a 'good' estimation technique, although every method has its limitations and bias rate.

The most common methods are grouped into: averaging estimation techniques (Walling and Webb, 1988), ratio estimation techniques (Beale, 1962), and regression estimation techniques (Horowitz, 2003). Recently, new regression techniques have been developed that relate observed SSC to streamflow, or other variables (i.e. time, season) (Hirsch et al., 2010); the estimated daily concentration is then multiplied by daily streamflow to obtain load. Although a number of studies have analysed aspects concerning load estimation, few of them have focused on the 'load estimation problem' in temporary river systems. The extreme variability of the hydrological regime, which characterises temporary streams (Oueslati et al., 2015; De Girolamo et al., 2017a; De Girolamo et al., 2017b), involves objective difficulties in the continuous measurement of SSC (De Girolamo et al., 2015a; Wohl et al., 2015) and, at the same time, implies a high degree of uncertainty in the evaluation of suspended sediment load.

In this context, the first objective of the present paper was to estimate suspended sediment load in the Celone River (SE, Italy), a typical temporary river, by using methodologies commonly applied to perennial rivers. The second objective was to identify a technique able to improve the accuracy of load estimations, reducing the uncertainty interval that can be applied to a temporary river system. Finally, by means of uncertainty analysis, we aimed to quantify the degree of confidence that users can assign to a given load estimation method. Our final aim was to provide a guideline for watershed managers for selecting methods of sediment load estimation, and to contribute to improving the understanding of the "load estimation problem" in watersheds influenced by Mediterranean climate.

3.2 Materials and Methods

The Study Area

The study area is the Celone River basin, located in northern Apulia (SE, Italy). The area of 72 km^2 drains into the Capaccio Reservoir, characterised by a full capacity of 25.82 Mm^3 (in May 2016, the filled volume was 16.8 Mm^3). In the mountainous area, characterised by steep slopes, and in a phase of accentuated erosion, the river channel is incised, and a large amount of suspended and bed load material is transported. Throughout the mountainous area, many check dams have been built to reduce bank erosion. The main channel assumes a shape of twisted channels in a flood plain, where most of the coarse material is deposited, and then continues with a meandering pattern. The drainage network of the basin assumes a dendritic pattern. The main river channel is about 24 km long, and the entire drainage network is about 80 km long. The main lithological units are flyshoid formations (flysch della Daunia) and grey-blue clays in the upper part of the basin, and alluvial deposits in the valley. The main soil types are classified as typic-haploxerroll, vertic-haploxeroll, and typic-calcixeroll, according to the US Department of Agriculture classification. The soils in the basin have a composition related to the lithology, and show a variable texture (clay, clay-loam, and sandy-clay-loam). The depth and soil physical and hydrological characteristics are highly variable; in the flat part of the basin, soils are deep (1.5–2 m), while in the hills and mountains, they are moderately deep (< 1 m).

The area is an agricultural basin; the main cultivations are cereals (mostly winter and durum wheat; 45%), sunflower (9%), pasture (6%), and olive groves (8%). Minor land uses (2%) include vegetables and vineyard. Forests (29%), mostly oaks and conifers, are present in the upper part of the basin. Urban areas (1%) are limited to three small villages; therefore, the human pressures contributing to soil erosion in the area are agricultural practices, especially conventional tillage that involves multiple operations with chisel plow and disks. In autumn and winter, most of the agricultural areas are not protected from erosion (seeded and ploughed fields for spring crops). The erosion is favoured by up and down tillage, which is employed in the mountainous and hilly parts of the basin. The erosion processes in the area are both distributed (sheet erosion) and localised (rill erosion). Erosion of the banks is also an active process. The climate in the Celone Basin is typically Mediterranean; rainfall events are mainly concentrated in winter and spring, and frequently occur for short durations and at high intensity. Precipitation also shows a high spatial variability, with events localised in small areas. The rainfall regime has a great influence on the flow regime of the Celone River, which is characterised by periods of intermittency of flow and flash floods and, consequently, on erosion and sediment transport. In the period 1960–1996, the average annual precipitation amount to 792 mm in the mountainous area (Faeto; 860 m a.s.l.), and 623 mm in the lowland area (Troia; 350 m a.s.l.). Mean temperature varies between 3.4 °C (January) and 20.3 °C (August) in the upper part, and between 7.2 °C (January) and 25.5 °C (August) in the valley (De Girolamo et al., 2015b; De Girolamo et al., 2017a).

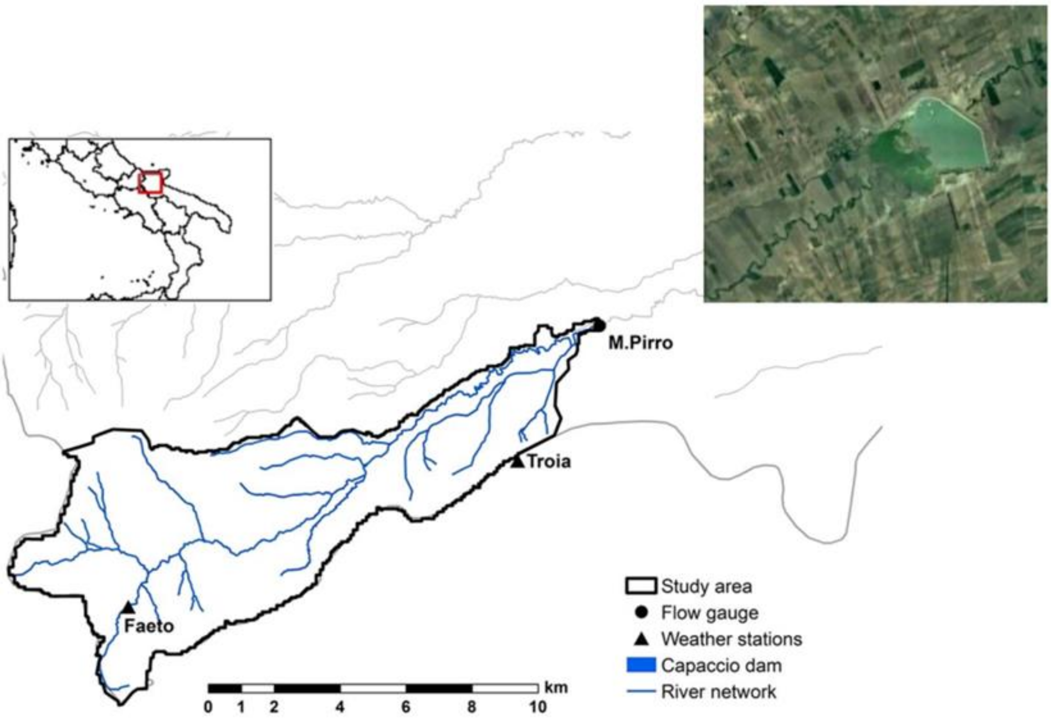

Fig.1. Study area, The Celone river basin

Time period	Rainfall (mm y-1) Faeto	Rainfall (mm y-1) Troia	Discharge[e] (mm day)		
			Min	Max	Mean
2010-2011	1140	638	0,005[c]	19,810	0,960
1960-1991	792[a] ± 135[b]	623[a] ± 110[b]	0,000[d]	19,230	0,417

a Mean value.

b Standard deviation.

c Masseria Pirro gauge (drainage area 72 km^2).

d S·Vincenzo gauge (drainage area 86 km^2).

e Mean annual flows normalized to the corresponding drainage area.

Tab.1. Basic hydrological data recorded in the catchment

Field data: Streamflow and suspended sediment concentration

From July 2010 to June 2011 (12 months), continuous measurements of streamflow, and infrequent measurements of SSC, were recorded at the Masseria Pirro gauging station, 8 km upstream of the Capaccio Reservoir (Fig. 1). An ISCO automatic sampler (model 6712FS; 24 bottles; pumped volume 1 L) was installed in the gauging station, which is connected to an ISCO 750 Area Velocity Flow Module, in order to have continuous measurements of the streamflow. Two sets of programming were used. The first one lets us set up time-spaced samplings. With this standard program, periodic samples were taken at fortnightly or monthly time intervals during summer and autumn periods, and once or twice a week from November to June. The second set lets us create complex programs for flood sampling applications. We adopted a sampling strategy triggered by water level changes during the rising limb of hydrograph and flow rates during the flood recession. During flood events, the time-interval was between 15 min and 2 h in the rising limb and between 2 h and 1 day in recession limb. With this sampling program, a large number of samples were collected over the study period (n = 216), covering all hydrological conditions (flood, normal, and low flow). The SSCs were analysed in a laboratory, using the APAT-IRSA analytical standard method (APAT-IRSA-CNR, 2003). Standard 0.45 µm pore-diameter cellulose filters were used to filter the samples, to quantify the total suspended concentration. For additional details concerning the gauging station and sampling, please refer to

De Girolamo et al. (2015a). The study period is representative of historical hydrological conditions in the basin (Table 1). We verified that rainfall recorded in two gauging stations was 43% and 2.4% higher than historical data (from 1960 to 1996). Whilst, the most relevant flood events are comparable to the major events recorded in the past at San Vincenzo gauge, an old station located 8 km downstream the new one (Masseria Pirro) (recurrence interval of 30 years).

Load estimates

The flux of sediment passing through a cross-section of a stream during a predetermined time-interval can be expressed mathematically by the relationship (Eq. 1):

$$L = \int_{t1}^{t2} Q_t SSC_T dt \qquad (1)$$

where Qt is the streamflow (L s−1) at time t, SSCt is the SSC (mg L−1) at time t (s), and L is the load (mg). To apply this relationship, it is necessary to know how discharge (Q) and SSC vary over time. When the measurements of SSC are discrete, as in this case, a relationship describing the variation of concentration over time, between two consecutive measurements, SSC(t), is needed. To this end, several load estimation techniques were developed, providing total load. The most common are grouped as follows:

(i) Averaging estimator methods

Commonly called interpolation or integration methods (Tennakoon et al., 2007), the averaging estimator methods (Av) are generally variations of the following two simple approaches. A first approach involves all the available measurements (flow and SSC) multiplying the average SSC by the average flow based on all days of the year to obtain an "average" daily load, which is then converted into the annual total load. The second approach involves multiplying the average SSC over a specified time period by the mean daily flow computed for those days when SSC measurements are taken to obtain a succession of estimated loads. Thus, the method "annual mean sample concentration-mean flow averaging" (A_AvCmFd, Eq. 4 in Appendix A) includes all the available measurements, hence, the mean daily flow is computed on all sampled flow (N = 365 values) and the mean SSC on days when concentration are taken (n = 81). The method "annual mean sample concentrationmean sample flow averaging" (A_AvCmFm, Eq. 2 in Appendix A) includes data only when both variables (SSC and flow) are measured (n = 81). In both these techniques, average daily SSC and average flow are determined separately. Finally, the calculation of load is carried out by multiplying these averages, and summing them up, for the examined time-interval. In the method "annual sample concentration-sample flow averaging" (A_AvCsFs, Eq. 3 in Appendix A), the load is first determined for those days when both variables are measured and then extended to the study period. In the method called "annual flow weighted mean concentration", the mean daily load, estimated by using only data from days when both variables are taken, is weighted by a factor which is the ratio of mean annual flow (N = 365) and mean sampled flow (n = 81) as reported in Appendix A (A_FWMC, Eq. 5).

(ii) Ratio estimator methods

The ratio methods are usually made up of two factors. The first factor is the same in the presented methods and corresponds to the biased load average value. Such factor is computed as the total annual flow multiplied by the ratio of the mean load value over the mean flow value. The second one is called correction factor (Tennakoon et al., 2007) and is meant to correct the bias introduced from estimating the population parameters (covariance and variance) from the sample. The most common correction factors are the Beale's factor (A_RtoBea, Eq. 8 in Appendix A, Beale, 1962) and the Kendall's correction factor (A_RtoKen, Eq. 7 in Appendix A, Kendall et al., 1983). Differently from load average values, the correction factor changes through the two formulas. In the Beale estimator method, the covariance of the bivariate sample distribution is estimated from the observations and standardized by the sample variance of flow. The Kendall correction factor is easier and contains the difference between the mean load and the product between concentration and flow averaged.

(iii) Regression estimator methods

The regression estimator methods (SRC) define an empirical relationship between Q, which is the independent variable, and SSC, which is the dependent variable. The relationship, called the suspended sediment rating curve, is a power function, derived by a log-transformed least-squares regression (Phillips et al., 1999) (Appendix A). In this formulation, a correction factor has to be introduced, since the final result of the log-transformed regression method is required in the original units, and the back-transformation leads to an underestimation of concentration and, consequently, to a bias (Ferguson, 1986). In the present work, to improve the SSC-Q log-transformed linear relationship, we applied the Duan (1983) retransformation factor, defined by Eq. 2, and called a 'smearing estimator' (CF). It does not require any assumption about the distribution of residuals.

$$CF = \frac{\sum_1^N 10^{\varepsilon i}}{N} \qquad (2)$$

where: εi = log (SSCi) − log (SSC'i) are the residuals, and N is the number of observations. Taking into account the large number of samples, and that the sampling strategy adopted in the Celone River included both regular sampling and floods, as suggested by Tan et al. (2005), we assumed that all of the methods were appropriate to be used for load calculations. Appendix A summarises the methods and equations used in the present study.

The GUMLEAF v0.1alfa model (Generator for Uncertainty Measures and Load Estimates using Alternative Formulae: Tan et al., 2005) was used to calculate load, by averaging and ratio methods.

Data Analysis

Simultaneous measures of streamflow and concentrations were used to define the sediment rating curves (n = 216 samples) with which the SSCs were computed for a subsequent load calculation. Meanwhile, daily values of streamflow and concentrations (n = 81) were used in the Av and Rto methods. In particular, for ordinary flow conditions, the instantaneous value of the SSC was considered as a mean daily value; meanwhile, for flood events, sub-daily data (minimum three measurements) were processed into daily data by using Eq. 3 to calculate daily load:

$$DailyL = 0{,}9\ \sum_{i=1}^{96} q_i C_{int} \qquad (3)$$

Where:
DailyL is the daily load (kg);
qi is measured streamflow (m3 s−1) at time t (1, 2, …, 96) (flow measurements were taken every 15 min, hence, 96-time intervals were recorded in a day);
Cint is the measured, or interpolated, concentration (mg L−1) at time t (1, 2, …, 96), 0.9 is the time-interval (15 × 60 = 900 s) over which the load was calculated, divided by the conversion factor (1000−1), between the different units used in the equation.
By dividing daily load by daily total discharge, and including the unit conversion factor, a mean daily concentration value of suspended sediment was obtained during floods.

Using Data Stratification

It is well known that stratification of an entire dataset into homogeneous subsets (strata) can be a suitable method to reduce bias in the load estimations (Cooper and Watts, 2002). To understand, in depth, how both discharge and seasonality of the hydrological regime influence the evaluation of load, we applied different types of stratifications to the entire dataset, based on flow regime and on seasonality.

The flow regime stratification is based on the assumption that the hydrological regime is the most important driver in suspended sediment transport (De Girolamo et al., 2015a), and that the most relevant part of the suspended load is moved during floods. Based on this assumption, the entire dataset was divided into three subsets, corresponding to three classes of flow identified on the flow duration curve: high, normal, and low flow. The flow duration curve explains the flows of various magnitudes, and the percentage of times river flow exceeds a specified value (Fig. 2).

We analysed three different stratifications, on the basis of flow regime, as follows: R_1 (0–5–70–100%); R_2 (0–10–70–100%); and R_3 (0–20–70–100%). The class of high flow changes in the three stratifications while the class of low flow is fixed within the range of 70–100% of time exceedance for all stratifications. This is because the flow duration curve shows a flex point at 70% of exceedance frequency, demonstrating a change in streamflow regime.

On the other hand, this range is generally used for designating low flows (Smakhtin, 2001). Classes within the range 0–5, 0–10%, and 0–20% of the time exceedance were designated as high flow for R_1, R_2, and R_3, respectively. As Table 2 shows, the coefficients of variation (CV) for SSC assume high values, especially for the high flow classes. The stratification R_3 shows the lower values of CV, both for normal and high flow.

	Exc. Freq, R_3 (%)	CV	Exc. Freq, R_2 (%)	CV	Exc. Freq, R_1 (%)	CV
High Flow	0-5	225	0-10	242	0-20	251
Normal Flow	5-70	185	10-70	213	20-70	243
Low Flow	70-100	109	70-100	109	70-100	109

Tab.2. CV of SSC for each subset of data identified on the basis of flow regime

The seasonal stratification (S_1) was made by dividing the entire dataset into two subsets: the wet season, from October to March, and the dry season, from April to September. Applying seasonal stratification, the correlation between streamflow and SSC is 0.26 for the wet season, and 0.24 for the dry season, and the CV of measured SSC is 247% and 259% for the dry and wet season datasets, respectively. The low correlation values garnered with such kind of stratification should not be surprising. In fact, such index is particularly sensitive to outlying values which populate both wet and dry subsets as confirmed by the high CV.

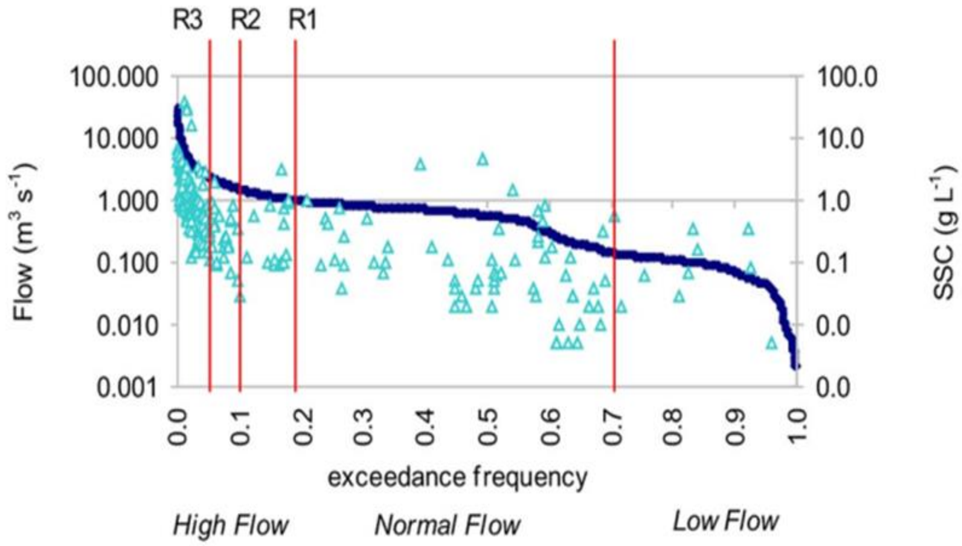

Fig.2. Flow duration curve and SSC. Stratification R_1: 0 ÷ 20% of exceedance frequency identifies high flow, 20–70% is normal flow, and 70–100% is low flow. Stratification R_2: 0 ÷ 10% of exceedance frequency identifies high flow, 10–70% is normal flow, and 70–100% is low flow. Stratification R_3: 0 ÷ 5% of exceedance frequency identifies high flow, 5–70% is normal flow, and 70–100% is low flow

Uncertainty

Experience has shown that uncertain information can adversely affect the decision-making process, and that awareness of the degree of reliability of information collected, in order to make a rational decision, is a key element in any management field. To cope with uncertainty, concepts have been introduced, such as the confidence levels associated with the available information, and suitable metrics to measure that. In simple words, uncertainty represents, in general, the lack of exact knowledge, irrespective of its causes (Refsgaard et al., 2007). In more detail, uncertainty can stem from many causes, or better, can be traced back to many sources. A first source of uncertainty arises from errors in the measurements; they can be systematic or accidental.

In the first case, it is relatively easy to clean the data, because the error is uniform, namely a constant or functional drift, and consequently it can be corrected with a small amount of algebra. Conversely, random errors, missing data, unrepresentative sampling techniques, or inaccurate scaling assumptions can be managed as random events, normally distributed (Taylor and Bunn, 1999), with a zero mean. The second uncertainty source is inherent in data variability, and so it can be considered a natural form of uncertainty.

This is generally accounted for by means of metrics, such as variance, or standard deviation. Finally, the last uncertainty source comes into play whenever there is a lack of knowledge about the right model to be applied during data processing. In this case, there can be several different models, all equally legitimate for the processing stage, each providing quite different results, but all equally plausible. This case is usually addressed by means of Monte Carlo-based methods. In the present work, the software GUMLEAF (Tan et al., 2005) has been applied to estimate the uncertainty associated with the computation of annual load. Such software applications are capable of accounting for only two kinds of uncertainty source, namely the inherent (or natural) uncertainty, and the knowledge uncertainty. For each load estimate, to account for knowledge uncertainty, one method out of 22 (Av and Rto methods, annual, seasonal, and regime stratification; see Appendix A) is randomly selected, by applying a Monte Carlo simulation, each method having an equal probability of being selected. The result of this simulation provides the mean and the variance for the method under consideration. Then, natural uncertainty is considered by assuming the load is normally distributed around the mean, and a load estimate is simulated by generating a normal random variable, with the mean and variance of the selected method.

3.3 Results

Hydrological regime and seasonality

The hydrological regime of the Celone River has a great influence on suspended sediment transport, with SSCs following the pattern of streamflow. The correlation between measured streamflow and SSC is 0.81 ($p < 0.01$), and the coefficient of determination ($R2 = 0.66$) indicates that 66% of variance of SSC may be explained by streamflow, while 34% is accounted for by other factors, such as rainfall intensity and its spatial distribution, vegetation cover, and soil management.
The highest value of SSC (37.6 g l^{-1}) was recorded during a flash flood event (21st July 2010) that occurred after a dry period, characterised by an extremely low streamflow (Fig. 3). During the wet season, when floods are frequent, SSCs assume a wide range of values. Flood events generally showed a relatively short duration (less than one day), and the hydrograph exhibited a rapid rising limb, with relevant differences between average daily flow (Qday) and instantaneous peak values (Qt) (De Girolamo et al., 2017b). A detailed analysis of the suspended sediment dynamics,

temporal variability of streamflow, and SSCs is reported in De Girolamo et al. (2015a).

Sediment rating curves

The sediment rating curves were developed as a log-transformed linear equation, and applied with and without the Duan's bias correction factor (CF) of the retransformation. Table 3 shows the correction factors for each subset of data for the three stratifications, based on flow regime, and for the two seasonal subsets, while the CF for the entire dataset was 1.7. The values assumed for normal flow are higher than those related to high and low flow.

This can be explained by the fact that CFs depend on the similarity between the SSC observed and predicted values. When the subset is very homogeneous (low standard deviation) predicted values tend to be very similar to the observations, and consequently the residuals are very small. A similar reason can explain the magnitude of the CF value related to the wet subset.

The sediment rating curves were built for the entire dataset, and for the above-mentioned data stratifications (Fig. 4). By using these equations, suspended sediment concentration values were estimated on a time interval of 15 min than load was computed with Eq. 1.

	R_1	R_2	R_3	Dry	Wet
High Flow	2,2	2,12	2,04	2,07	7,84
Normal Flow	3,13	3,62	4,69		
Low Flow	1,24	1,24	1,24		

Tab.3. Duan's bias correction factor (CF) for each group of data, stratified on the basis of hydrological regime, and on a seasonal basis

Comparison of load estimation techniques

Using the entire dataset

By using the entire dataset (prefix "A_" in Appendix A and Fig. 5), the annual sediment load assumes values that are very dissimilar, depending on the method used for the computation. As Fig. 5 shows, the magnitude remains in the range of 2.2 t ha^{-1} yr^{-1} (A_Src) to 11.23 t ha^{-1} yr^{-1} (A_AvCsFs). The averaging methods applied by using the entire dataset (prefix "A_Av" in Fig. 5 and Appendix A) show the highest variability ranging from 2.65 t ha^{-1} y^{-1} (A_AvCmFd) to 11.23 t ha^{-1} y^{-1} (A_AvCsFs), with a standard deviation of 3.6. The methods called A_AvCsFp and A_AvCmFm estimate 10.37 t ha^{-1} yr^{-1} and 4.96 t ha^{-1} yr^{-1}, respectively.

Conversely, annual load estimated by using Rto methods (prefix "A_Rto" in Appendix A and Fig. 5) show similar results, from 5.99 t ha^{-1} y^{-1} (A_RtoSim) to 6.07 t ha^{-1} y^{-1} (A_RtoKen) with a St. Dev. = 0.08. Loads estimated by the sediment rating curves, log-linear equations without and with CF (prefix "A_Src" in Fig. 5 and Appendix A), applied on a 15 min time-scale, show an intermediate variability, ranging from 2.20 t ha^{-1} y^{-1} to 3.7 t ha^{-1} y^{-1}, which are lower than the estimates computed with averaging and ratio methods.

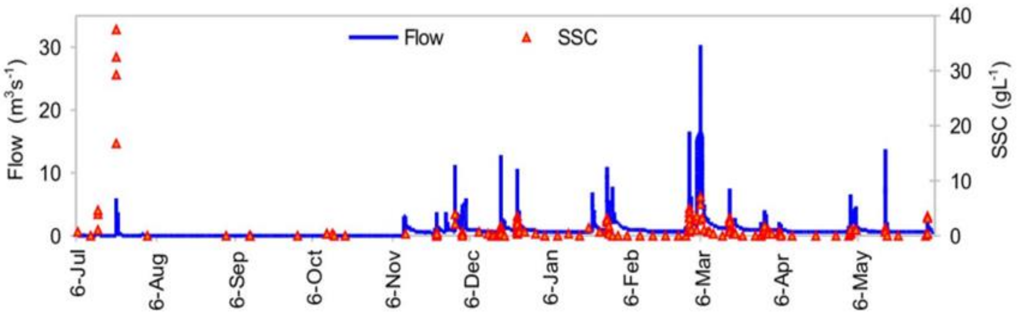

Fig.3. Streamflow Q [m3 s−1] and suspended sediment concentration SSC [g1 L−1] measured at the Masseria Pirro gauging station, July 2010 to June 2011

Using subsets of data on hydrological regime and seasonal basis

Stratification of the entire dataset into three subsets, based on flow regime (methods with the prefix "R_" in Appendix A,), led to an improvement in the precision (lowering of the variance) of the load estimations (Fig. 5). In particular, R_3 (0–5–70–100% exc. freq.) estimated an annual load ranging from 2.61 to 6.06 t ha^{-1} y^{-1}, whilst for the stratification R_2 (0–10–70–100% exc. freq.), loads are included in the range of 2.55 to 5.78 t ha^{-1} y^{-1}, and for the R_1 stratification (0–20–70–100% exc. freq.), the load ranges from 2.40 to 5.20 t ha^{-1} y^{-1}. The method called 'annual sample concentration - sample flow averaging' (A_AvCsFs, described in Appendix A) shows the highest reduction in variability in annual load estimation, passing from 11.2 to 5.90 t ha^{-1} y^{-1} (R_1_AvCsFs; Fig. 5), and 4.7 t ha^{-1} y^{-1} (R_3_AvCsFs in Fig. 5), when applying the stratification on the basis of hydrological regime.

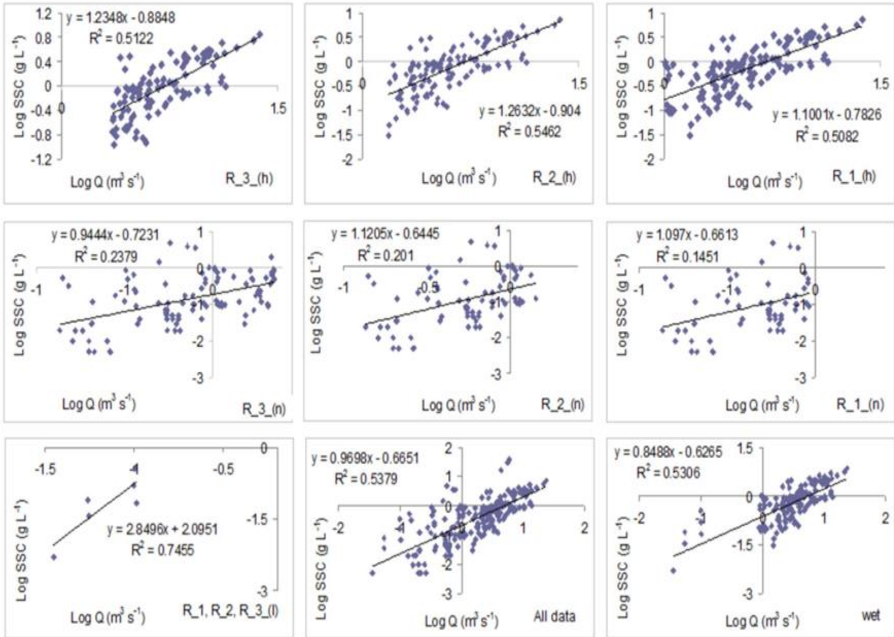

Fig.4. Model fitting stage of curve sediment rate. At the top, the model fitted for high-flow (h) related to the R_3 (0–5% exc freq), R_2 (0–10% exc freq), and R_1 (0–20% exc freq) stratification. In the middle, the model fitted for normal flow related to the R_1, R_2, and R_3 stratification. At the bottom, the model fitted for low flow (70–100% exc freq.), for all data, and for the wet season.

The Rto methods (described in Appendix A) give annual load values in a restricted range, from 4.19 (R_3_RtoSim) to 4.89 t ha^{-1} y^{-1} (R_1_RtoBea), with a reduction of about 1.1–1.8 t ha^{-1} y^{-1}, depending on the stratification respect to the values obtained with the entire dataset (Fig. 5). Sediment rating curves developed for the subsets of data divided on flow regime stratification show an increase in values (Src in Fig. 5). The stratification on the basis of flow regime works well for all the methods, creating a convergence of the estimates towards the true value. These results indicate that annual load estimated using the sediment rating curve, applied to the entire dataset, was underestimated, while it was overestimated with the averaging method "A_AvCsFs", and with all the ratio/Rto methods (Fig. 5).

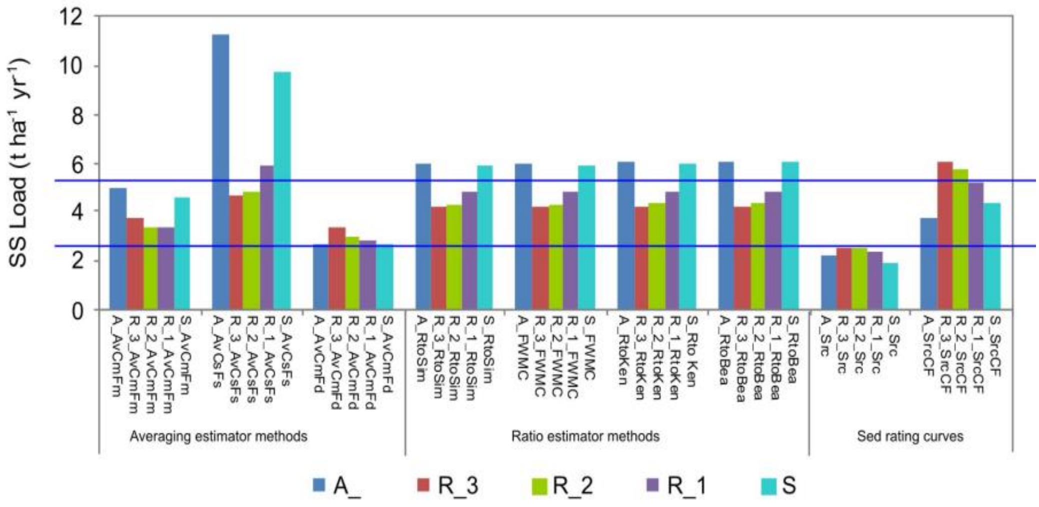

Fig.5. Annual suspended sediment load, estimated with different methods by using the entire dataset (A_) and subsets of the data (R_1, R_2, R_3; and S). Flow regime stratifications: R_1(0–20–70–100% exceedance of frequency); R_2 (0–10–70–100% exceedance of frequency) and R_3 (0–5–70–100% exceedance of frequency). Seasonal stratification: S. Horizontal bluelines identify the interval that includes the true value. (For interpretation of the references to colour in this figure legend, the reader is referred to the web version of this article.).

The seasonal stratification adopted in the present study, dry and wet periods, shows a limited increase in the precision of annual load estimates, less significant than that obtained via applying stratification based on the flow regime. Indeed, as Fig. 5 shows, all the averaging methods show results very close to those obtained using the entire dataset, ranging from 2.62 (S_AvCmFd) to 9.74 t ha^{-1} y^{-1} (S_AvCsFs).

Similarly, load estimates obtained using the Rto with the seasonal stratification are not dissimilar from the values obtained without data stratification. For the sediment rating curves, the seasonal stratification does not work in increasing the accuracy, predicting the values 1.92 (S_Src) and 4.42 t ha^{-1} y^{-1} (S_Src_CF), without and with CF, respectively.

Flood and high flow contribution to annual load

By using the sediment rating curves, log-linear with and without CF, we estimated suspended sediment load transported in high, normal, and low flow conditions (Table 4). As expected, the majority of the sediment load is transported in high flow conditions: 94, 89, 86%, for R_1, R_2, and R_3, respectively. The low flow contribution to the annual load is very low (< 1%). Therefore, when the correction factor was used in the load calculations, the results are more than doubled, with a slight reduction of the percentage for the high flow class, and an increase for the normal flow. A comparative analysis of measured and generated suspended sediment load for the highest flood event (4–7th March; Fig. 2) shows that the actual load is underestimated by the log-linear equation.

Flow Stratification	High t $ha^{-1}y^{-1}$	%	Normal t $ha^{-1}y^{-1}$	%	Low t $ha^{-1}y^{-1}$	%	Tot. t $ha^{-1}y^{-1}$
Without CF							
R_1 (0-20)	2,27	94,3	0,12	4,9	0,02	0,7	2,40
R_2 (0-10)	2,27	89,2	0,26	10,1	0,02	0,7	2,55
R_3 (0-5)	2,23	85,6	0,36	13,7	0,02	0,7	2,61
With CF							
R_1 (0-20)	4,62	88,8	0,56	10,7	0,02	0,4	5,20
R_2 (0-10)	4,83	83,5	0,93	16,1	0,02	0,4	5,78
R_3 (0-5)	4,91	81,1	0,12	18,5	0,02	0,4	6,06

Tab.4. Loads and relative percentage estimated for high, normal, and low flow conditions for the three different stratifications, using the log-linear equation without and with CF.

Actual load was computed integrating on daily time scale the 15-min discharge and SSC (Eq. 3, where SSC is measured or linearly interpolated concentration between two consecutive measurements). Measured load is estimated at 10112 t, whilst loads estimated using the sediment rating curves are 9275, 8991, and 8056 t for R_3, R_2, and R_1, respectively. In contrast, the loads are overestimated if CF is used in the calculations: 20,425, 19,061, and 16,434 t, respectively. As Fig. 6 shows, the measured value is included in the range of values identified by the loglinear equation, without and with CF. Hence, we can conclude that the log-linear equation, applied with and without CF, is able to identify an interval in which the actual value of load is included. The mean error between measured and generated values was quantified as 31% for the stratification R_3, and much higher (70%) when we applied the CF. For stratifications R_2 and R_1, the error is 32 (61% with CF) and 36 (48% with CF), respectively.

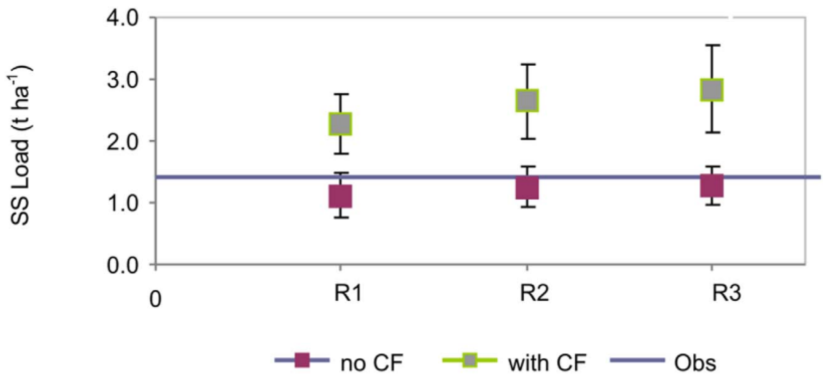

Fig.6. Load transported during the highest peak recorded in the study period (4-7th March 2011), computed with three sediment rating curves, with and without CF, and measured load. Error bars show relative mean absolute error

Uncertainty

The uncertainty associated with estimation methods of annual sediment load was assessed through a method based on a Monte Carlo simulation (implemented in Gumleaf software), repeated 1000 times, with the goal of conveying the uncertainty inherent each method into some numerical descriptor. After the application of Gumleaf, the simulation's outcomes were summarised by means of three parameters, namely mean, standard deviation, and coefficient of variation. By analysing these parameters, it is possible to assess the uncertainty associated with each method. In particular, the coefficient of variation (CV), that is, the ratio between standard deviation and the mean, is commonly regarded as an index well suited for describing variability in a numerical set. It is an index of the lower the better kind. Analysis of the CV brings up the very different characteristics of each method; in fact, it ranges between 8% and 85%, a very large interval. The methods with lower values of CV can be considered to be more robust, because their results are insensitive to small changes in the input dataset. In Table 5, the last row shows the effects of stratification, related to each method.

The CV% ranges between about 6% and 13%. This means that stratifications can have a significant effect, even if of variable intensity, according to the considered method, in annual load estimation. The last column shows the effects of a specific stratification on all the methods; the lowest CV% indicates that, in correspondence with that stratification, the methods tend to produce similar annual load estimations.

Therefore, downstream of this analysis, the stratification called '0–5–70–100%' tends to assimilate the load estimations of all the methods. Consequently, such stratification can be suggested as the most suitable for application. Analogously, the last row in Table 5 shows the response of a specific method under the change of stratification, showing that the method least influenced by, or more stable due to, the stratification change is 'R_AvCmFm'. On the contrary, the method 'R_AvCsFs' that shows the highest CV value is more unstable under the stratifications, providing estimated loads very dissimilar from one stratification to another (from 4.7 to 5.89 t ha^{-1} yr^{-1}). In Fig. 7, the graphic outcome of Gumleaf is represented, and the uncertainty related to each method is described in the form of a boxplot. The mean values range between about 81,000 t (A_AvCsFs) to 19,000 t ("S_AvCmFd"). The method associated with the maximum vertical lengths of the boxes is the one called 'A_AvCsFs', while the minimum is in correspondence with 'S_AvCmFd'. It is noteworthy that the second minimum is 'R_AvCmFd', a method sensitive to the stratification, and that, in general, such methods are represented by smaller boxes.

Stratification	R_AvCmFm (t ha-1y-1)	R_AvCsFs (t ha-1y-1)	R_AvCmFd (t ha-1y-1)	R_FWMC (t ha-1y-1)	R_RtoSim (t ha-1y-1)	R_RtoKen (t ha-1y-1)	R_RtoBea (t ha-1y-1)	CV%
R_1 (0-20-70-100)	3,42	5,89	2,87	4,81	4,81	4,88	4,89	20,97
R_2 (0-10-70-100)	3,39	4,82	3,07	4,30	4,30	4,37	4,35	14,03
R_3 (0-5-70-100)	3,78	4,70	3,36	4,19	4,19	4,25	4,22	9,47
CV %	6,12	12,82	7,97	7,50	7,50	7,46	7,89	

Tab.5. Outcomes of three different stratifications (R_1, R_2, R_3), based on hydrological regime: suspended sediment loads and related CV.

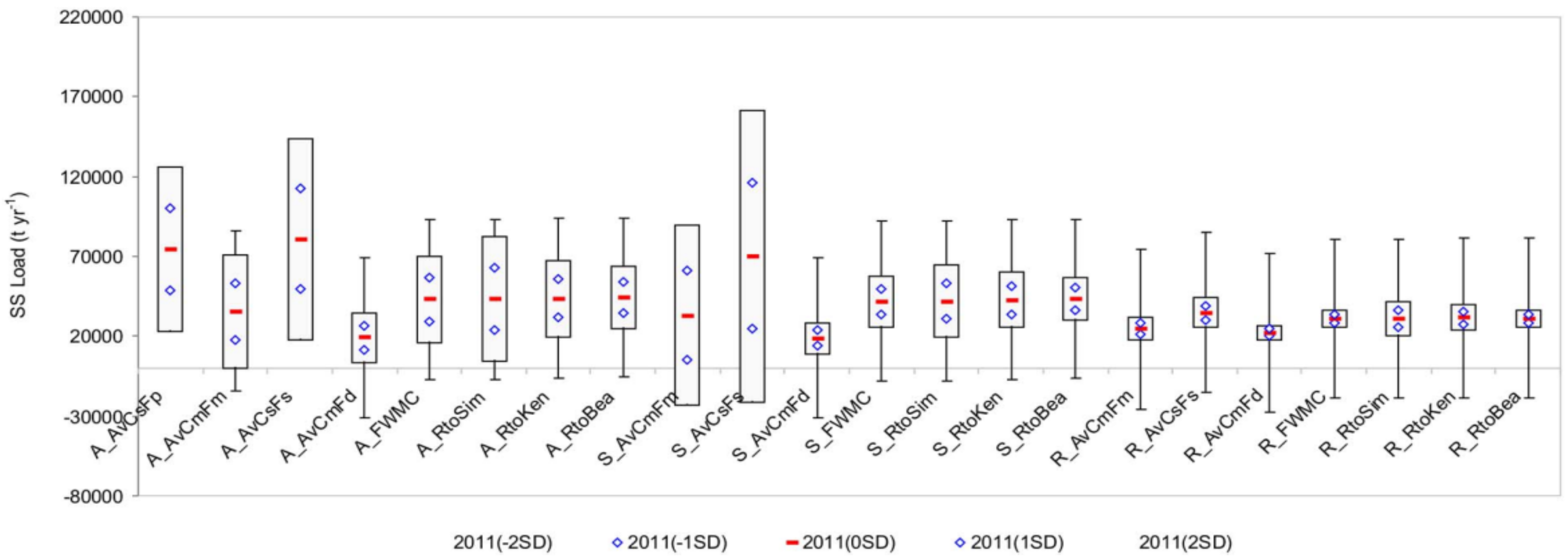

Fig. 7. Boxplot representing the uncertainty associated with each method after Gumleaf application. The stratification R is for R_3 (0–5–70–100% of exc. freq.). The vertical length of the boxes indicates the uncertainty associated with each method, the red '-'within the box represents the mean value. (For interpretation of the references to colour in this figure legend, the reader is referred to the web version of this article.

3.4 Discussion

Influence of flow regime on loads

The precision and accuracy of suspended sediment load estimation is strictly dependent on the sampling frequency, on the method used for sampling (manual sampling, automatic sampling of water, measurement of turbidity), on the technique used for load estimation, on the duration of the sampled period, and its characteristics (wet or dry year).

The results of the present study show that, in the Celone basin, influenced by a Mediterranean climate, the hydrological regime is the key factor in sediment transport. Consequently, the sampling program has to be carefully designed, bearing in mind the flow regime, the characteristics of the basin, and the final objective of the sampling, which is load estimation. The time and frequency of samplings should capture temporal concentration changes, covering the entire range of observed streamflow (Harmel et al., 2006). An enhancing of river monitoring network would certainly be desirable, but currently, in most of the European Union countries only discrete samples are collected on aregular time basis, their numbers varying among the countries (from four to 24: De Girolamo and Lo Porto, 2012; Ullrich and Volk, 2010). Actually, the monitoring policy adopted by the EU Member States is dictated by a careful balance between the available economic resources and the capability of building a reliable framework representing the environmental state. From what we describe above, we understand that the prescribed observations of sediment concentration (quarterly or monthly samples) cannot be sufficient for reliable load estimation, especially if samples are taken with a frequency and timing that does not take into account the hydrological regime. Also, fixed-interval, such as weekly or 10-day, samples could be poorly suited for load estimation because they could miss floods that have generally a short duration, in the Celone River (based on measured data over a long period at San Vincenzo gauge) as well as in most small temporary rivers (Alexandrov et al., 2003; D'Ambrosio et al., 2016). On the other hand, direct and continuous measurement of sediment load could constitute a relatively challenging activity difficult to conduct for long periods. The present work allowed us to derive the following considerations. In summer, from August to the end of October, the Celone River system shows an extremely low flow (mean daily flow < 0.1 l s^{-1}), with very low SSC, consequently, load delivered in this period is negligible compared to the wet season (2.7–5.4% of annual load, depending on calculation method). Hence, a few samples could be sufficient to estimate load.

However, during flash flood events that occur in summer, very high values of SSC could be recorded. Generally, in terms of load the contribution of these events to annual load is negligible, but depending on the magnitude and frequency of the specific flash flood events, and especially for very intensive rainfalls, load could be significant. Contrarily, a few large flood events, recorded in the wet season, are responsible for almost all the annual sediment transport, as several authors have already pointed out (Harrington and Harrington, 2013; Rovira and Batalla, 2006). It was found in the study area that the largest flood, having a duration of three days, was responsible for 1.4 t ha^{-1} yr^{-1} (depending on calculation technique, about 25–50% of annual load), and > 80% of annual load was transported in 18 days.

Hence, it is evident that flood events have to be sampled in order to have a reliable estimation of total load, and that it is important to sample both the rising and falling limbs of the hydrograph. In addition, it was recorded that equal peaks of flow show different values of SSC, due to different vegetation cover status, rainfall intensity, or antecedent soil moisture conditions (De Girolamo et al., 2015a).

Hence, it is important to sample floods occurring in different period of the year (late autumn, early to late winter, and early spring). Unfortunately, these events are unpredictable, and a correct sampling strategy needs an automated procedure. Automatic samplers offer the possibility to take regular samples and to operate during floods, but their use requires special effort, in terms of both time and cost.

Depending on the flood duration, and the modality of the setting up of the instrument, a limitation may arise from the number of bottles (24). Turbidity measurements could overcome this limit, as the continuous measurements, generally obtained using infrared devices, are able to provide a relationship with SSC; however, both these systems provide estimations that could be subject to errors associated with physical characteristics of the sediment (large grain size and their distribution), and that could cause an underestimation of SSC, especially in very high concentration conditions (Regüés and Nadal-Romero, 2013).

Selecting an appropriate load estimation method

In our study, annual suspended sediment load estimation shows a wide range of values, with respect to the applied estimation approach. Each method was found to be affected by a different degree of uncertainty, which may have several implications when the estimated loads are used in modelling sediment transport (i.e. for model calibration or validation) (Ullrich and Volk, 2010), and that has to be taken into account in watershed management.

Identifying and selecting an appropriate method for estimating sediment load is not an easy task. Tan et al. (2005) summarised the data requirements and applicability of several methods. Thus, when data are sparse (monthly, or less frequent), they suggested using averaging or ratio methods, if no significant relationship between Q and SSC exists, and regression methods if a significant relationship between Q and SSC exists. In the case of a representative flood event, where data and regular sampling is weekly or fortnightly, they suggest using averaging or ratio methods with seasonal or flow regime stratification.

According to their framework, linear interpolation methods can only be applied for continuous samplings. In our study, we found that the averaging methods applied to the entire dataset show very dissimilar results, confirming previous studies (Salles et al., 2008; Moatar and Meybeck, 2005; Littlewood et al., 1998; Walling and Webb, 1985), which pointed out that none of the averaging methods can be considered universally an accurate and precise estimator. In the Celone

Basin, the methods called A_AvCsFp and A_AvCsFs overestimated loads (10.37 t ha^{-1} yr^{-1} and 11.23 t ha^{-1} yr^{-1}, respectively), and the largest uncertainty was associated with these estimates. Meanwhile, the method called A_AvCmFd strongly underestimated annual load (2.65 t ha^{-1} yr^{-1}). Littlewood et al. (1998) pointed out that the precision of the averaging methods increased as sampling frequency increased; however, our study demonstrates that, even if the frequency of samples is high and they capture flow regime variability, the precision of averaging methods may be not satisfactory. The large range of values provided by these methods is due to the different assumptions on which they are based. The average values of concentrations and flow used in the equations are estimated differently in each method, and the results strongly depend on the number of samples, on streamflow variability, and on the time between two successive samples (Richards et al., 2012); however, applying data stratification based on hydrological regime, greatly improved the results for some methods (i.e. A_AvCsFs and A_AvCmFm), and less for others (i.e. A_AvCmFd). Data stratification on a seasonal basis does not seem to work efficiently in improving the performances of the averaging methods.

The averaging methods used require caution when estimating suspended sediment load in Mediterranean temporary rivers, even if, as in this case, the SSC measurements cover the entire flow range. The results of different ratio methods are very similar one to another. Applying the stratification of data on a seasonal basis, the loads are more or less the same as the whole dataset.

According the results garnered from the available dataset, this strategy seems not to be suitable for temporary river systems.

Conversely, all the stratification strategies adopted in this study based on hydrological regime produced an increase in accuracy. The results show that, in the latter case, estimated loads are included in the range proved to be acceptable, and where the actual load is included. Generally, these methods are reliable when continuous, or a large number of flow data is available, even if the SSC measurements are few, and their accuracy increases with the correlation between Q and SSC (Preston et al., 1989; Richards and Holloway, 1987). Hence, the ratio methods seem to be suitable to estimate loads in Mediterranean river systems if the dataset is representative of the flow regime, and if a stratification based on flow regime is adopted. The regression methods used in the present study, the so-called sediment rating curves, were developed as a log-linear equation, and used to generate SSC at 15-min intervals, in order to estimate annual load with and without the back-transformation correction. The results show that load is underestimated. Indeed, several studies had already found a substantial underestimation of actual high concentrations, and an overestimation of the actual low concentrations (Horowitz, 2003; Asselman, 2000; Walling and Webb, 1988; Ferguson, 1986). We improved the performance of the sediment rating curve by dividing the entire dataset (Q, SSC) into hydrological regime groups, and applying Duan's CF for the back-transformation. Generally, the reliability of these methods depends on the correlation between SSC and flow; however, Harrington and Harrington (2013) suggested comparing loads generated using rating curves to the true value before selecting this method, as the goodness-of-fit could not ensure that the rating curve will be a good predictor. The results of the present study confirm that they provide a very good performance when the Q-SSC correlation is > 0.5, as suggested by Quilbé et al. (2006). The results show that the actual load of the major events is included in the range identified by the sediment rating curve, applied without and with CF. All the selected flow regime stratifications provided good results. The stratification R3 (0–5–70–100 exc. freq.) tended to assimilate the load estimation of all methods and, hence, it can be suggested as the best stratification; however, we have to take into account that the mean error of this stratification is the lowest (31%) when it was applied without CF, but it is the highest (70%) when CF is used. Moreover, the stratification R_1 (0–20–70–100) shows the maximum mean error in estimating load without CF, and the minimum error in the estimation with CF. Therefore, a suitable strategy for refining the load estimation interval could be to select the minimum error without CF for the lower, and the minimum error with CF as the upper, boundary. These results can be extended to the annual time-scale, as most of the sediment load (81–86%) is transported in high flow conditions. In the Celone basin, acceptable estimates of annual load have to be included in the range from 2.61 to 5.20 t ha^{-1} yr^{-1}. This interval of values can be found in other studies conducted in Mediterranean basins (Alexandrov et al., 2003; Van Rompaey et al., 2005; Achite and Ouillon, 2007; Estrany et al., 2011; Liquete et al., 2009).

3.5 Conclusion

In the present chapter, we addressed the 'load estimation problem' for a temporary river system. The most common, direct methods used for estimating load from continuous flow measurements, and discrete values of concentrations, were applied and compared, in order to quantify annual suspended sediment load, and identify those computational approaches that are suitable for temporary rivers. The main conclusions drawn are as follows.

• Load assumes a wide range of values with respect to the applied load estimation technique.

• Some averaging methods are not suitable for estimating sediment load in temporary, flashy rivers, characterised by high variability in streamflow. For these methods, stratification of the dataset in groups of data based on season, does not improve their performance, while stratification based on flow regime improves their performance significantly.

• Ratio methods generally overestimate load, but if data stratifications based on flow regime are adopted, the accuracy improves.

• Sediment rating curves have proved to be a valuable method for generating SSCs, when the correlation between flow and SSC is higher than 0.5; however, suspended sediment load is underestimated when SSC is derived from the log-linear regression equation. By introducing Duan's back-transformation CF, load is overestimated. The sediment rating curve development requires measurements of SSC in all flow conditions, especially in flood events, during which very high concentrations are observed.

• A good performance is obtained by using flow regime data stratification. Each of the three different stratifications analysed here greatly improved load estimation, reducing the range of variability of all the methods. The stratification defined by 0–5–70–100% of exceedance frequency on the flow duration curve tends to assimilate the load estimations of all the methods. Consequently, such stratification can be suggested as the most suitable application.

• The data stratification based on season, adopted in this study (wet and dry seasons), has proved to be less effective than stratification based on hydrological regime for all the methods. This strategy seems to not be suitable for temporary river systems.

• The uncertainty associated with sediment load estimation is an important piece of information for watershed management, helping managers in quantifying sediment load before making decisions concerning the measures needed to reduce soil erosion. The results of this research may assist similar studies aimed at quantifying suspended sediment load in temporary, flashy streams. Further studies are needed to investigate over a long period the interaction between sediment transport and human activity, and to identify the best management practices to reduce sediment erosion in a river basin.

Appendix A: Suspended sediment concentration and load equations

	Abbreviation	Load Equation	Description
1	A_AvCsFp	$k \sum_{i=1}^{n} \left(c_i * \sum_{p=1}^{N_{pi}} q_{pi} \right) = k \sum_{i=1}^{n} (c_i * Q_{pi})$	Sample period flow-weighted averaging = Sample conc x mean flow between sampling period in a year
2	A_AvCmFm	$kN \left(\sum_{i=1}^{n} \frac{c_i}{n} * \sum_{i=1}^{n} \frac{q_i}{n} \right) = kN\overline{cq}$	Annual mean Sample conc-mean Sample flow averaging = mean Sample conc x mean Sample flow in a year
3	A_AvCsFs	$kN \left(\sum_{i=1}^{n} \frac{c_i * q_i}{n} \right) = kN\bar{l}$	Annual Sample conc-Sample flow averaging = Sample conc x Sample flow in a year
4	A_AvCmFd	$k \left(\sum_{i=1}^{n} \frac{c_i}{n} \right) \left(\sum_{j=1}^{N} q_j \right) = k\bar{c}Q$	Annual mean Sample conc-mean flow averaging = mean Sample conc x mean Annual flow in a year

5	A_FWMC	$k\left(\sum_{i=1}^{n}(c_i * q_i)\right)\left(\frac{\sum_{j=1}^{N} q_j}{\sum_{i=1}^{n} q_i}\right) = k\bar{l}\frac{Q}{q} = k\hat{R}Q$	*Annual flow-weighted mean conc = sample conc x sample flow in a year weighted by ratio of mean annual flow/mean sample flow*
6	A_RtoSim	$k\left(\frac{\sum_{i=1}^{n}\frac{c_i * q_i}{n}}{\sum_{i=1}^{n}\frac{q_i}{n}}\right)\left(\sum_{j=1}^{N} q_j\right) = k\frac{\bar{l}}{\bar{q}}Q = k\hat{R}Q$	*Annual simple ratio estimator (load estimate similar to FWMC method, but variance estimate differs)*
7	A_RtoKen	$k\left[\left(\frac{N-1}{n-1}\right)(\bar{l} - \overline{cq})\right]\hat{R}Q$	*Annual Kendall's ratio estimator*
8	A_RtoBea	$k\left[\frac{1 + \left(\frac{1}{n} - \frac{1}{N}\right)\left(\frac{S_{lq}}{\bar{l}\bar{q}}\right)}{1 + \left(\frac{1}{n} - \frac{1}{N}\right)\left(\frac{S_q{}^2}{\bar{q}^2}\right)}\right]\hat{R}Q$	*Annual Beale's ratio estimator*
9	S_AvCmFm	$\sum_{S=1}^{T_s}\left[kN_s\left(\sum_{i=1}^{n_s}\frac{c_i}{n_s} * \sum_{i=1}^{n_s}\frac{q_i}{n_s}\right)\right] = \sum_{S=1}^{T_s}(kN_s\overline{c_s}\overline{q_s})$	*Seasonal-stratified mean Sample conc-mean Sample flow averaging = sum of mean Sample conc x mean Sample flow of all seasons in a year*
10	S_AvCsFs	$\sum_{S=1}^{T_s}(kN_s\overline{l_s})$	*Seasonal-stratified sample conc-sample flow averaging = sum of sample conc x sample flow of all seasons in a year*

11	S_AvCmFd	$\sum_{S=1}^{T_s}(k\bar{c}_s Q_s)$	Seasonal-stratified mean sample conc-mean flow averaging = sum of mean sample conc x mean seasonal flow of all seasons in a year
12	S_FWMC	$\sum_{S=1}^{T_s}(k\widehat{R_s}Q_s)$	Seasonal-stratified flow-weighted mean conc = sum of Sample conc x Sample flow weighted by ratio of mean Seasonal flow/mean Sample flow of all seasons in a yr
13	S_RtoSim	$\sum_{S=1}^{T_s}(k\widehat{R_s}Q_s)$	Seasonal-stratified simple ratio estimator
14	S_RtoKen	$\sum_{S=1}^{T_s}\left(k\left[\left(\frac{N_s-1}{n_s-1}\right)(\bar{l_s}-\bar{c}_s\bar{q}_s)\right]\widehat{R_s}Q_s\right)$	Seasonal-stratified Kendall's ratio estimator
15	S_RtoBea	$\sum_{S=1}^{T_s}\left(k\left[\frac{1+\left(\frac{1}{n_s}-\frac{1}{N_s}\right)\left(\frac{[S_{lq}]_s}{\bar{l}_s\bar{q}_s}\right)}{1+\left(\frac{1}{n_s}-\frac{1}{N_s}\right)\left(\frac{{[S_q]_s}^2}{{\bar{q}_s}^2}\right)}\right]\widehat{R_s}Q_s\right)$	Seasonal-stratified Beale's ratio estimator

16	R_AvCmFm	$k\sum_{R=1}^{T_R}\left[N_R\left(\sum_{i=1}^{n_R}\frac{c_i}{n_R}*\sum_{i=1}^{n_R}\frac{q_i}{n_R}\right)\right]=k\sum_{R=1}^{T_R}(N_R\overline{c_R}\overline{q_R})$	*Flow regime-stratified mean sample conc-mean sample flow averaging = sum of mean sample conc x mean sample flow of all regimes in a year*
17	R_AvCsFs	$k\sum_{R=1}^{T_R}(N_R\overline{l_R})$	*Flow regime-stratified sample conc-sample flow averaging = sum of sample conc x sample flow of all regimes in a year*
18	R_AvCmFd	$k\sum_{R=1}^{T_R}(\overline{c_R}Q_R)$	*Flow regime-stratified mean sample conc-mean flow averaging = sum of mean sample conc x mean regime flow of all regimes in a year*
19	R_FWMC	$k\sum_{R=1}^{T_R}(\widehat{R_R}Q_R)$	*Flow regime-stratified flow-weighted mean conc =sum of Sample conc x Sample flow weighted by ratio of mean Seasonal flow/mean Sample flow of all regimes in a yr*
20	R_RtoSim	$k\sum_{R=1}^{T_R}(\widehat{R_R}Q_R)$	*Flow regime-stratified simple ratio estimator*
21	R_RtoKen	$\sum_{R=1}^{T_R}\left(k\left[\left(\frac{N_R-1}{n_R-1}\right)(\overline{l_R}-\overline{c_R q_R})\right]\widehat{R_R}Q_R\right)$	*Flow regime-stratified Kendall's ratio estimator*

22	R_RtoBea	$\sum_{R=1}^{T_R}\left(k\left[\frac{1+\left(\frac{1}{n_R}-\frac{1}{N_R}\right)\left(\frac{[S_{lq}]_R}{\overline{l_R}\overline{q_R}}\right)}{1+\left(\frac{1}{n_R}-\frac{1}{N_R}\right)\left(\frac{[S_q]_R^{\ 2}}{\overline{q_R}^2}\right)}\right]\widehat{R_R}Q_R\right)$	Flow regime-stratified Beale's ratio estimator
23	A_Src	$Log\ ci = a\ Log\ Qi$	Annual sediment rating curve
24	A_SrcCF	$Ci = CF * 10^{aLogQ_i}$	Annual sediment rating curve with back transformation correction factor (CF)
25	S_Src	$Log\ Ci = a1Log\ Qi\ (Dry);\ Log\ Ci = a2Log\ Qi\ (Wet)$	Seasonal-stratified concentration and flow data
26	S_SrcCF	$Ci = CF_1 * 10^{a_1 LogQ_i}(Dry);\ Ci = CF_2 * 10^{a_2 LogQ_i}\ (Wet)$	Seasonal-stratified concentration and flow data with back transformation correction factor (CF)
27	R_Src	$Log\ Ci = a_1 LogQ_i\ (High);\ Log\ Ci = a_2 LogQ_i\ (Normal); Log\ Ci = a_3 LogQ_i\ (Low);$	Flow regime-stratified data (R_1; R_2; R_3)

28	R_src_CF	$Ci = CF1 * 10\ a1Log\ Qi\ (High);\ Ci = CF2 * \ 10a2Log\ Qi(Normal);\ Ci = CF3 * 10\ a1Log\ Qi\ (Low);$	*Flow regime-stratified data (R_1; R_2; R_3) with back transformation correction factor (CF)*

Notation:
k = scaling factor, to account for days in a duration (year or season or flow regime) with flow gap (if any) by single proportion; ci , qi = sampled concentration, sampled flow; Npi , Qpi , qpi = measures between mid of consecutive samples I (flow days, total flow, sampled flow); n, nS, nR = number of sampled concentration days over a duration (year, season, flow regime); N, NS, NR = number of measured flow days over a duration (year, season, flow regime; Q, QS, QR = total measured flow over a duration (year, season, flow regime); $\bar{q}$, $\bar{q}S$,$\bar{q}R$ = average sampled flow over a duration (year, season, flow regime); $\bar{l}$, $\bar{l}S$, $\bar{l}R$ = average load over a duration (year, season, flow regime); $\hat{R} = \frac{\bar{l}}{\bar{q}}$, $\widehat{R_R} = \frac{\bar{l}R}{\bar{q}R}$, $\widehat{R_S} = \frac{\bar{l}S}{\bar{q}S}$ = load-flow ratio over a duration (year, season, flow regime); T, TS, TR = total number of strata (year, season, flow regime)

Abbreviation:
A_ , R_ , S_ indicates the type of stratification: annual, flow regime based and seasonal; Av is for Averaging Method; Rto is for Ratio method; Src is for Sediment rating curve; Cs = sample concentration; Cm = mean sample concentration; Fs = sample flow; Fm = mean sample flow; Fp = flow over period of consecutive samples; Fd = flow over a duration (year, season, flow regime); FWMC = flow-weighted mean concentration; Sim = Simple; Ken = Kendall; Bea = Beale; CF = Correction Factor; $\widehat{R_R} = \frac{\bar{l}R}{\bar{q}R}$ is the load flow ratio over a duration based on flow regime ; $\widehat{R_S} = \frac{\bar{l}S}{\bar{q}S}$ is the load flow ratio over a duration based on seasonality; $\hat{R} = \frac{\bar{l}}{\bar{q}}$ is the load flow ratio over year

Di Pillo et al. 2020, Catena, Submitted

04 –Drivers of SS transport

Abstract

Suspended sediment transport in streams generally responds not only to water discharge but to a large number of spatial-temporal variables. This study aims to evaluates drivers of suspended sediment (SS) transport through the analysis of flood events (n = 23) occurred during a one-year sampling campaign (2010 to 2011) in the Celone River basin (Puglia, S-E, Italy). High resolution data of rainfall, streamflow (Q), and suspended sediment concentrations (SSC) were used. Hysteresis index (HI) was calculated for each event to classify Q-SSC relationships and to analyze basin's response to different storm events. A Principal Component Analysis (PCA) was adopted to find the most influencing factors among 18 variables, previously investigated to test their sphericity and suitability for the PCA itself. Results showed as flood events had predominantly a negative HI (18 over 21), ranging from +3,77 to -17,8, suggesting a delayed transport mechanism, also re-suspension and exhaustion mechanisms were detected by analyzing HI shift, from positive to negative and vice versa. PCA showed that three components were able to describe the 75,47% of the variation in the data. PC1 and PC2 explained alone more than 64% of the variance. Among the initial 18 variables, PCA revealed that the major factors influencing SS transport where rainfall kinetic energy at the two gauging stations (KE_Diga; KE_Faeto), total rainfall depth recorded at the nearest SS gauging station (Htot_diga),

Keywords: Intermittent rivers, suspended sediment transport, drivers of soil erosion, hysteresis index, principal component analysis.

SSCmax and SS load, Qmax, Qmid, Vtot, and time duration of flood event (Tflow) and both measured time shift between hyetograph and hydrograph.

4.1 Introduction

Soil erosion is an issue that in recent years is becoming of great importance, especially in those areas of the Mediterranean Region where river basins are already affected by water scarcity (Bangash et al. 2013, De Girolamo et al. 2012, Cudennec et al. 2007) and water/soil pollution due to agricultural practices (De Girolamo et al. 2017a, Casali et al. 2008,). Eroded sediment particles during the transport and deposition processes cause variations in the morphologic and hydraulic characteristics of the river (Nones et al. 2016, Lane et al. 2007), reservoir/barrage siltation (Di Pillo et al. 2019, Kondolf et al. 2014, Bazzoffi et al. 2005), and depletion of the water quality since sediments are the main vehicle for nutrients and pollutants deriving from anthropogenic activities (D'Ambrosio et al. 2018, De Girolamo et al. 2017b, Horowitz et al. 2008).

In order to quantify and minimize these problems, an understanding of erosion and sediment transports processes are needed. At this scope, several authors developed various approaches to quantify erosion rate (Santos et al 2017, Yang et al. 2012, de Vente et al. 2007, Lu et al. 2005) and sediment loads by using models (Ahanger et al. 2013, Francke et al. 2008, Zhang et al. 2012) or field measurements (Erikson et al.

2013) including the uncertainty analysis associated to the estimations (Reg§ès et al. 2013, Navratil et al. 2011).

However, a few studies have investigated the driving forces of suspended sediment (SS) transport (Vercruysse et al. 2017, Duvert et al. 2010).

In ungauged river basins, where data availability is limited, modelling approaches (USLE, MUSLE, RUSLE-EPM etc.) provide a quantification of soil erosion, identifying critical source areas and deposition patterns (Tan et al. 2018). However, these approaches do not identify the dominant forces responsible of the process.

For perennial river systems theoretical relationships among the major variables influencing the SS transport, the so called "drivers", have long been studied (Anderson H.W. 1957). In particular, at event scale, different studies (Perks et al. 2016, Dominic et al. 2015, Oerung et al. 2011, Mano et al. 2009) were carried out. For intermittent river systems, the drivers are not sufficiently analysed (Alexandrov et al. 2007, 2009, Bisantino et al. 2011), especially by using high resolution data (Gao et l. 2013, Oerung et al. 2010). Indeed, the response of these rivers to the drivers could be different from perennials because of the strongest variability of flow regime as pointed out by De Girolamo et al. 2018. Hence, the role of rainfall and flow regime on SS transport needs to be investigate in these river systems. In addition, as a lag time can exist between streamflow (Q) and SS concentrations (SSC) (De Girolamo et al., 2015), the analysis of hysteretic relationships between these variables needs to be investigate. Previous studies pointed out that hysteresis analysis can give a relevant contribution in understanding the mechanisms of runoff generation (Spence et al., 2010) and on hydrological connectivity (Murphy et al., 2014; Zuecco et al., 2016, Pagano et al.2019) or in identifying the sediment source areas contributing to the SS transport. The most common approaches to analyse the hysteretic loops are based on bivariate plots or on indices (Zhang et al., 2014, Butturini et al. 2008).

Indexing approach is more suitable in a poor data catchment since it requires a few SSC data (i.e. only punctual concentrations on rising and falling limb of the hydrograph) instead of a continuous data collection (Lawler et al. 2006).

This paper aims at finding the main drivers of SS transport for an intermittent stream through an accurate analysis of flood events. The relationships among rainfall, discharge and SSC were analysed, in addition to the hysteretic loops (Lloyds et al. 2016) in the Celone catchment (S-E, Italy), where high-resolution data were available. This study is the continuation of previous works carried out in the study area to analyse temporal variability of SS transport and to quantify SS load (SSL) (De Girolamo et al., 2015; De Girolamo et al., 2018). Results can contribute to better understand hydro-sedimentary patterns in intermittent streams and may be very useful in watershed management.

4.2 Material and Methods

Study area

The Celone river basin is a small foothill catchment located in the Apulia region (S-E of Italy), it is a sub catchment (85,9 km^2) of the Candelaro river basin (2200 km^2). In the middle course of the river a reservoir was realized in 2000, the Torrebianca dam that is the major man-made hydraulic work of the area (25,82 Mm^3 at full capacity, filled volume of 16,34 Mm^3 on May 2017). The basin is well drained with a total length of the drainage network of 109 km, elevation within the basin varies from 218 m.a.s.l. to 1142 m.a.s.l. (av. elevation 386 m.a.s.l.).

The climate is typically Mediterranean, with mean annual rainfall rangeing from 792 to 623 mm, respectively for Faeto gauge (860 m.a.s.l.) and Troia gauge (350 m.a.s.l.), within the basin. Average temperature ranges from 3,4°C (January) to 20,3° C (August) in the upper part and from 7,2°C (January) to 25,5°C (August) in the valley area.

The catchment could be zoned both on the geomorphological and hydrologic-hydraulics characteristics (Di Pillo et al. 2019), in three homogeneous sub-areas, the upstream zone, the flood plain zone and the valley zone. The upstream mountain area is characterized by non-irrigated crops and pastures, with high presence of forests. Here, the slope is accentuated (av. slope 22,86%), and the river is a single-channel deeply incised. To reduce bank erosion, several check dams along the course were realized in the past. In the flood-plain area, the river assumes a braided morphology, slopes decrease (av. Slope 12,48%) and there is a deposition of sediment. Land use is characterized by olive cultivations, cereals and sunflowers. In the valley area, where the river flows into the reservoir, slopes decreasing more (av. Slope 5,63%), cultivated lands increase and river get sinuous. On the whole, into the entire catchment land use is mainly cultivated, cereals (45%), sunflowers (9%), pasture (6%), olive groves (8%) vegetable and vineyards (2%), with oak and conifers forests (29%) in the upper part. Urban areas are less than 1%. Anthropogenic activities, such as agricultural practices, are the major cause of soil erosion. Indeed, the frequent up and down tillage practices contribute to increase soil losses, especially in autumn and winter.

Flyshoid formations (flysch della Daunia) and grey-blue clays are the main lithological units (De Girolamo et al., 2018) in the upper part of the basin, meanwhile alluvial deposits are predominant in the valley. The soils in the basin have a composition related to the lithology, and show a variable texture (clay, clay-loam, and sandy-clay-loam). The main soil types are classified as typic-haploxerroll, vertic-haploxeroll, and typic-calcixeroll, according to the US Department of Agriculture classification. The depth and soil physical and hydrological characteristics are highly variable; in the flat part of the basin, soils are deep (1.5–2 m), while in the hills and mountains, they are moderately deep (< 1 m).

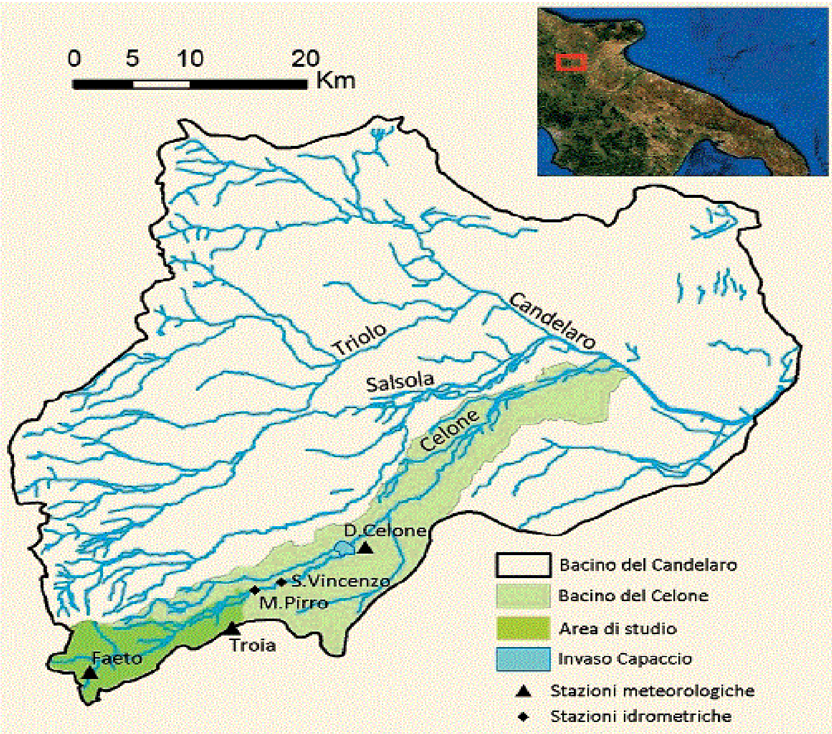

Figure 1. Study area, gauging stationS

Data Campaign: Rainfall, Qand SSC

Continuous measurements of Q, were taken from July 2010 to June 2011 at the Masseria Pirro's gauging station, 8 km upstream the Torrebianca dam's closing setion. An ISCO 750 Area Velocity Flow Module recorded 5 min Q values, while for the measurement of SSC an ISCO automatic sampler (model 6712FS; 24 bottles; pumped volume 1L) provided infrequent samplings, based on two different settings. The first setting was based on regular time intervals. The second sampling strategies, oriented to take samples during floods, was triggered by water level changes during the rising limb of hydrograph and a decrease of flow rates during the flood recession. During flood events, the time-interval was between 15 min and 2 h in the rising limb and between 2 h and 1 day in recession limb. With this sampling program, a large number of samples were collected over the study period (n = 216), covering all hydrological conditions (flood, normal, and low flow). The SSCs were analysed in a laboratory, using the APAT-IRSA analytical standard method (APAT-IRSA-CNR, 2003). Standard 0.45 µm pore-diameter cellulose filters were used to filter the samples, to quantify the total suspended concentration. For additional details concerning the gauging station and sampling, please refer to De Girolamo et al. (2015a).

During the study period, 23 storm events occurred. In the present study, due to the gaps in measurements of variables, only 21 events were processed. Storm event initiation were defined as a consistent consecutive increase in streamflow values (Megnounif et al. 2013) In multiply events, if peaks were distinct, the single events were divided. In particular, 6 events grouped two at a time were observed $Q_{initial}$ was estimated if, after the Q_{min} in the falling limb of the previous event, an increase of Q was detected. Rainfall at daily, and sub-daily time scale (5-min. and 30-min) measured at the Faeto gauging station, located in the upstream basin (900m asl), and Diga Celone gauging station located in the plain area were considered. Data were provided from the decentralized functional center, Civil Protection section of the Apulia region, recorded for the same study period.

Variables detection

Estrany et al. (2009) and Gao et al. (2008) pointed out that the relationship between SSC and Q is nonlinear, but complex and multivariate. Indeed, SS transport is related to hydrological regime, sediment supply, and is broadly influenced by climatic conditions, topographic conditions, and land use. Some authors have evaluated the semi-permanent controlling factors in SS transport, defined as catchment-related variables such as morphology, land use, land use changes, total area, erodible area, vegetation cover or connectivity, aiming at analysing the temporal variability in suspended sediment dynamics, to detect long-term effects of variability in these control factors, or to compare similar basins (Duvert et al. 2017, Tamene et al. 2006, Stegen et al. 2001).

Generally, driving forces in SS transport has been clustered as (i) flow event variables, (ii) rainfall variables, (iii) time shift variables, (iv) antecedent soil moisture conditions or antecedent precipitation of the analysed flood event (from 12h to 10d before or more). However, concerning the latest factors, no strict relationship between SS and antecedent soil water content or rainfall conditions were found (Oerung et al. 2010).

In this study, given the fast response of the basin to rainfall events and the consequently flashy characteristics of the floods, we evaluated only the Antecedent Moisture Conditions as the major indicator of the sediment disposability 24h before the flood events measured at Faeto and Diga Celone gauging stations.

In the present work, 18 variables were selected, grouped in these four clusters, as showed in Tab.1. and Fig.2. Because of the fast response of the basin to rainfall events and the consequent flashy character of floods, only the antecedent rainfalls recorded 24h before were considered.

Variable	Cluster	Description
Qi [m3/s]		Initial water discharge of the flow event
Qmax[m3/s]	Flow event	Maximum water discharge of the flow event
Qmid[m3/s]		Midpoint of water discharge
Vtot [m3]		Volume of water flowed during flow event
SSCmax [g/l]		Maximum concentration of SS during flow event
SSCmean [g/l]	SSC	Mean concentration of SS during flow event
SST [kg]		Total suspended sediment yeld
Htot_Diga [mm]		Total rainfall depth measured at Diga Celone gauging station
Htot_Faeto [mm]		Total rainfall depth measured at Faeto gauging station
Imax_Diga30-min [mm/h]	Rainfall	Maximum rainfall intensity that caused flow event measured at Diga Celone gauging station
Imax_Faeto30-min [mm/h]		Maximum rainfall intensity that caused flow event measured at Faeto gauging station
KE_Diga [mm]		Rainfall kinetic energy measured at Diga Celone gauging station (Brandt 1990)
KE_Faeto [mm]		Rainfall kinetic energy measured at Faeto gauging station (Brandt 1990)
ΔT Qmax-hmax_Diga [min]		Time lag between hyetograph-hydrograph peaks measured between Diga Celone and Masseria Pirro

ΔT Qmax-hmax_Faeto [min]	Time	Time lag between hyetograph-hydrograph peaks measured between Faeto and Masseria Pirro
Tflow event [min]		Duration of the flow event
AMC_Diga [mm]		Antecedent moisture condition of the soil 24h before the flow event at Diga Celone gauging station
AMC_Faeto [mm]	Soil condition	Antecedent moisture condition of the soil 24h before the flow event at Faeto gauging station

Tab. 1. Selected variables

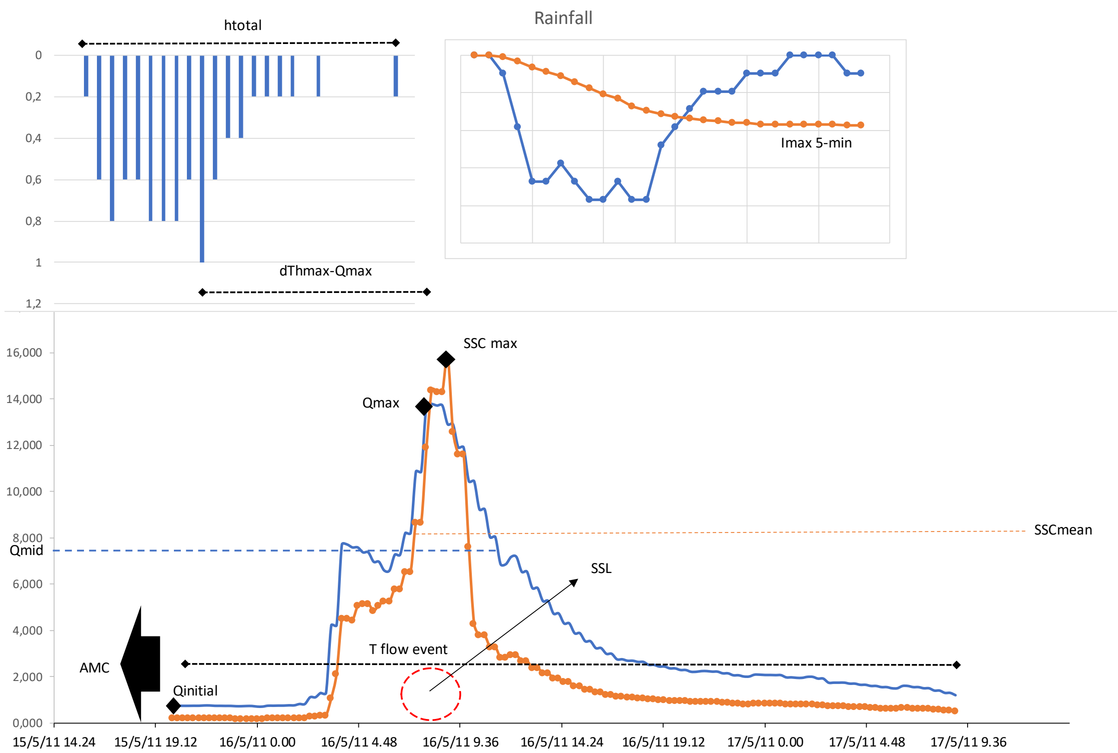

Figure 2. Graphical identification of main selected variables

Statistical Analysis

In the present chapter, to describe the interdependence among the selected controlling variables the Pearson's correlation was applied. In addition, to reduce the number of variables the Principal Component Analysis (PCA) was applied. PCA is a statistical application of dimensional reduction of controlling variables in a smallest set of variables, often developed also to simplify or well calibrate subsequent analysis (i.e. prediction models, sediment rating curves etc) (Wuttichaikitchaoren et al. 2004), that allow to find a new coordinate system in which few variables could explain the maximum of the variance.

Generally, to apply the PCA, the set of variables must be adequate, explanatory and suitable (Field 2005). For this purpose, as recommended by Halim et al. 2007, the Kaiser-Meyer-Olkin (KMO) test for measuring the sampling adequacy and the Bartlett's test of sphericity were applied. IBM® SPSS statistics 23 was used to analyze the dataset for preliminary verifications, to find statistical correlations (Pearson's method) and to run PCA. Before performing the PCA the adequacy and sphericity of variables was investigated (Hair et al. 2006; Pallant 2005).

To validate the PCA the a-parameter test developed by Cronbach 1951 was assessed (Eq. 1):

$$\alpha = \frac{N^2 \overline{cov}}{\sum S_{var}^2 - \sum cov_{var}} \quad (1)$$

Where N is the number of variables, $\overline{cov}$ is the average covariance between variables, S_{var}^2 is the variable variance, and cov_{var} is the covariance, a result of a = 0,83 further verified PCA.

Event scale analysis and Hysteresis classification

The Hysteresis Index (HI) was estimated for each event with the aim to analyze patterns of hysteresis for an intermittent river. Indeed, indexing approach is a dimensionless classification of hysteresis that, notwithstanding the loose of precision in the capacity of describing the shape of the loops, could allow the comparison between different catchment's behavior.

Many authors have proposed different indexes to describe the hysteretic loops. Langlais et al. (2005) fitted two different regression lines to both the rising and the falling limb of the splitted hydrograph, Butturini developed an index (Butturini et al. 2008) evaluating the subtended area of hysteresis loop that could describes the enrichment or dilution of the sediment during the single storm event, Lloyds et al. 2016 carried out a critical revision of many indices proposing a reviewed version of the Lawler index (Lawler et al. 2006).

In the present work, the index proposed by Lawler et al. 2006 was used to evaluate hysteresis. The index was already used by other authors (Mc Donalds and Lamoureux 2009, Outram et al. 2014, Sheriff et al. 2016) in rural and agricultural watershed having similarities with the study area.

This index was calculated as a ratio between the suspended sediment concentration during the rising limb (SSC_{RL}) and the falling limb (SSC_{FL}) of the hydrograph at the mid-point of discharge, avoiding in this way the often-noisy sections of the beginning and the end of the loops (Lawler et al. 2006).

We first determinate the midpoint (Q_{mid}) as:

$$Q_{mid} = 0{,}5\,(Q_{max} - Q_{min}) + Q_{min} \qquad (2)$$

Where Q_{min} and Q_{max} are the initial and maximum peak event values, respectively.

The corresponding SSC values at Q_{mid} on the rising (SSC_{RL}) and falling (SSC_{FL}) hydrological limbs were determined, defining two possibilities $SSC_{RL} > SSC_{FL}$ or $SSC_{RL} < SSC_{FL}$,. Hysteresis Index where thereafter calculated with Eq. 3 or Eq. 4, respectively

$$HI = (SSC_{RL}/SSC_{FL}) - 1 \qquad (3)$$

And:

$$HI = \left(-\frac{1}{(SSC_{RL}/SSC_{FL})}\right) + 1 \qquad (4)$$

The magnitude, in absolute value, indicates the synchronicity between Q and SSC peaks, with positive and negative deviations respectively for clockwise and anticlockwise hysteresis.

Magnitude of HI index may also suggest an insight regarding the distance of the sediment source from the monitoring point (Aich et al. 2016), the more negative the index is, the more distant is the source, and conversely for positive values, the higher they are, the more proximal is the source. The limitation of this approach is that figure 8 and complex hysteretic loops could be difficult to describe.

4.3 Results and discussion

Rainfall, Q, and SSC

Storm events were concentrated mainly during spring season (March - May), in particular in March were observed 8 distinct storm events (23% of total events).

Total rainfall depth causing floods (htot) ranged from 1 to 36 mm at Diga Celone gauging station, exceeding 7 times the average amount recorded during floods (11,49 mm), and from 2,6 to 26,2 mm at Faeto gauging station, exceeding 9 times the average (13,28 mm). Maximum rainfall intensity (Imax 30min) recorded during flood events showed a wide variability ranging from 0,8 to 23,6 mmh^{-1} and from 4 to 48,8 at the Diga Celone and Faeto gauging stations, respectively. These values were recorded respectively on March and June. The associated kinetic energy (Brandt, 1990), evaluated for both two stations varied from 149,95 mm on May to 2599,91 mm on March. It is important to highlight that in May crops confer high protection to the soil that is less erodible, meanwhile, in March cultivated lands are less protected by vegetation (i.e. durum wheat production).

During flood events, Qmax varied from 0,36 to 30,18 m^3s^{-1} exceeding 6 times the mean value of 8,39 m^3s^{-1} (SD = 7,30 m^3s^{-1}), Q_{ini} varies from 0,09 to 6,517 m^3s^{-1}. High values of Q_{ini} were observed during multiple peak events when the baseflow was high.

SSC measured during the study period were highly variable, ranging from 0.005 to 37.6 g l^{-1} and the values recorded during the selected floods ranged from 0,1 to 7,13 g l^{-1}. During March, where 8 distinct flood events occurred, there was a falling in suspended sediment concentration over consecutive floods, showing both sediment depletion caused from continuous runoff and sediment dilution by increased baseflow.

Sediment load during the selected floods varied from 1387 kg in October (Tflow event 858 min), to 8939629 kg in March (Tflow event 5907 min). During spring seasons 13463 of 17154 tons of sediment were flushed whereas during wet periods this amount is lower due to the exhaustion mechanism gave from the longer precipitation period. Major features of mean, maximum and minimum magnitude of observed variables are summarized in tab.2.

	MAX	MIN	MEAN	SD
Qmax	30,18	0,36	8,40	7,30
Qmid	16,03	0,20	4,72	3,74
Qinitial	6,52	0,09	1,43	1,33
SSCmax	7,13	0,10	2,13	1,83
SSCmean	2,42	0,05	1,09	0,79
SST	8939629,70	1387,30	816873,11	1946446,09
Vtot	2511580,00	6693,90	389108,71	542797,94
Kemm Diga	2599,91	102,35	591,01	682,07

Kemm Faeto	1870,56	149,96	595,11	441,06
htot Diga	36,00	1,00	11,49	10,22
htot Faeto	26,20	2,60	13,28	7,39
Imax 30min Diga	23,60	0,80	8,74	5,62
Imax 30min Faeto	48,80	4,00	14,53	10,47
AMC [mm] Diga	13,00	0,00	4,17	4,58
AMC [mm] Faeto	31,60	1,20	9,68	8,50
ΔtQmax-hmax Diga [min]	1430,00	40,00	450,48	309,91
ΔtQmax-hmax Faeto [min]	2150,00	40,00	554,29	435,58
T flow event [min]	5907,00	258,00	1734,14	1241,74

Tab. 2 Min, Max mean values and SD for observed variables

Correlation among variables

The main relevant factors influencing SS transport mechanism were identified through the Pearson's correlation matrix (Tab.3). Variables related to the SS transport (SSCmax, SSCmean, SST) have shown a strong positive correlation with the discharge variables (Qmax, Qmid, Qinitial) and KE of both gauging stations. Indeed, the correlation between the SS transport variables and KE was higher for Diga Celone that is nearest to the measuring point, explaining a high hydrological response of SSC to the KE of rainfall, thus categorizable as flash flood type (Zabaleta et al. 2007).

A positive correlation between SS variables and Tflow, htot and Vtot was found, meanwhile, a low correlation between SS variables and Imax of both gauging stations was observed.

A weak correlation between SS variables and the AMC for both gauging was observed. However, AMC was positively correlated with Qinitial (R = 0,74 and 0,49) respectively for Faeto and Diga Celone station) a common behaviour with the Carapelle catchment previously investigated by Pagano et al. (2019).

Qmax	1,00																	
Qmid	1,00	1,00																
Qinitial	0,62	0,66	1,00															
SSCmax	0,84	0,83	0,56	1,00														
SSCmean	0,74	0,74	0,35	0,93	1,00													
SST	0,82	0,82	0,85	0,77	0,57	1,00												
Vtot	0,86	0,86	0,80	0,79	0,59	0,98	1,00											
KE Diga	0,76	0,75	0,54	0,77	0,64	0,82	0,86	1,00										
KE Faeto	0,76	0,75	0,48	0,69	0,62	0,75	0,75	0,70	1,00									
htot Diga	0,60	0,59	0,42	0,62	0,50	0,68	0,69	0,88	0,54	1								
htot Faeto	0,42	0,39	0,10	0,47	0,49	0,41	0,35	0,27	0,58	0,34	1,00							
ImaxDiga	0,28	0,28	0,19	0,20	0,14	0,22	0,22	0,24	0,32	0,47	0,30	1,00						
ImaxFaeto	-0,16	-0,18	-0,24	0,09	0,20	-0,16	-0,22	-0,32	-0,17	-0,29	0,51	-0,02	1,00					
AMC Diga	0,14	0,15	0,74	0,16	0,03	0,41	0,39	0,27	0,31	0,24	0,02	0,50	-0,18	1,00				
AMC Faeto	-0,02	0,00	0,49	0,04	-0,11	0,27	0,19	0,02	0,13	0,01	-0,03	0,31	-0,11	0,80	1,00			
dTq-h Diga	-0,21	-0,19	-0,08	-0,20	-0,12	-0,19	-0,18	-0,03	-0,26	-0,03	-0,56	-0,14	-0,34	0,03	0,01	1		
dTq-h Faeto	-0,23	-0,20	0,06	-0,24	-0,16	-0,12	-0,13	-0,09	-0,26	-0,06	-0,56	-0,20	-0,33	0,03	-0,02	0,91	1	
T flow event	0,67	0,67	0,62	0,75	0,55	0,85	0,89	0,76	0,59	0,55	0,29	0,11	-0,03	0,37	0,11	-0,16	-0,13	1

Tab. 3. Pearson's correlation matrix among the 12 selected variables, bold values are significant at 0,05

A positive correlation between initial discharge value, potential rainfall erosivity and antecedent moisture content at Diga Celone gauging station, where cultivated lands are prevalent, was observed also by Rodríguez-Blanco et al. (2010), concluding that in rural catchments, persistent rainfall in saturated soil with low infiltration capacity may cause the occurrence of floods.

With regard to time delay between peak rainfall and peak discharge (dthmaxQmax), it is negatively related with both Q and SS variables, as highlighted also by Pagano et al. 2019 who evidenced the same dynamic in the Carapelle watershed, which has similar environmental features to the Celone basin. This aspect further explains the delayed transport mechanism (i.e. the faster the flood peak arrives the lower the suspended sediment peak that flows out), highlighting the fast-hydrological response of the basin to rainfall.

Principal component analysis

The preliminary verification tests of adequacy and sphericity confirmed the suitability of all variables for the PCA, the KMO score was 0,59 (>0,5, minimum value for a good PCA) (Hair et al. 2006), whereas Bartlett's test of sphericity was 529,15 with a significance of 0,000 rejecting null hypothesis and proved adequate correlation among variables (Pallant 2005). In addition, the a-parameter test developed by Cronbach 1951 was applied and the result of 0,85 further verified the PCA.

PCA results give three principal components with eigenvalues > 1, which are able to explain more than 75% of the variance (Tab.3).

The first component (PC1) is able to describes alone the 48,45% of the variance, the most representative variables (> 0,75) resulted discharge variables (Qmax, Qmid), total volume of water (Vtot), SS variables (SSCmax, SST), rainfall erosivity (KE_Diga, KE_Faeto), Tflow event and the total rainfall depth measured at Diga Celone gauging station (Htot_Diga). Thus, categorized by the greater loading values, the first component contains the major features of the main dominant forces of water erosion (both KE, Htot_Diga and SSC variables), and transport capacity variables (discharge variables, total volume and duration of flow event).

The second component (PC2) describes alone the 15,47% of the variance. The factors showing higher loading values (> 0,5) were the time shift between the peak of rainfall and the peak of discharge (at both stations). This result highlights that in these kind of rivers, flashy and intermittent, the lag time plays a fundamental role. PC1 and PC2 cumulatively describes 63,93% of the total variance by containing 11 of the initial 18 considered variables, by adding also the third component, we could explain 75,37% of the whole variance (Tab.4, Tab.5).

Total Exlpained variance

	Initial Eigenvalues			Loadings		
Componente	Totale	% di varianza	% cumulativa	Totale	% di varianza	% cumulativa
1	8,721	48,452	48,452	8,721	48,452	48,452
2	2,786	15,477	63,928	2,786	15,477	63,928
3	2,060	11,443	75,372	2,060	11,443	75,372
4	1,137	6,318	81,690			
5	1,006	5,588	87,278			
6	,635	3,528	90,806			
7	,484	2,691	93,497			
8	,447	2,484	95,981			
9	,348	1,933	97,915			
10	,149	,828	98,743			
11	,100	,553	99,296			
12	,078	,435	99,730			
13	,024	,132	99,863			
14	,014	,076	99,939			
15	,006	,034	99,973			
16	,003	,017	99,990			
17	,002	,009	99,999			
18	,000	,001	100,000			

Tab. 4. PCA analysis total explained variance

	Component		
	PC1	PC2	PC3
Qmax	,911	-,066	-,196
Qmid	,908	-,029	-,194
Qini	,726	,374	,195
SSCmax	,894	-,154	-,184
SSCmean	,746	-,260	-,306
SST	,944	,143	,047
Vtot	,956	,151	-,025
KEdiga	,877	,167	-,211
KEfaeto	,830	-,088	,044
Htotdiga	,757	,137	-,104
Htotfaeto	,498	-,681	,195
Imaxdiga	,355	,022	,513
Imaxfaeto	-,123	-,695	,153
AMCdiga	,368	,461	,716
AMCfaeto	,176	,415	,790
dtQ_H_diga	-,251	,736	-,388
dtQ_H_faeto	-,245	,757	-,381
Tflow	,828	,079	-,048

Tab. 5. PCA analysis, explained components

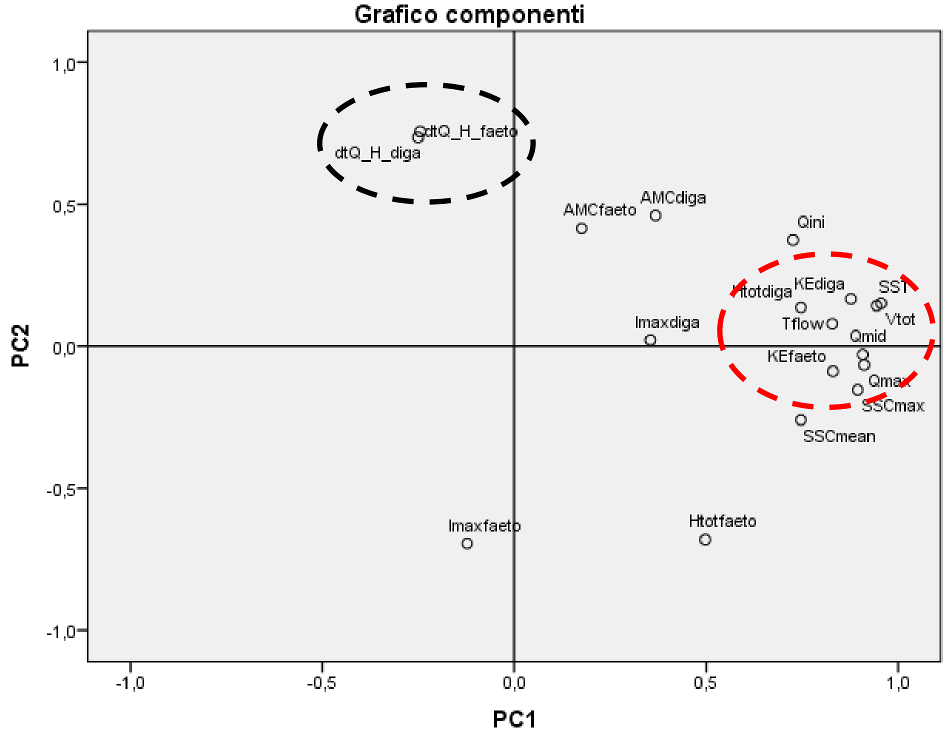

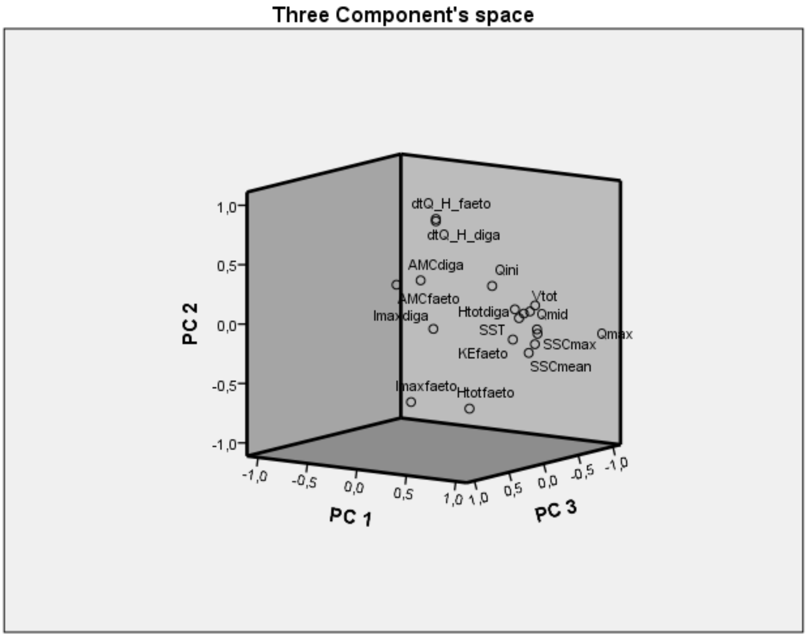

Figure 3. Plotted variables in two component's space, on the right top panel PC1 showing high values for Qmax, Qmid, Vtot, SSCmax, SST, KE Diga Celone, KE Faeto, Tflow event, Htotdiga, and on the left top panel PC2 dominated by dthmax-Qmax Diga and dtHmax-Qmax Faeto

Hysteresis classification of flood events

Hysteresis analysis of flood events showed a prevalent delayed behavior of sediment transport, 19 events over 23, highlighting a distal localization of sediment sources. This was previously investigated also by Di Pillo et al. 2019 that identified the upper area of the river basin as the principal source of fine material before the sink, localized in the valley zone, where medium-grain size material deposited as a consequence of the sudden decrease in bed slope.

When positive HI index was observed, 4 events over 23, the magnitude ranges from HI= 3,77 to HI= 0,32. The higher positive HI value (3,77) was observed on July 2010, when the higher values of Suspended Sediment Concentration (37,62 mg l^{-1}) was reordered. Two switches from positive to negative HI were observed on December 2010 and March 2011, these phenomena could be linked to the nearly sediment depletion during wet condition (biblio). A switch from negative to positive HI was recorded in the dry season (July 2010), attributable to the re-suspension mechanisms of medium and fine grain size materials previously deposited, during a medium-low flow event (Qmax= 0,95 m^3s^{-1}), near the measuring point, after re-mobilized with a successive high flow event (Qmax = 5,7 m^3s^{-1}). Negative HI index varies from -0,02 to -17,8, the average negative values was of -1,63, when wet condition continued thorough multiple consecutive storm events, after the switch trends in negative HI was sustained. When terrain surfaces were covered (from March to June) HI tends to zero. Overall, given the little extent of the watershed absolute values of hysteresis index tends to assess on ≈ -1.

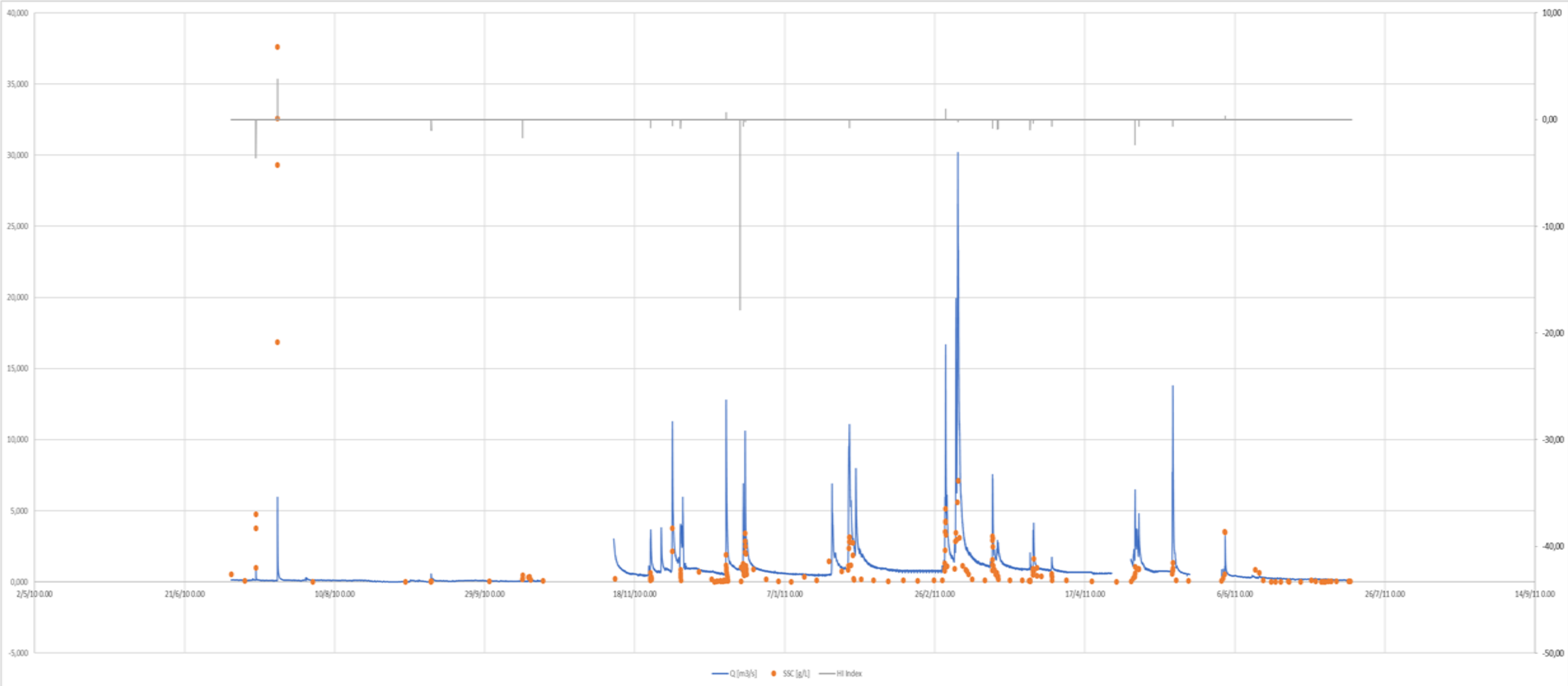

Figure 4. Plotted time series of Q [m3/s] and SSC [g/l] together with evaluated HI index for single flood event

4.4 Conclusion

Good estimation of erosion rates and sediment transport in intermittent rives is fundamental for designing the best maintenance practices of semi-arid watershed. In this study we first investigate the hydro-sedimentary behavior i.e. Q-SSC dynamic at event scale during one year of sampling (2010-2011) in a small flashy river, the Celone. During the study period 23 flood events covering all hydrological condition were observed, Hysteresis Index was calculated for every event. Sediment dynamics have shown a delayed mechanism, 19 over 23 events with a negative HI, confirming the prevalence of distal sediment transport, 4 events show a positive HI index, these events overcomes after dry periods when sediment availability increase, especially near to the measuring point. Shift from positive to negative HI where observed showing sediment exhaustion after subsequent flood events than negative trend was maintained, also a shift from negative to positive HI was observed when moderate floods transport sediment near to the measuring point, immediately available for the successive event.

The drivers of erosion and sediment transport were detected through statistical analysis as Pearson's correlations and Principal Component Analysis. High correlation was found between discharge and suspended sediment variables as expected, inasmuch also good correlation with rainfall potential erosivity, duration of flood events and SS' variables was found, highlighting the important role of runoff dynamics for intermittent rivers. Low correlation with antecedent moisture conditions and 30-min rainfall intensity was observed, confirming that hydrological response is more important than individual soil or rainfall conditions (Lana-Renault et al. 2006).

Principal component analysis aimed to reduce the variables space choosing the most representative ones. Analysis showed as two components of dominant factors PC1 and PC2 could explain more than 63% of the variance of all variables considered. These factors were mainly composed of 11 variables over the initial 18, thus space reduction was achieved, variables was grouped as, dominant force of erosion, transport capacity variables, duration of flood events and lag time between peaks or hydrograph and sedigraph therefore cutting out variables as AMC, rainfall intensity, mean values of suspended sediment concentration and initial value of discharge in a flood, often recognized as relevant drivers for perennial rivers.

Di Pillo et al. 2019, J. Mater. Envir. Sci. 10(3), 225-235

05 – Reservoir siltation and sediment source areas identification

Key words: Silting of reservoir, Physical-based modelling, Water res. management, Sediment source areas,

Abstract

The chapter presents a first attempt to quantify the siltation in a man-made reservoir (Torrebianca) in South-East Italy. The FLORENCE model was used to quantify siltation and a multi-scale modelling approach was developed to identify the main source areas of the transported material. The total specific wet sediment production at the reservoir was quantified in 13.15 t ha-1 yr-1. The Celone river basin is the major source of both sediment and water feeds into reservoir. At sub-basin scale the modelling results show that within the Celone river basin the main source areas of sediment were the upstream zone and the valley area. The floodplain area, where the river assumes a braided morphology features, instead acts as a sink for the coarse material. Based on these results, it was estimated that, from 2000 to 2017, in the absence of appropriate removal operations, the reservoir may have lost 13.77%. These results suggest that a better management measures to reduce sediment transport and silting are needed.

5.1 INTRODUCTION

In Italy there are overall 1224 hydraulic operas, 665 crossbeam and 564 between tanks and reservoirs, mainly located in Umbria, Molise (Centre of Italy) Sardegna (Italian island) and Puglia (South-east of Italy), designed to meet the irrigation and industrial requirements. On the whole these operas provided to hold back an amount of 2475 Mm3 of water (Bazzoffi and Vannino 2009). These works, however, require, in addition to regular maintenance works necessary for the continued operation of all the components, also a focus, concerning the dumping of sediments in the basin itself, which in recent years is becoming increasingly important with respect to other issues (Bazzoffi et al. 2005, Di Silvio 2004, Graf et al. 2010, Kondolf et al. 2014, Valent et al. 2019).

The silting phenomenon is caused generally by heterogeneous factors (Chandran and Janky 2005, Kovacs et al. 2012, Krasa et al. 2005, Shi 2005, Yang et al. 2007) depending by intrinsic characteristics of the underlying basins, such as the soil texture and its hydrological and physical characteristics, morphology and slope of the area, rainfall and hydrological regime.

Over the years, several studies methods and tools were developed to predict reservoir sedimentation, from the Empirical methods, to the newest physical-based and Numerical methods (Huang et al. 2018, Jothiprakash and Garg 2008, Verstraeten and Poesen 2000). Overall it is clear from the literature that empirical methodologies are simpler to use than the other ones, moreover they require less measured data and are also quicker to assess. However, their simplicity makes them useful now only in the first approximation to understand the order of magnitude of the phenomenon (Morris and Fan 1997). Physical-based and numerical methods, due to the increasing develop of computational software and to the innovation in the analysis of spatial data thorough Geographic Information System and remote sensing, are the most used methods to predict the siltation of reservoirs (Borrelli et al. 2014, Panagos et al. 2015, Huang et al. 2018, Abouabdillah et al. 2014, Rosgen 2000).

Nowadays, most of the studies are conducted with the use of models based on different assumptions (Alatorre et al. 2010, De Vente et al. 2013, Jothiprakash and Garg 2008, Kirkby et al. 2003, Minear and Kondolf 2009, Mueller et al. 2010, Van Rompaey et al. 2005). Despite these advances, the evaluation of reservoir siltation still has many aspects that need further clarification. These features regard a more accurate estimate of the volumes of sediments deposited in the reservoir, which are needed to calibrate and validate the models. In addition, it is important to identify an exact schedule of dredging and purging operations, together with proper planning for the reuse and disposal of the sediments, as recommended by the newest national and European legislation (D.Lgs art. 114 03/04/2006, D.M.A.T.T. 30/06/2004 Criteri per la redazione del progetto di gestionedegliinvasi, Water Framemework Directory (WFD) 2000/60/CE). Moreover, also a precise detection of areas that contribute most to the sediment production, the so-called sources areas, is needed to have a broader understanding of the changing dynamics of the basin itself (Collins et al. 2017, De Vente et al. 2006, Gomes-Minella et al. 2004, Gov. of India 2019, Theuring et al. 2013).

On the other hand, source areas identification is needed to implement a Program of Measures oriented to reduce erosion and sediment transport. In Mediterranean watersheds characterized by a large variability in physical and morphological characteristics, experimental activities at field or plot scale are difficult to conduct and their results cannot be extrapolated or up-scaled. Thus, sources areas identification is a difficult task that is generally performed by using model.

However, most of the conceptual and empirical models at basin scale, commonly used to quantify erosion and identify source areas, such as Annualized Agricultural Non-Point Source (AnnAGNPS) (Bingner and Theurer 2005), Soil and Water Assessment Tool (SWAT) (Bazzoffi et al. 2005), are not able to simulate landslides, gully erosion, wind erosion and bank erosion. This limit may have a great influence on the quantification of sediment load which may results underestimated [Abdelwahab et al. 2013, Abouabdillah et al. 2014). In basins where there are mass movements due to landslides or the bank collapse and erosion is relevant, neural networking models developed by using an IPS (Intelligent Problem Solver) procedure may be a valid tool for estimate sediment load.

The aims of the present chapter are to (i) quantify the sediment production at basin scale for the Celone and Lorenzo river basin (Apulia, Italy); (ii) identify the sediment production for sub-basins identifying main sources areas; (iii) estimating the silting and the volume reduction of the reservoir. We used the FLORENCE model v. 1.0 (FLOw of wateRshedsedimENts Calculator based on geographic fEature), a neural networking model that take in account every components of sediment production, such as superficial erosion, gully erosion, bank erosion and mass movements. Despite the amount of spatial analysis, necessary to run the model, it doesn't need any relevant data concerning water or sediment discharge, so it would be useful for those reservoirs fed by ungauged basins.

The purpose is to contribute to improve the knowledge concerning the sediment transport in the area upstream the reservoir, where there are no previous studies, and to test the capability of the FLORENCE model in estimating silting providing a useful tool to reservoir operator and water resources managers who need inexpensive and quick tool for managing reservoir.

5.2 Materials and Methods

Study Area

The study area is composed by the Celone river basin (85.9 km2) and the Lorenzo river basin (51.9 km2), which are the two inflow in the Torrebianca reservoir, in Puglia (SE of Italy). The area is characterized from an average elevation of ca. 386 m.a.s.l. that ranges from 1142 m.a.s.l. to 218 m.a.s.l. (Fig.1). The greatest part of it is localized between 200 and 500 m.a.s.l. (43%), the average slope of the basins is of scilicet 12.5%.

The total length of the drainage system which converges into the reservoir is of 109 km. It is mainly an agricultural area, in which the most available cultivations are durum wheat (46%), sunflower (9%), pastures (6%) and olive groves (8%), there are also frequent deciduous forests (29%).

Insight the study area there are also three wastewater treatment plants which bear to a request for about 4900 inhabitant equivalents, which comes out from the three small villages. In the basin, the agricultural practices may have great influence on the hydrological regime, through the drainage capability of the soil, strictly linked to the use of lands (Van Rompaey and Krasa 2007), and on the water quality of the river (Buck et al. 2004, De Girolamo et al. 2012, Honish et al. 2002, Pratt and Chang 2012, Tong and Chan 2002), mainly due to the diffuse use of fertilizers and also on the disposability of sediment sources [Valent et al. 2019, De Araujo et al. 2006, Hamed et al. 2002, Tian et al. 2010), through the rearrangement of soil caused by frequent tillage, especially during the driest periods [Buck et al. 2004, De Girolamo et al. 2017, De Girolamo et al. 2015).

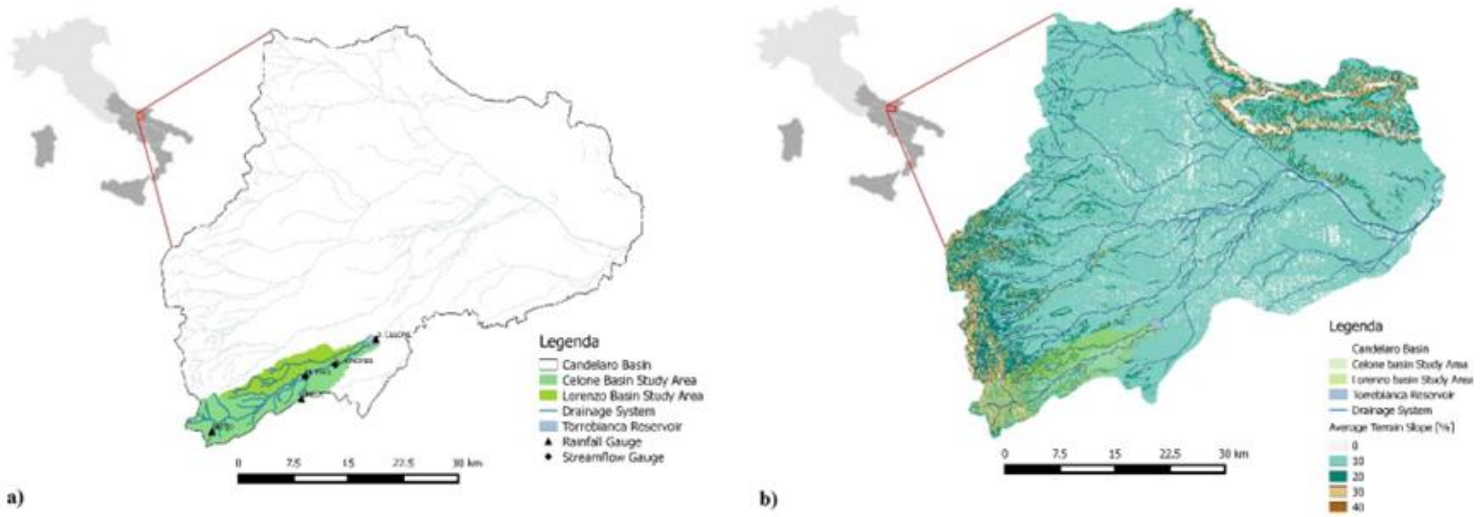

Fig.1. Study area (a), Average Terrain slope (b), (From Di Pillo et al. 2019)

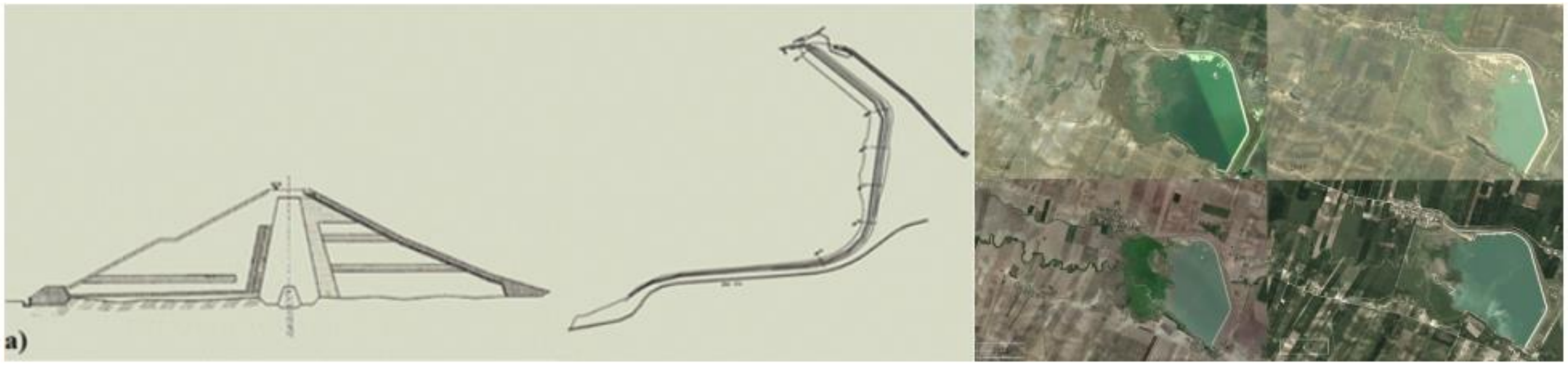

Fig.2. Plan view and cross-sectional view of the opera (a), view of different filling conditions of the reservoir, due to different water level both in wet and dry periods in 2004, 2007, 2012 and 2015 (b) (From Di Pillo et al. 2019).

The Torrebianca reservoir is the most important hydraulic work in this area, it supplies water for agricultural use. It is a zoned heart dam; whose construction began in 1990 to be terminated in 1997 (Consorzio per la bonifica della Capitanata 2007). The main characteristics of the dam are summarized in table 1. and Fig 2. shows the plan and cross section of the work, below a satellite image. The volume in May 2017 was 16.342x106 m3 and its capacity at fully supply is 25.82x106 m3, flow rates hesitate from the spillway, respectively, of the bottom and the derivation is 220m3s-1, 89m3s-1, 7m3s-1.

Torrebianca Reservoir		
Parameter	Value	Unit
Dam Height	20,98	[m]
Quota of Maximum storage	150,05	[m.a.s.l.]
Total volume of reservoir	$25{,}82*10^{6}$	[m^3]
Useful volume adjustment	$16{,}8*10^{6}$	[m^3]
Liquid mirror surface at quota of max. storage	3,15	[km^2]
Liquid mirror surface at quota of max. regulation	2,97	[km^2]

Tab.1. Technical characteristic of the Torrebianca dam (From Di Pillo et al. 2019)

FLORENCE model

To evaluate the sedimentation process upstream the Torrebianca reservoir we applied the FLORENCE model v. 2.0 (FLOw of watershed sedimENts Calculator based on geographic fEature), a tool capable to estimate the basin's specific sediment production over a long period as estimation of the average annual volume of wet sediment [m3km-2y-1].

The model wasdeveloped by the CRA-ABP (Consiglio per la Ricerca e la sperimentazione in Agricoltura- CRA-ABP Centro di Ricerca per l'Agrobiologia e la Pedologia di Firenze) to predict the reservoir siltation (Bazzoffi & Vannino 2009).

This tool relates the volume of sediment, deposited in artificial reservoirs, with physiographic variables, climatic and land use of the underlying basins. The sediment production estimation already takes in account the sub basin's internal re-deposition, furthermore, the model takes in account every components of sediment production, such as superficial erosion, gully erosion, bank erosion and mass movements.

This is a neural networking model developed by using an IPS (Intelligent Problem Solver) procedure (Logananthara et al. 2000, Van Do 2012). This procedure has led to the identification of the best neural network, starting from a 23 variables data set in FLORENCE, then growth to 24 variables with the introduction of the SDR (Sediment delivery Ratio) (Bazzoffi 2008, 2009, ISPRA 2013, ITCOLD 2016). The sensitivity analysis for the input variables of FLORENCE is shown in table 2.

Variable	SDR	Area	Av. Temp.	Drain. Density	Rainfall	Erodib. Area	N° Landslides	Av. Slopes
Rank	1,05	1,11	1,13	1,15	1,18	1,22	1,12	1,05
Ratio	8,00	6,00	4,00	3,00	2,00	1,00	5,00	7,00

Tab.2. Sensitivity analysis for the eight FLORENCE input variables

In FLORENCE, eight inputs data set described through the paper are needed. FLORENCE model has already been applied in Italy with success (Casciolo et al. 2010, Dono et al. 2005). It requires a GIS software (ArcMap, QGIS) for the spatial analysis of the input data. In the present work QGIS was used for all the spatial data elaborations. The model can be used for estimating the contribution of sub-areas, characterized by homogeneous features, to the total load. We applied the web application FLORENCE v. 1.0 (http://florence.homelinux.com/login.php) tool at two different spatial scales discretization of the study area. In a first application, we considered both the Celone and Lorenzo river basins, with the specific aim to evaluate the total sediment production of the whole area draining into the reservoir. Then, we evaluate only the sediment production of Celone basin, which was previously found to be the major source of both, water and sediments, for the dam.

We further divided the study area of the Celone into three sub-spatial units to find the major sediment sources within the basin itself. Three sub-areas which are homogeneous units in terms of rainfall characteristics, average slope and soil texture, were identified. Spatial data were re-analyses in GIS space to set up the model.

Spatial data analysis

According to the user's guide of the model (http://abp.entecra.it/florence/istruzioni.pdf), we first assessed the drainage area after selecting the closing section [km^2], after that we estimated the erodible surface of the basin, given as a portion of the area itself [km^2], calculated by multiplying each portion of the surface with a specific land use by a given coefficient of erodibility that ranges from 0 (not erodible) to 1 (totally erodible).

We used the Corine Land Cover 2012 for the scope (http://www.sinanet.isprambiente.it/it/sia-ispra/downloadmais/corine-land-cover), which was reclassified through field surveys.

In the study area, in recent decades, land use changes were not recorded. We estimated the stream drainage density [km^{-1}] as the ratio between the surface area of the basins and the length of its river network. The average slope of the area was evaluated through an analysis of the Digital Elevation Model of the area. Then, other inputs are automatically calculated by the model itself.

Climatic data such as average temperature [°C] and rainfall [mm] are included in the model database and also the numbers of the landslides on the area are evaluated by the model once selected the municipalities included in the basin, in part or in whole. The ability to take into account, in the calculation of total wet sediment production, the influence of gully erosion, landslides and mass movements is a key point. In fact, compared to other physically based models, FLORENCE can consider the susceptibility of the stream to these phenomena, including in its database the number of known landslides in the selected municipalities. Such susceptibility is generally very high for small basins in the southern Mediterranean [Andriani et al. 2009, 2015, conforti et al. 2011, Leoni et al. 2011) possibly contributing to the production of sediment for many t ha^{-1} $year^{-1}$.

Multiscale Modelling

In the Celone basin, due to the presence of a first alluvial plain in the middle course of the river, there is a deposition of the coarse material. Here the river assumes a braided morphology features. We have applied the FLORENCE model differentiating three sub-areas. The aim was, on the one hand, to understand how a different spatial distribution of sub-basins influences the model results and, on the other hand, to estimate the Celone basin contribution to the entire phenomenon of silting of Torrebianca reservoir. We modelled the production of wet sediment through the above described spatial analysis for each sub-area.

First Modelling data inputs			
Input	Unit	Celone and Lorenzo river basin	Celone river basin
Area	Km^2	137,77	85,9
Drainage Density	Km^{-1}	0,791	0,704
Erodible Area	Km^2	97,87	59,47
Av. Slope	%	12,82	12,71

Table3:Calculated inputs for the modelling procedure applied at basin scale

The division of the entire Celone drainage area in three sub-areas was made taking in account the homogeneity of each sub area, both from the point of view of geo-morphological characteristics (i.e. hillslope, containment of the slopes, soil composition and land use) and hydrological/hydraulics characteristics (i.e. geometry and steepness of the river bed, and river morphology). This subdivision has led to the identification of three homogeneous subareas described as follows:

The upstream zone: it is characterized by high slope gradients (22.86%) that gives a high containment to the river (Rinaldi et al. 2010) which here is incised. The land use mainly consists of forest territories, with some parts of the area destined to non-irrigated crops and pastures, providing a poor erodible surface (11.47 km^2).

The floodplain area: here the containment action of the slopes is minimal, almost absent, due to the reduction of its steepness (12.48%); this reduction contributes to change the river morphology (Rosgen et al. 2001) that becomes braided with a deposition of the coarse material. The changes of the morphology bring also an increase of the erodible area (18.22 km2), encouraging cultivability the surrounding land (Clarke & Rendell 20009.

The valley area: this is the final stretch of the river that flows in the reservoir, here the hillslopes and the bed slopes continue to decrease (5.63%), the river morphology returns to single channel, whereas the sinuosity increases. Here the agriculture is intensive, and the management practices support the increase of erodibility (29.78 km^2) (Capolongo et al. 2008, Sharma et al. 2011).

Second Modelling data inputs				
Input	Unit	Upstream zone	Floodplain area	Valley Area
Area	Km^2	27,92	25,95	32,12
Drainage Density	Km^{-1}	0,62	0,82	0,75
Erodible Area	Km^2	11,47	18,22	29,78
Av. Slope	%	22,86	12,48	5,63

Table4:Calculated inputs for the modelling procedure applied at sub-basin scale

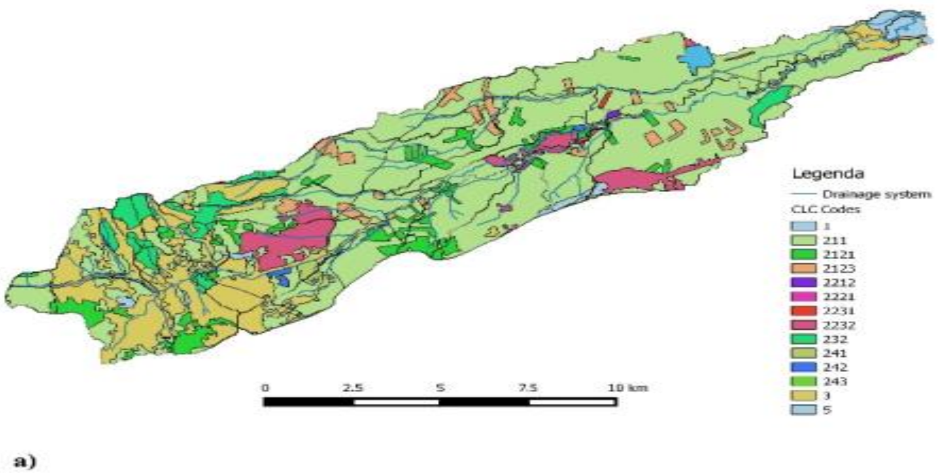

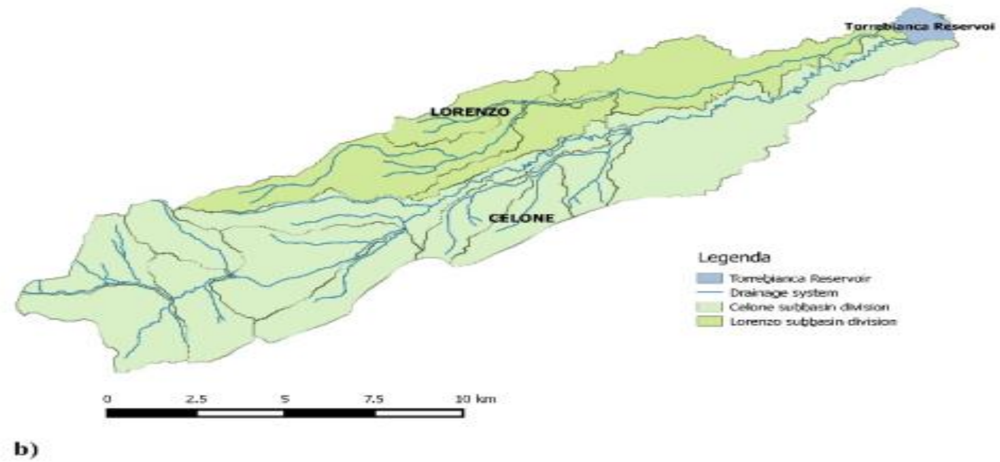

Fig.3. Land use (a), Celone and Lorenzo basins subdivision (b) (From Di Pillo et al. 2019)

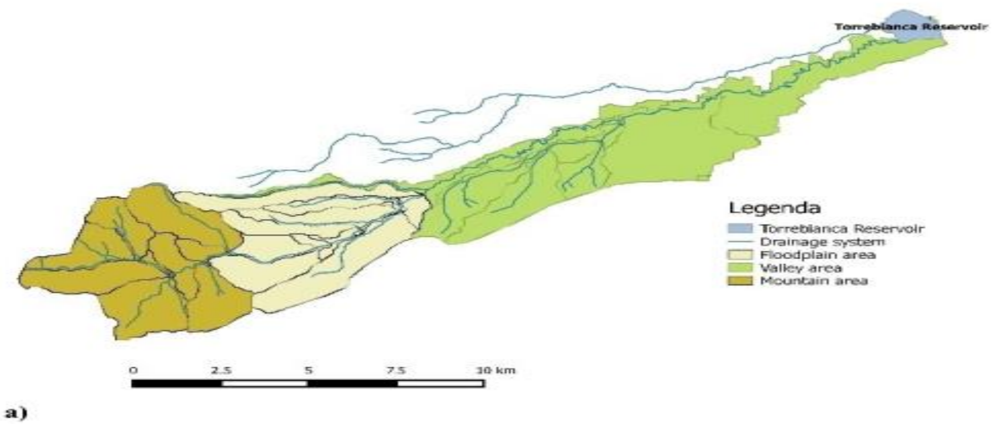

Fig.4. Subareas division of the Celone river basin (a), floodplain area satellite images (b) (From Di Pillo et al. 2019)

5.3 Results and Discussion

Sediment Produciton

The results of the model applied to the whole drainage area showed a total production of wet sediment of 1518.63 m^3 $km^{-2}y^{-1}$, whilst considering only the Celone river basin it amounted to 1474.48 m^3 $km^{-2}y^{-1}$. These values were then processed to obtain data of weight of sediment production, which are 13.15 t $ha^{-1}y^{-1}$ and 12.78 t $ha^{-1}y^{-1}$, respectively. We considered, in the absence of additional studies necessary for a more targeted characterization of the stratigraphic of the bottom of the riverbed, an average density value of the sediment equal to 0.866 t m^{-3} (Bazzoffi et al. 2009). The results show that the contribution to total sediment yield per hectare from the Lorenzo basin is higher than that calculated for the Celone basin, however, in absolute terms considering the drainage area the contribution of the Celone is higher than that of Lorenzo. At sub-basin scale, analysing the modelling results of the first sub-area, we have found that the wet sediment production was of scilicet 1011.55 $m^3km^{-2}y^{-1}$, which corresponds to 8.76 t $ha^{-1}y^{-1}$, once reported in the specific production of sediment with the above transformation. This value is comparable with other specific sediment production data for mountain basins of small extent (de Vente et al. 2006, Nelson et al. 2002, Shi et al. 20149. The same procedures are also been adopted for the second (floodplain area) and third (valley area) sub area, individually, the results are shown in tab.5.

	Outputs	
Input	Volume of wet sediment [$m^3km^{-2}y^{-1}$]	Specific sediment production [$tha^{-1}y^{-1}$]
Celone and Lorenzo river basin	1518,63	13,15
Celone river basin	1474,48	12,78
Upstream zone of Celone river basin	1011,55	8,76
Floodplain area of Celone river basin	662,7	5,74
Valley area of Celone river basin	1085,35	9,4

Table5: Calculated outputs for the entire modelling procedure

Silting phenomenon and water resource reduction

The amount of wet sediment in terms of volume obtained for the entire drainage area, 1518.63 $m^3km^{-2}y^{-1}$, was subsequently adopted as input to assess the silting thorough two indexes (Tian et al. 2010): the average annual silting rate, TI% (Eq.1), and then the silting degree of the global volume of the dam, GI% (Eq.2).

$$T_i = (V_{int}/V_{ti}) * 100 \qquad \text{(Eq.1)}$$

$$G_i = ((V_{int} * \Delta T)/V_{ti}) \qquad \text{(Eq. 2)}$$

Where:

Vint is the wet sediment volume of the entire drainage into the reservoirs (1518.63x137.77);

Vti is the adjustment volume of water of the reservoir at the initial time step (25.82x106 m^3);

ΔT is the working period of the opera (17 yr^{-1}).

The first index, TI, shows that the Torrebianca reservoir is affected by a silting of 0.81% of percentage of its volume corresponding to 2.09x105 m^3 yr^{-1}. This implies that during 17 years of operation, from 2000 to 2017, in the absence of appropriate removal operations, the reservoir may have lost 13.77%. of its volume i.e. scilicet 3.56x106 m^3.

According to other studies for the Mediterranean region (Patra et al. 2019, Shi et al. 2014, Schleiss et al. 2013), it means that the filling up by sediment is the most dangerous factor to manage, notwithstanding water losses in a reservoir could be caused also by other factors, like evaporation of surface water or seepage 8Panagos et al. 2015, Mugabe et al. 2003).

Multi scale modelling validation

For the Celone river basin, considering the whole basin, the results (12.78 t $ha^{-1}y^{-1}$) are in line with that of other small and medium sized reservoirs of the Mediterranean region 8Borrelli et al. 2014, de Vente et al. 2013, 2007, 2006, Abdelwhab et al. 2013, Nadal-Romero et al. 2011, Vanmaercke et al. 2011). Moreover, for the same river basin, the suspended sediment load, already evaluated in previous studies [74], were estimated in a range between 1.41 and 11.23 t $ha^{-1}y^{-1}$, this range seem to be comparable with the model output, once considered the bed load part of the transport phenomenon, as the model's output is a total production of sediment [Rovira et al. 2005, Turowski et al. 2010, Vericat & Batalla 2010), unfortunately, neither measurements of total sediment or previous studies are available concerning the Lorenzo sub-watershed.

Once divided the Celone river basin into three homogeneous macro-areas, the results show that the upstream zone has an elevated specific total sediment yield production that can be justified by high average slopes and medium-high erodible area. In the transition areas, between upstream and floodplain area, the specific total sediment production tends to decrease, passing from 8.76 t $ha^{-1}y^{-1}$to 5.74 t $ha^{-1}y^{-1}$. This behavior is explained by the sudden drop of the slopes which passes from 22.86 % to 12.4 % leading to a sharp decrease in the current carrying capacity and therefore to the immediate release of the sediment coarser fractions 8Alekseevskiy et al. 2008, Ali et al. 2012, Zhang et al. 2009), giving to the riverbed a characteristic braided morphology. We can also appreciate this release phenomenon by analyzing the satellite images of this zone Fig.4. In this macro-area, the transport phenomenon is mostly in suspension, further corroborating the comparison between the fitted suspended sediment loads already evaluated by De Girolamo et al. (2018). In the plain area, the third macro-area, there is an absence of forest and the land use is prevalently agricultural land (90% of the entire area) that implies an increase of erodible area compared with the rest of the basin. In addition, here there is a remobilization of a part of coarser grains, landing to a specific total sediment production of 9.4 t $ha^{-1}y^{-1}$.

In light of this, we can assume that the main source area of the sediments are precisely the downstream zone and the upstream zone, while the intermediate zone, floodplain area, would act on the transport phenomenon such a filter action for grains with larger diameter. This behavior has an important reply once considered the temporary characteristic of the river. In fact, the middle area itself could became an important source area of medium-large grain, deposited during the low and medium flow regime, which are more frequent than the high flow where this material could be re-mobilized by the hidden and intense peaks of discharge, properly of this kind of rivers.

5.4 Conclusion

This chapter represent a first attempt to estimate sediment transport and silting in an area where data availability is limited. In light of the growing impact that the issue of reservoir sedimentation would have, especially on European and Italian reservoirs in the next few years, the present work would give a contribute to the current knowledge concerning the silting phenomenon. The FLORENCE model proved to be a useful tool for quantifying the sediment transport especially in ungauged basins, in which direct estimate of sediment transport represents a hard and costly task linked to an appropriate data campaign. Despite its simplicity, the model is useful for estimating the magnitude of the silting phenomenon at the reservoir closing section with appropriate accuracy. In addition, it is able to identify sources areas, feeding sediment transport, providing useful indications to the water resources managers on the zone that could be re-organized, re-projected or re-arranged to minimize the problem. Furthermore, by implementing and interpreting a similar multi-scale modelling procedure it is possible to identify the areas that are main responsible of sediment production. In this case, the fact that there are previous studies concerning the sediment transport has also allowed us to compare this result with them, finding a match.

06 – Concluding Remarks

This thesis work aimed to give a deep explaination of the complex mechanisms that underlying hydro-sedimentaru behaviour of intermittent river systems.

We started from a one year (June 2010 – July 2011) continuous measurements of discharge (Q) and discrete samplings of Suspended Sediment Concentration (SSC),n*216 total samplings of SSC were taken, covering all hydrological conditions.

Given the hydrological peculiarities of the Celone river, an temporary stream, that has an hydrological regime quite specific that shows a high an drapid variability in streamflow, flash floods and an extreme low flow or absence of flow, peculiarities that exert a great influence on erosion and sediment transport, we tried to afford the so called "Load Estimation Problem" starting from the fact that there is a general lack of adequate formulas because of most of them were assessed for perennial rivers one, notwithstanding this kind of streams (temporary) is quite common in several regions around the world.

Our general proposes were both to improve the understanding of suspended sediment transport phenomenon and to provide a guide, which can be useful to water resources managers, for designing a monitoring program and for selecting a method to estimate sediment load.

With this spirit we estimate suspended sediment load by using almost all methodologies commonly applied in perennial rivers, tying to identify a technique able to improve the accuracy, reducing uncertainty interval specifically for a temporary river system and than by means of the uncertainty analysis, quantify the degree of confidence that users can assign to a given load estimation method

Results of this first step identify the hydrological regime as the key factor in sediment load estimations in Mediterranean basins. In addition, the results of available previous studies in literature, were only partially confirmed by them; for instance, we found that the seasonal stratification of the entire dataset in subsets, suggested by several author in their studies about perennial rivers, doesn't work very well in temporary streams. Meanwhile, the stratification on flow regime increases the accuracy of all methods in estimating loads. Hence, this technique is suggested in temporary rivers. Analysing several possible flow regime stratifications we also identified those which are more suitable.

After this step, starting from the non-linear, but complex and multivariate relationship between Q and SSC, we assessed an event scale analysis, based on the same data-set, trying to find drivers of transport mechanism.

Among the great number of independent variables suitable to assess the multivariate analysis, we have chosen 18, the most significant of those analyzed by other authors, with the specific aim to observe differences, also in the driving factors, between perennial and temporary rivers.

By using a Principal Component Analysis, we were able to identify 11 variables among the initial 18 that can be taken as dominant forces in the suspended sediment transport mechanism of the Celone river. As expected some variables i.e. AMC, initial flood discharge, and rainfall intensity, already described as fundamental to take in account in the Q-SSC relationship description for perennial river systems, were excluded .

Also an hysteresis analysis of Q-SSC loops during single flood events were conducted, following an antecedent and organic characterization already done by De Girolamo et al. 2015, but assessing it through an indexing approach with two aims, to were able to compare different basins with similar characteristics, since the HI index were dimensionless and to understand the ability of this mehodology to effectively describe hysteresis, also by loosing specific features as the shape of the loops etc..

The analysis confirmed that the description of the overall hysteresis behaviour i.e. anticlockwise with a distal transport mechanism, were detected, also other punctual mechanisms such as sediment exhaustion after subsequent floods and re-suspension of near source sediments were right described, we than concluding that notwithstanding could be difficult to analyse eight shaped or complex loops and when high resolution data sets are available it is preferable to carry out in-depth analysis of hysteresis loops, when we are in a data-scarce situation indexing description of hysteresis as a first approach might be useful thanks also to the ability to be implemented with few concentration and discharge data.

Finally, to highlight consequences that sediment transport could have in the absence of correct management strategies, we assessed a first attempt to quantify the siltation of the Torre Bianca reservoir, 8 km downstream the gauging station, that provides water for agricultural and industrial uses as well as the largest hydraulic work in the area.

Analysis was carried out through a physical-based model, able to quantify the long-term sediment production at the basin scale. With the further aim to identify also those zones most inclined to sediment delivery we divided the study area in three homogeneous sub-areas. We than started modelling, observing that, basin scale sediment production where in line with total sediment load estimated in the first step, moreover with a multiscale modelling we also observed that within the Celone basin, different erosion-sedimentation and resuspension mechanisms took place. The analysis shows also that over the years different managing action will be needed to maintain the usable life of the dam, reducing water disposability loss.

REFERENCES

Abouabdillah, A., White, M., Arnold, J.G., De Girolamo, A.M., Oueslati, O., Maataoui, A., Lo Porto, A., 2014. Evaluation of soil and water conservation measures in a semi-arid river basin in Tunisia using SWAT. Soil Use Manag. 30 (4), 539–549. http://dx.doi.org/10.1111/sum.12146.

Achite, M., Ouillon, S., 2007. Suspended sediment transport in a semiarid watershed, Wadi Abd, Algeria (1973–1995). J. Hydrol. 343 (3–4), 187–202. http://dx.doi.org/10.1016/j.jhydrol.2007.06.026.

Achite, M., Ouillon, S., (2007). Suspended sediment transport in a semiarid watershed, Wadi Abd, Algeria (1973–1995). J. Hydrol. 343 (3–4), 187–202. http://doi:10.1016/j.jhydrol.2007.06.026

Ahanger, M. A., Asawa, G. L., & Lone, M. A. (2008). Experimental study of sediment transport hysteresis. Journal of Hydraulic Research, 46(5), 628-635.

Ahanger, M. A., Asawa, G. L., & Lone, M. A. (2013). Hysteresis effect on sediment rating curves. J. Acad. Ind. Res, 1(8).

Aich, V., Zimmermann, A., & Elsenbeer, H. (2014). Quantification and interpretation of suspended-sediment discharge hysteresis patterns: How much data do we need?. Catena, 122, 120-129.

Alekseevskiy, N. I., Berkovich, K. M., & Chalov, R. S. (2008). Erosion, sediment transportation and accumulation in rivers. *International Journal of Sediment Research*, *23*(2), 93-105.

Alexandrov, Y., Cohen, H., Laronne, J. B., & Reid, I. (2009). Suspended sediment load, bed load, and dissolved load yields from a semiarid drainage basin: A 15-year study. Water resources research, 45(8).

Alexandrov, Y., Laronne, J.B., Reid, I. (2007). Intra-event and inter-seasonal behaviour of suspended sediment in flash floods of the semiarid Northern Negev, Israel. Geomorphology 85(1–2): 85–97

Alexandrov, Y., Laronne, J.B., Reid, I., 2003. Suspended Sediment Transport in Flash Floods of the Semiarid Northern Negev, Israel (November 2015). pp. 346–352. Retrieved from. http://www.cabdirect.org/abstracts/20033080936.

APAT-IRSA-CNR, 2003. Metodi analitici per le acque. In: APAT Manuali e Linee Guida. 29. pp. 1–1153.

Aronica, I., & Paltrinieri, E. (1954). Bonifica montana nel comprensorio dell'Alto Simeto. Ist. Poligrafico dello Stato.

Anderson, H. W. (1957). Relating sediment yield to watershed variables. Eos, Transactions American Geophysical Union, 38(6), 921-924.

Andriani, G. F., Diprizio, G., & Pellegrini, V. (2015). Landslide susceptibility of the La Catola Torrent catchment area (Daunia Apennines, southern Italy): a new complex multi-step approach. In *Engineering Geology for Society and Territory-Volume 5* (pp. 387-392). Springer, Cham.

Arthington, A.H., 2012. Effects of dams on habitat and aquatic biodiversity. In: Environmental Flows, pp. 113–124. (October 2012). https://doi.org/10.1525/california/9780520273696.003.0008

Asselman, N.E.M., 2000. Fitting and interpretation of sediment rating curves. J. Hydrol. 234 (3–4), 228–248. http://dx.doi.org/10.1016/S0022-1694(00)00253-5.

Bagarello, V., Di Stefano, C., Ferro, V., Pampalone, V., 2017. Predicting maximum annual values of event soil loss by USLE-type models. Catena 155, 10–19. http://dx.doi.org/10.1016/j.catena.2017.03.002

Bangash, R. F., Passuello, A., Sanchez-Canales, M., Terrado, M., López, A., Elorza, F. J., ... & Schuhmacher, M. (2013). Ecosystem services in Mediterranean river basin: climate change impact on water provisioning and erosion control. Science of the Total Environment, 458, 246-255.

Bazzoffi, P., Abbattista, F., Vanino, S., Napoli, R., Fais, A., & Nino, P. (2005). LOSS OF WATER STORAGE CAPACITY OF RESERVOIRS IN SOUTHERN ITALY: ECONOMIC IMPLICANCES OF SEDIMENTATION. In Proceedings of OECD Workshop on Agriculture and Water: Sustainability, Markets and Policies.

Beale, E.M.L., 1962. Some uses of computers in operational research. In: Industrielle Organisation. 31. pp. 51–52.

Bisantino, T., Bingner, R., Chouaib, W., Gentile, F., & Trisorio Liuzzi, G. (2015). Estimation of runoff, peak discharge and sediment load at the event scale in a medium-size Mediterranean watershed using the AnnAGNPS model. Land degradation & development, 26(4), 340-355.

Bisantino, T., Gentile, F., & Trisorio Liuzzi, G. (2011). Continuous monitoring of suspended sediment load in semi-arid environments. Sediment transport, 296-312.

Bisantino, T., Gentile, F., Milella, P., Trisorio Liuzzi, G., 2010. Effect of time scale on the performance of different sediment transport formulas in a semiarid region. J. Hydraul. Eng. 136 (1), 56–61. http://dx.doi.org/10.1061/(ASCE)HY.1943-7900.0000125.

Bischoff, K.B. Levenspiel, O. Fluids dispersion generalization and comparison of mathematical models—I generalization of models. *Chem. Eng. Sc.* **1962**, *17(4)*, 245-255.

Borrelli, P., Märker, M., Panagos, P., & Schütt, B. (2014). Modeling soil erosion and river sediment yield for an intermountain drainage basin of the Central Apennines, Italy. *Catena*, *114*, 45-58.

Brandt, C. J. (1990). Simulation of the size distribution and erosivity of raindrops and throughfall drops. Earth Surface Processes and Landforms, 15(8), 687-698.

Bussi, G., Francés, F., Montoya, J. J., & Julien, P. Y. (2014). Distributed sediment yield modelling: Importance of initial sediment conditions. *Environmental modelling & software*, *58*, 58-70. http://dx.doi.org/10.1016/j.envsoft.2014.04.010.

Butturini, A., Alvarez, M., Bernal, S., Vazquez, E., & Sabater, F. (2008). Diversity and temporal sequences of forms of DOC and NO3-discharge responses in an intermittent stream: Predictable or random succession?. Journal of Geophysical Research: Biogeosciences, 113(G3).

Capolongo, D., Pennetta, L., Piccarreta, M., Fallacara, G., & Boenzi, F. (2008). Spatial and temporal variations in soil erosion and deposition due to land-levelling in a semi-arid area of Basilicata (Southern Italy). *Earth Surface Processes and Landforms: The Journal of the British Geomorphological Research Group*, *33*(3), 364-379.

Casalí, J., Gastesi, R., Álvarez-Mozos, J., De Santisteban, L. M., de Lersundi, J. D. V., Giménez, R., ... & López, J. J. (2008). Runoff, erosion, and water quality of agricultural watersheds in central Navarre (Spain). agricultural water management, 95(10), 1111-1128.

Casalí, J., Giménez, R., De Santisteban, L., Álvarez-Mozos, J., Mena, J., & de Lersundi, J. D. V. (2009). Determination of long-term erosion rates in vineyards of Navarre (Spain) using botanical benchmarks. Catena, 78(1), 12-19.

Chahor, Y., Casalí, J., Giménez, R., Bingner, R. L., Campo, M. A., & Goñi, M. (2014). Evaluation of the AnnAGNPS model for predicting runoff and sediment yield in a small Mediterranean agricultural watershed in Navarre (Spain). Agricultural Water Management, 134, 24-37.

Chandran, R., & Jansky, L. (2005). Sustainable management of sediments at reservoirs: a comparative study from Asia, Africa and Europe. In *Proceedings of the 11th world lakes conference, Nairobi, Kenya, 31 October-4 November 2005: volume I/ed. by EO Odada and...[et al]. pp. 33-39* (pp. 33-39).

Collins, A. L., Pulley, S., Foster, I. D., Gellis, A., Porto, P., & Horowitz, A. J. (2017). Sediment source fingerprinting as an aid to catchment management: a review of the current state of knowledge and a methodological decision-tree for end-users. *Journal of environmental management*, *194*, 86-108.

Cooper, D.M., Watts, C.D., 2002. A comparison of river load estimation techniques: application to dissolved organic carbon. Environmetrics 13 (7), 733–750. http://dx.doi.org/10.1002/env.525.

Cronbach, L. J. (1951). Coefficient alpha and the internal structure of tests. psychometrika, 16(3), 297-334.

Cudennec, C., Leduc, C., & Koutsoyiannis, D. (2007). Dryland hydrology in Mediterranean regions—a review. Hydrological Sciences Journal/Journal des Sciences Hydrologiques, 52(6), 1077-1087.

Damnati, B., Ibrahimi, S., & Radakovitch, O. (2013). Quantifying erosion using 137Cs and 210Pb in cultivated soils in three Mediterranean watershed: Synthesis study from El Hachef, Raouz and Nakhla (North West Morocco). Journal of African Earth Sciences, 79, 50-57.

Dang, T. H., Coynel, A., Orange, D., Blanc, G., Etcheber, H., & Le, L. A. (2010). Long-term monitoring (1960–2008) of the river-sediment transport in the Red River Watershed (Vietnam): Temporal variability and dam-reservoir impact. Science of the Total Environment, 408(20), 4654-4664.

D'Ambrosio, E., De Girolamo, A. M., & Rulli, M. C. (2018). Assessing sustainability of agriculture through water footprint analysis and in-stream monitoring activities. Journal of Cleaner Production, 200, 454-470.

D'Ambrosio, E., De Girolamo, A.M., Barca, E., Ielpo, P., Rulli, M.C., 2016. Characterising the hydrological regime of an ungauged temporary riversystem: a case study. Environ. Sci. Pollut. Res. 24 (16), 13950–13966. http://dx.doi.org/10.1007/s11356-016-7169-0.

D'Ambrosio, E., De Girolamo, A. M., Spanò, M., Corbelli, V., Capasso, G., Morea, M., ... & Ricci, G. F. (2019). A spatial analysis to define data requirements for hydrological and water quality models in data-limited regions. Water, 11(2), 267.

De Girolamo, A.M., Lo Porto, A., 2012. Land use scenario development as a tool for watershed management within the Rio Mannu Basin. Land Use Policy 29 (3), 691–701. http://dx.doi.org/10.1016/j.landusepol.2011.11.005.

De Girolamo, A.M., Pappagallo, G., Lo Porto, A., 2015a. Temporal variability of suspended sediment transport and rating curves in a Mediterranean river basin: the Celone (SE Italy). Catena 128, 135–143. http://dx.doi.org/10.1016/j.catena.2014.09.020.

De Girolamo, A.M., Gallart, F., Pappagallo, G., Lo Porto, A., 2015b. Assessing flow regime alterations in a temporary river. J. Hydrosci. Hydraul. Eng. 63 (3), 263–272. http://dx.doi.org/10.1515/johh-2015-0027.

De Girolamo, A.M., D'Ambrosio, E., Pappagallo, G., Rulli, M.C., Lo Porto, A., 2017a. Nitrate concentrations and source identification in a Mediterranean river system. Rendiconti Lincei 28, 291–301. http://dx.doi.org/10.1007/s12210-016-0593-8.

De Girolamo, A.M., Balestrini, R., D'Ambrosio, E., Pappagallo, G., Soana, E., Lo Porto, A., 2017b. Antropogenic input of nitrogen and riverine export from a Mediterranean catchment. The Celone, a temporary river case study. Agric. Water Manag. 187, 190–199. http://dx.doi.org/10.1016/j.agwat.2017.03.025.

De Girolamo, A. M., Di Pillo, R., Porto, A. L., Todisco, M. T., & Barca, E. (2018). Identifying a reliable method for estimating suspended sediment load in a temporary river system. Catena, 165, 442-453.

de Vente, J., Poesen, J., Verstraeten, G., Govers, G., Vanmaercke, M., Van Rompaey, A., ... & Boix-Fayos, C. (2013). Predicting soil erosion and sediment yield at regional scales: where do we stand?. Earth-Science Reviews, 127, 16-29.

de Vente, J., Poesen, J., Govers, G., Boix-Fayos, C., 2009. The implications of data selection for regional erosion and sediment yield modelling. Earth Surf. Process. Landf. 34 (15), 1994–2007. http://dx.doi.org/10.1002/esp.1884.

de Vente, J., Poesen, J., Arabkhedri, M., & Verstraeten, G. (2007). The sediment delivery problem revisited. Progress in Physical Geography, 31(2), 155-178.

Di Pillo, R., De Girolamo, A. M., & Todisco, M. T. (2019). Modelling the silting-up of a small reservoir fed by a temporary river: the Torrebianca reservoir study case (Puglia, SE Italy), Journal of Material and Environmental sciences, 10(3), 225-235.

Di Silvio. (2004) *Autorità di Bacino della Basilicata, Studi e Ricerca*, Vol. 4. Parte, I. I. IL FENOMENO DI INTERRIMENTO DEGLI INVASI ARTIFICIALI.

Dominic, J. A., Aris, A. Z., & Sulaiman, W. N. A. (2015). Factors controlling the suspended sediment yield during rainfall events of dry and wet weather conditions in a tropical urban catchment. Water resources management, 29(12), 4519-4538.

Duan, N., 1983. Smearing estimate: a nonparametric retransformation method. J. Am. Stat. Assoc. 78 (383), 605–610. http://dx.doi.org/10.2307/2288126.

Duru, U., Wohl, E., & Ahmadi, M. (2017). Factors controlling sediment load in the Central Anatolia Region of Turkey: Ankara River basin. Environmental management, 59(5), 826-841.

Duvert, C., Gratiot, N., Evrard, O., Navratil, O., Némery, J., Prat, C., & Esteves, M. (2010). Drivers of erosion and suspended sediment transport in three headwater catchments of the Mexican Central Highlands. Geomorphology, 123(3-4), 243-256.

Einstein, H. A. (1950). The bed-load function for sediment transportation in open channel flows (No. 1026). US Government Printing Office.

Engelund, F., & Fredsøe, J. (1976). A sediment transport model for straight alluvial channels. Hydrology Research, 7(5), 293-306.

Estrany, J., Garcia, C., Walling, D.E., Ferrer, L., 2011. Fluxes and storage of fine-grained sediment and associated contaminants in the Na Borges River (Mallorca, Spain). Catena 87 (3), 291–305.

Field, A. (2005). Discovering statistics using SPSS, Newberry Park.

Ferguson, R.I., 1986. River loads underestimated by rating curves. Water Resour. Res. 22 (1), 74–76. http://dx.doi.org/10.1029/WR022i001p00074.

Foteh, R., Garg, V., Nikam, B. R., Khadatare, M. Y., Aggarwal, S. P., & Kumar, A. S. (2018). Reservoir Sedimentation Assessment Through Remote Sensing and Hydrological Modelling. *Journal of the indian Society of Remote sensing*, *46*(11), 1893-1905.

Gallart, F., Pérez-Gallego, N., Latron, J., Catari, G., Martínez-Carreras, N., Nord, G., 2013. Short- and long-term studies of sediment dynamics in a small humid mountain Mediterranean basin with badlands. Geomorphology 196, 242–251. http://dx.doi.org/10.1016/j.geomorph.2012.05.028.

Gao, P., Pasternack, G. B., Bali, K. M., & Wallender, W. W. (2007). Suspended-sediment transport in an intensively cultivated watershed in southeastern California. *Catena*, *69*(3), 239-252.

García-Rama, A., Pagano, S.G., Gentile, F., Lenzi, M.A., 2016. Suspended sediment transport analysis in two Italian instrumented catchments. J. Mt. Sci. 13 (6), 957–970.

Gentile, F., Bisantino, T., Corbino, R., Milillo, F., Romano, G., Liuzzi, G.T., 2010. Monitoring and analysis of suspended sediment transport dynamics in the Carapelle torrent (southern Italy). Catena 80 (1), 1–8. http://dx.doi.org/10.1016/j.catena.2009.08.004.

Giandotti, M. (1934). Previsione delle piene e delle magre dei corsi d'acqua, Ministero dei LL. PP., Servizio Idrografico Italiano. Memorie e Studi Idrografici, 8.

Gonzalez-Hidalgo, J. C., Batalla, R. J., & Cerda, A. (2013). Catchment size and contribution of the largest daily events to suspended sediment load on a continental scale. *Catena*, *102*, 40-45. doi:10.1016/j.catena.2010.10.011.

Graf, W. L., Wohl, E., Sinha, T., & Sabo, J. L. (2010). Sedimentation and sustainability of western American reservoirs. *Water Resources Research*, *46*(12).

Suszka, L., & Graf, W. H. (1987). Sediment transport in steep channels at unsteady flow. In Proceedings of XXII congress, IAHR, Lausanne, Switzerland. p (pp. 167-175).

Harmel, R.D., Cooper, R.J., Slade, R.M., Haney, R.L., Arnold, J.G., 2006. Cumulative uncertainty in measured streamflow and water quality data for small watersheds. Trans. ASABE 49 (3), 689–701.

Harrington, S.T., Harrington, J.R., 2013. An assessment of the suspended sediment rating curve approach for load estimation on the rivers Bandon and Owenabue, Ireland. Geomorphology 185, 27–38.

Hirsch, R.M., Moyer, D.L., Archfield, S.A., 2010. Weighted regressions on time, discharge, and season (WRTDS), with an application to chesapeake bay river inputs. J. Am. Water Resour. Assoc. 46 (5), 857–880. http://dx.doi.org/10.1111/j.1752-1688.2010.00482.x.

Horowitz, A.J., 2003. An evaluation of sediment rating curves for estimating suspended sediment concentrations for subsequent flux calculations. Hydrol. Process. 17 (17), 3387–3409. http://dx.doi.org/10.1002/hyp.1299.

Horton, R. E. (1945). Erosional development of streams and their drainage basins; hydrophysical approach to quantitative morphology. Geological society of America bulletin, 56(3), 275-370.

ITCOLD - Comitato Nazionale Italiano delle Grandi Dighe. La gestione dell'interrimento dei serbatoi artificiali italiani, situazione attuale e prospetive, repot gruppi di lavoro.(2016)

Lloyd, C. E. M., Freer, J. E., Johnes, P. J., & Collins, A. L. (2016). Using hysteresis analysis of high-resolution water quality monitoring data, including uncertainty, to infer controls on nutrient and sediment transfer in catchments. *Science of the Total Environment*, *543*, 388-404.

Lawler, D. M., Petts, G. E., Foster, I. D., & Harper, S. (2006). Turbidity dynamics during spring storm events in an urban headwater river system: The Upper Tame, West Midlands, UK. *Science of the Total Environment*, *360*(1-3), 109-126.

Lloyd, C. E. M., Freer, J. E., Johnes, P. J., & Collins, A. L. (2016). Testing an improved index for analysing storm discharge–concentration hysteresis. *Hydrology and Earth System Sciences*, *20*(2), 625-632.

Kendall, A., Stuart, A., Ord, J.K., 1983. Advanced Theory of Statistics, 4th ed. vol. 3 Griffin, London.

Kheirfam, H., Sadeghi, S.H., Darki, B.Z., Homaee, M., 2017. Controlling rainfall-induced soil loss from small experimental plots through inoculation of bacteria and cyanobacteria. Catena 152, 40–46.

Kirkby, M.J., Irvine, B.J., Jones, R.J.A., Govers, G., Boer, M., Cerdan, O., ... Van Lynden, G., 2008. The PESERA coarse scale erosion model for Europe. I. - Model rationale and implementation. Eur. J. Soil Sci. 59 (6), 1293–1306. http://dx.doi.org/10.1111/j.1365-2389.2008.01072.x.

Langlois, J. L., Johnson, D. W., & Mehuys, G. R. (2005). Suspended sediment dynamics associated with snowmelt runoff in a small mountain stream of Lake Tahoe (Nevada). *Hydrological Processes: An International Journal*, *19*(18), 3569-3580.

Larned, S.T., Datry, T., Arscott, D.B., Tockner, K., 2010. Emerging concepts in temporaryriver ecology. Freshw. Biol. 55 (4), 717–738. http://dx.doi.org/10.1111/j.1365-2427.2009.02322.x.

Lee, C.J., Hirsch, R.M., Schwarz, G.E., Holtschlag, D.J., Preston, S.D., Crawford, C.G., Vecchia, A.V., 2016. An evaluation of methods for estimating decadal stream loads. J. Hydrol. 542, 185–203. http://dx.doi.org/10.1016/j.jhydrol.2016.08.059.

Leoni, G., Barchiesi, F., Catallo, F., Dramis, F., Fubelli, G., Lucifora, S., ... & Puglisi, C. (2009). GIS methodology to assess landslide susceptibility: application to a river catchment of Central Italy. *Journal of maps*, *5*(1), 87-93.

Letcher, R.A., Jakeman, A.J., Calfas, M., Linforth, S., Baginska, B., Lawrence, I., 2002. A comparison of catchment water quality models and direct estimation techniques. Environ. Model. Softw. 17 (1), 77–85. http://dx.doi.org/10.1016/S1364-8152(01)00054-8.

Liquete, C., Canals, M., Ludwig, W., Arnau, P., 2009. Sediment discharge of the rivers of Catalonia, NE Spain, and the influence of human impacts. J. Hydrol. 366 (1–4), 76–88. http://dx.doi.org/10.1016/j.jhydrol.2008.12.013.

Littlewood, I.G., Watts, C.D., Custance, J.M., 1998. Systematic application of United Kingdom river flow and quality databases for estimating annual river mass loads (1975–1994). Sci. Total Environ. 210–211, 21–40.

López-Tarazón, J.A., Estrany, J., 2017. Exploring suspended sediment delivery dynamics of two Mediterranean nested catchments. Hydrol. Process. 31 (3), 698–715. http://dx.doi.org/10.1002/hyp.11069.

Jones, J. I., Murphy, J. F., Collins, A. L., Sear, D. A., Naden, P. S., & Armitage, P. D. (2012). The impact of fine sediment on macro-invertebrates. River Research and Applications, 28(8), 1055-1071.

McDonald, D. M., & Lamoureux, S. F. (2009). Hydroclimatic and channel snowpack controls over suspended sediment and grain size transport in a High Arctic catchment. *Earth Surface Processes and Landforms*, *34*(3), 424-436.

Megnounif, A., Terfous, A., & Ouillon, S. (2013). A graphical method to study suspended sediment dynamics during flood events in the Wadi Sebdou, NW Algeria (1973–2004). *Journal of hydrology*, *497*, 24-36. https://doi.org/10.1016/j.jhydrol.2013.05.029

Moatar, F., Meybeck, M., 2005. Compared performances of different algorithms for estimating annual nutrient loads discharged by the eutrophic river Loire. Hydrol. Process. 19 (2), 429–444. http://dx.doi.org/10.1002/hyp.5541.

Mukhopadhyay, B., Smith, E.H., 2000. Comparison of statistical methods for estimation of nutrient load to surface reservoirs for sparse data set: application with a modified model for phosphorus availability. Water Res. 34 (12), 3258–3268.

Nadal-Romero, E., Martínez-Murillo, J. F., Vanmaercke, M., & Poesen, J. (2011). Scale-dependency of sediment yield from badland areas in Mediterranean environments. *Progress in Physical Geography*, *35*(3), 297-332.

Navratil, O., Esteves, M., Legout, C., Gratiot, N., Nemery, J., Willmore, S., & Grangeon, T. (2011). Global uncertainty analysis of suspended sediment monitoring using turbidimeter in a small mountainous river catchment. *Journal of Hydrology*, *398*(3-4), 246-259. doi:10.1016/j.jhydrol.2010.12.025

Oeurng, C. and Sauvage, Sabine and Coynel, Alexandra and Maneux, Eric and Etcheber, Henri and Sanchez-Pérez, José-Miguel *Fluvial transport of suspended sediment and organic carbon during flood events in a large agricultural catchment in southwest France.* (2011) Hydrological Processes, vol. 25 (n°15). pp. 2365-2378 http://dx.doi.org/10.1002/hyp.7999

Oueslati, O., De Girolamo, A.M., Abouabdillah, A., Kjeldsen, T.R., Lo Porto, A., 2015. Classifying flow regimes of Mediterranean streams using multivariate analysis. Hydrol. Process. 29 (22), 4666–4682. http://dx.doi.org/10.1002/hyp.10530.

Panagos, P., Borrelli, P., Poesen, J., Ballabio, C., Lugato, E., Meusburger, K., ... Alewell, C., 2015. The new assessment of soil loss by water erosion in Europe. Environ. Sci. Pol. 54, 438–447. http://dx.doi.org/10.1016/j.envsci.2015.08.012.

Pagano, S. G., Rainato, R., García-Rama, A., Gentile, F., & Lenzi, M. A. (2019). Analysis of suspended sediment dynamics at event scale: comparison between a Mediterranean and an Alpine basin. *Hydrological Sciences Journal*, 1-14. https://doi.org/10.1080/02626667.2019.1606428.

Patault, E., Alary, C., Franke, C., Gauthier, A., & Abriak, N. E. (2019). Assessing temporal variability and controlling factors of the sediment budget of a small agricultural catchment in Northern France (the Pommeroye). *Heliyon*, *5*(3), e01407.

Phillips, J.M., Webb, B.W., Walling, D.E., Leeks, G.J.L., 1999. Estimating the suspended sediment loads of rivers in the LOIS study area using infrequent samples. Hydrol. Process. 13 (7), 1035–1050. http://dx.doi.org/10.1002/(SICI)1099-1085(199905)13:7<1035::AID-HYP788>3.0.CO;2-K.

Preston, S.D., Bierman, V.J., Silliman, S.E., 1989. An evaluation of methods for the estimation of tributary mass loads. Water Resour. Res. 25 (6), 1379–1389.

Quilbé, R., Rousseau, A.N., Duchemin, M., Poulin, A., Gangbazo, G., Villeneuve, J.P., 2006. Selecting a calculation method to estimate sediment and nutrient loads in streams: application to the Beaurivage River (Québec, Canada). J. Hydrol. 326 (1–4), 295–310.http://dx.doi.org/10.1016/j.jhydrol.2005.11.008.

Refsgaard, J.C., van der Sluijs, J.P., Højberg, A.L., Vanrolleghem, P.A., 2007. Uncertainty in the environmental modelling process - a framework and guidance. Environ. Model. Softw. 22 (11), 1543–1556. http://dx.doi.org/10.1016/j.envsoft.2007.02.004.

Regüés, D., Nadal-Romero, E., 2013. Uncertainty in the evaluation of sediment yield from badland areas: suspended sediment transport estimated in the Araguás catchment (central Spanish Pyrenees). Catena 106 (October), 93–100. http://dx.doi.org/10.1016/j.catena.2012.05.006.

Ricci, G.F., De Girolamo, A.M., Abdelwahab, O.M.M., Gentile, F., 2018. Identifying sediment source areas in a Mediterranean watershed using the SWAT model. Land Degrad. Dev published on-line. https://doi.org/10.1002/ldr.2889.

Richards, R., Holloway, J., 1987. Monte Carlo studies of sampling strategies for estimating tributary loads. Water Resour. Res. 23 (10), 1939–1948.

Richards, R.P., Alameddine, I., Allan, J.D., Baker, D.B., Bosch, N.S., Confesor, R., De Pinto, J.V., Dolan, D.M., Reutter, J.M., Scavia, D., 2012. Discussion: nutrient inputs to the Laurentian Great Lakes by source and watershed estimated using SPARROW watershed models. J. Am. Water Resour. Assoc. 49 (3), 715–724.

Rouse, H. (1937). Modern conceptions of the mechanics of fluid turbulence. Trans ASCE, 102, 463-505.

Rovira, A., Batalla, R.J., 2006. Temporal distribution of suspended sediment transport in a Mediterranean basin: the lower Tordera (NE SPAIN). Geomorphology 79 (1–2), 58–71. http://dx.doi.org/10.1016/j.geomorph.2005.09.016.

Salles, C., Tournoud, M.G., Chu, Y., 2008. Estimating nutrient and sediment flood loads in a small Mediterranean river. Hydrol. Process. 22, 242–253. http://dx.doi.org/10.1002/hyp.6580.

Santos, J. C. N. D., Andrade, E. M. D., Medeiros, P. H. A., Palácio, H. A. D. Q., & Araújo Neto, J. R. D. (2017). Sediment delivery ratio in a small semi-arid watershed under conditions of low connectivity. Revista Ciência Agronômica, 48(1), 49-58.

Schleiss, A. J. (2013). Sedimentation of reservoirs. *Encyclopedia of natural hazards*, 901-905.

Seeger, M.; Errea, M.P.; Beguería, S.J.; Arnáez, Martí-Bono C. & García-Ruiz, J.M. (2004). Catchment soil moisture and rainfall characteristics as determinant factors for discharge/suspended sediment hysteretic loops in a small headwater catchment in the Spanish Pyrenees. *Journal of Hydrology*, 288, 299–311

Sharma, A., Tiwari, K. N., & Bhadoria, P. B. S. (2011). Effect of land use land cover change on soil erosion potential in an agricultural watershed. *Environmental monitoring and assessment*, *173*(1-4), 789-801.

Sherriff, S. C., Rowan, J. S., Fenton, O., Jordan, P., Melland, A. R., Mellander, P. E., & Huallachain, D. O. (2016). Storm event suspended sediment-discharge hysteresis and controls in agricultural watersheds: implications for watershed scale sediment management. *Environmental science & technology*, *50*(4), 1769-1778.

Shi, Z. H., Huang, X. D., Ai, L., Fang, N. F., & Wu, G. L. (2014). Quantitative analysis of factors controlling sediment yield in mountainous watersheds. *Geomorphology*, *226*, 193-201.

Smakhtin, V.U., 2001. Low flow hydrology: a review. J. Hydrol. 240 (3–4), 147–186. http://dx.doi.org/10.1016/S0022-1694(00)00340-1.

Soler, M.; Regüés, D.; Latron, J. & Gallart, F. (2007). Frequency–magnitude relationships for precipitation, stream flow and sediment load events in a small Mediterranean basin (Vallcebre basin, Eastern Pyrenees). *Catena,* 71, 164-171

Tabatabaei, M., Solaimani, K., Roshan, M.H., Kavian, A., 2014. Daily suspended sediment load estimation by meta-heuristic optimization approaches and fuzzy-C-means clustering method. Idian J. Sci. Technol. 7, 1488–1497. http://dx.doi.org/10.17485/ijst%2F2014%2Fv7i10%2F51872.

Tayfur, G., Karimi, Y., & Singh, V. P. (2013). Principle component analysis in conjuction with data driven methods for sediment load prediction. *Water resources management*, *27*(7), 2541-2554. https://dx.doi.org/10.1007/s11269-013-0302-7.

Tan, K.S., Fox, D., Etchells, T., 2005. GUMLEAF: Generator for Uncertainty Measures and Load Estimates Using Alternatie Formulae. (1 June).

Taylor, J.W., Bunn, D.W., 1999. Investigating improvements in the accuracy of prediction intervals for combinations of forecasts: a simulation study. Int. J. Forecast. 15 (3), 325–339. http://dx.doi.org/10.1016/S0169-2070(99)00002-3.

Tennakoon, S.B., Marsh, N., Arene, S., 2007. A software tool for the estimation of pollutant loads in rivers and streams using time series data. In: MODSIM 2007 International Congress on Modelling and Simulation. 80. Modelling and Simulation Society of Australia and New Zealand, pp. 74–80.

Tzoraki, O., & Nikolaidis, N. P. (2007). A generalized framework for modeling the hydrologic and biogeochemical response of a Mediterranean temporary river basin. Journal of Hydrology, 346(3-4), 112-121.

Ullrich, A., Volk, M., 2010. Influence of different nitrate-N monitoring strategies on load estimation as a base for model calibration and evaluation. Environ. Monit. Assess. 171 (1–4), 513–527. http://dx.doi.org/10.1007/s10661-009-1296-8.

Valent, P., Výleta, R., & Danáčová, M. (2019). A Joint Sedimentation-Flood Retention Assessment of a Small Water Reservoir in Slovakia: A New Hope for Old Reservoirs?. *Geosciences*, 9(4), 158.

Van Rompaey, A., Bazzoffi, P., Jones, R.J.A., Montanarella, L., 2005. Modeling sediment yields in Italian catchments. Geomorphology 65 (1–2), 157–169. http://dx.doi.org/10.1016/j.geomorph.2004.08.006.

van Rijn, L. C. (1984). Sediment transport, part III: bed forms and alluvial roughness. Journal of hydraulic engineering, 110(12), 1733-1754.

Van Rijn, L. C. (1987). Mathematical modelling of morphological processes in the case of suspended sediment transport.

Van Rijn, L. C. (1993). Principles of sediment transport in rivers, estuaries and coastal seas (Vol. 1006, pp. 11-3). Amsterdam: Aqua publications.

Vanmaercke, M., Poesen, J., Maetens, W., de Vente, J., & Verstraeten, G. (2011). Sediment yield as a desertification risk indicator. *Science of the Total Environment*, *409*(9), 1715-1725.

Velikanov, M. A. (1954). Gravitational theory of sediment transport. Journal of Science of the Soviet Union, Geophysics, 4(GTS translation 62-15004).

Vericat, D., Batalla, R.J., 2006. Sediment transport in a large impounded river: the lower Ebro, NE Iberian peninsula. Geomorphology 79 (1–2), 72–92. http://dx.doi.org/10.1016/j.geomorph.2005.09.017.

Vercruysse, Kim, Grabowski, Robert C., Rickson, R.J., Suspended sediment transport dynamics in rivers: Multi-scale drivers of temporal variation, *Earth Science Reviews* (2017), https://dx.doi.org/10.1016/j.earscirev.2016.12.016.

Vigiak, O., Malagó, A., Bouraoui, F., Vanmaercke, M., Obreja, F., Poesen, J., ... Grošelj, S., 2017. Modelling sediment fluxes in the Danube River basin with SWAT. Sci. Total Environ. 599-600, 992–1012. http://dx.doi.org/10.1016/j.scitotenv.2017.04.236.

Walling, D.E., Webb, B.W., 1985. Estimating the discharge of contaminants to coastal waters by rivers: some cautionary comments. Mar. Pollut. Bull. 16 (12), 488–492. http://dx.doi.org/10.1016/0025-326X(85)90382-0.

Walling, D.E., Webb, B.W., 1988. The reliability of rating curve estimates of suspended sediment yield: some further comments. In: Sediment Budgets (Proceedings of the Porto Alegre Symposium). 174. pp. 337–350.

Wohl, E., Bledsoe, B.P., Jacobson, R.B., Poff, N.L., Rathburn, S.L., Walters, D.M., Wilcox, A.C., 2015. The natural sediment regime in rivers: broadening the foundation for ecosystem management. Bioscience 65, 358–371. http://dx.doi.org/10.1093/biosci/biv002.

Wuttichaikitcharoen, P., & Babel, M. (2014). Principal component and multiple regression analyses for the estimation of suspended sediment yield in ungauged basins of Northern Thailand. *Water*, 6(8), 2412-2435. https://dx.doi:10.3390/w6082412.

Zuecco, G., Penna, D., Borga, M., & van Meerveld, H. J. (2016). A versatile index to characterize hysteresis between hydrological variables at the runoff event timescale. *Hydrological Processes*, *30*(9), 1449-1466.

Zhang, W., Wei, X., Jinhai, Z., Yuliang, Z., & Zhang, Y. (2012). Estimating suspended sediment loads in the Pearl River Delta region using sediment rating curves. *Continental Shelf Research*, *38*, 35-46. https://dx.doi:10.1016/j.csr.2012.02.017

Zhang, Q., Xiao, M., Liu, C. L., & Singh, V. P. (2014). Reservoir-induced hydrological alterations and environmental flow variation in the East River, the Pearl River basin, China. Stochastic environmental research and risk assessment, 28(8), 2119-2131.

PUBLICATION LIST

Thecnical note:

A.M. De Girolamo, **R. Di Pillo**, A. Calabrese, A. Lo Porto G. Pappagallo & M.T. Todisco. Sediment Transport in a Mediterranean river (Celone, Puglia). Comparison of Calculation tools. L'Acqua, Italian Hydrotechnical Association Vol. 01/2017; pp. 77-86 ISSN: 1125-1255

Conference proceedings:

A.M. De Girolamo, **R. Di Pillo**, A. Lo Porto, G. Pappagallo & M.T. Todisco, Trasporto solido in sospensione: Metodi di calcolo a confronto in un fiume temporaneo. XXXV Conv. Naz. di Idraulica e Costruzioni idrauliche, Bologna, 2016. ISBN: 9788898010400, https://:doi: 10.6092/unibo/amsacta/5400

R. Di Pillo, A.M. De Girolamo, M.T. Todisco. Stima della produzione specifica di sediment ed identificazione delle source area attraverso un approccio multiscale: (Celone, Puglia, S-E Italy). XXXVI Conv. Naz. Di Idraulica e costruzioni idrauliche, Ancona, 2018. ISBN: 978889437907.

R. Di Pillo, A.M. De Girolamo, M.T. Todisco. Analisi dell'isteresi Q-SSC mediante l'Hysteresis Index in un fiume intermittente: Il Celone (Puglia, Italia). XXXVII Conv. Naz. Di Idraulica e costruzioni idrauliche, Reggio Calabria, 2020. (submitted 07/01/2020).

Referred Journals:

A.M. De Girolamo, **R. Di Pillo**, A. Lo Porto, M.T. Todisco, E. Barca. Identifying a reliable method for estimating suspended sediment loads in a temporary river system, Catena 165 (2018) 442-453, https://doi.org/10.1016/j.catena.2018.02.015

R. Di Pillo, A.M. De Girolamo, M.T. Todisco. Modelling the silting-up of a small reservoir fed by a temporary river: the Torrebianca reservoir study case (Puglia, SE Italy). Journal of Materials and Environmental Sciences, 10,3 (2019), 225-233.

R. Di Pillo, M.T. Todisco, Transport and adsorption of pollutants in saturated porous media: Integration into unlimited domain. Pollution Research, ISSN 0257-8050 (Submitted 30/07/2019, under peer review)

R. Di Pillo, A.M. De Girolamo, A. Lo Porto, M.T. Todisco, E. Barca. Detecting divers of suspended sediment in a Mediterranean Temporary river system: a multivariate event-based analysis. Catena ISSN 0341-8162 (submitted 29/01/2020).